TURKISH REPUBLIC
ERCIYES UNIVERSITY
GRADUATE SCHOOL OF NATURAL AND
APPLIED SCIENCE
DEPARTMENT OF ENERGY SYSTEMS
ENGINEERING

INVESTIGATION OF ELECTRICITY AND HYDROGEN PRODUCTION POTENTIAL FROM SOLAR/WIND HYBRID SYSTEM IN IRAQ

Masad Mezher HASAN

Supervisor
Assoc. Prof. Dr. Gamze GENÇ

MSc. Thesis

March 2017
KAYSERİ

TURKISH REPUBLIC

ERCIYES UNIVERSITY

GRADUATE SCHOOL OF NATURAL AND APPLIED SCIENCE

DEPARTMENT OF ENERGY SYSTEMS ENGINEERING

INVESTIGATION OF ELECTRICITY AND HYDROGEN PRODUCTION POTENTIAL FROM SOLAR/WIND HYBRID SYSTEM IN IRAQ

(MSc Thesis)

Masad Mezher HASAN

Supervisor
Assoc. Prof. Dr. Gamze GENÇ

March 2017

KAYSERI

SCIENTIFIC ETHICS SUITABILITY

I declare that all information in this work was obtained in accordance with academic and ethical rules. All results and material that not been at the essence of this work are also transferred and expressed by giving reference as required by these rules and behavior.

MASAD MEZHER HASAN

SUITABILITY FOR GUIDE

The MSc thesis entitled "INVESTIGATION OF ELECTRICITY AND HYDROGEN PRODUCTION POTENTIAL FROM SOLAR/WIND HYBRID SYSTEM IN IRAQ" has been prepared in accordance with Erciyes University Graduate Education and Teaching Institute Thesis Preparation and Writing Guide.

Student	Supervisor
Masad Mezher HASAN	Assoc. Prof. Dr. Gamze GENÇ
Signature	Signature

Chairman of the Department of Energy Systems Engineering

Prof. Dr. Hüseyin YAPICI

ACCEPTANCE AND APPROVAL PAGE

This study entitled "INVESTIGATION OF ELECTRICITY AND HYDROGEN PRODUCTION POTENTIAL FROM SOLAR/WIND HYBRID SYSTEM IN IRAQ" prepared by Masad Mezher HASAN under the supervision of Assoc. Prof. Dr. Gamze GENÇ was accepted by the jury as MSc thesis in Energy Systems Engineering department.

17/03/2017

JURY:

Supervisor	: Assoc. Prof. Dr. Gamze GENÇ	.....
Juror:	: Assist. Prof. Dr. Gülşah ELDEN	.....
Juror:	: Assist. Prof. Dr. Muhammet ÇELİK	.....

APPROVAL:

That the acceptance of this thesis has been approved by the decision of the Institute's Board of Directors with the 04/04/2017.. date and 2017/16-04. numbered decision.

..05.../.04.../ 2017.

Prof. Dr. Mehmet AKKURT

Director of the Institute

DEDICATION

To my father ... who has been there for me in every step of the way,

To my mother ... whose prayers have paved the way for all my successful endevours,

To my brothers and their beautiful families,

To all my friends ... who have blessed my life with their existence.

ACKNOWLEDGMENTS

I would like to thank my adviser Assoc. Prof. Dr. Gamze GENÇ for her guidance and help in each step of the research. I would also like to thank all the academic staff at the Energy Systems Engineering Department for their support.

I would like to express my gratitude first to the great leader Mustafa Kemal Atatürk, the founder of the Turkish Republic, and to the Republic of Turkey for the support and hospitality during my research.

I also want to thank the Meterological Department at the Ministry of Agriculture for their cooperation in providing the researcher with all the necessary data, especially their dear employee Shahd Al-Kaissi for her constant investment in the research.

I thank all those who provided me with help in this research.

INVESTIGATION OF ELECTRICITY AND HYDROGEN PRODUCTION POTENTIAL FROM SOLAR/WIND HYBRID SYSTEM IN IRAQ

Masad Mezher HASAN

Erciyes University, Graduate School of Natural and Applied Sciences

MsC Thesis, March 2017

Supervisor: Assoc. Prof. Dr. Gamze GENÇ

ABSTRACT

Increasing demand for energy makes it imperative to search for more energy sources, which must be environmentally friendly and inexhaustible, in contrast to the current resources of energy (fossil fuel) that cause a lot of damages. Recently, interest in renewable energy sources has increased in order to overcome the dependency on fossil fuels to reduce the pollution, toxic emissions, and global warming.

In this thesis, it is aimed to investigate the potentials of electricity and hydrogen production with a solar (PV)/wind hybrid energy system for the cities of Basra, Wasit and Anbar in Iraq. In line with this aim, a hybrid energy system consists the various wind turbines having different rated powers (500 kW, 900 kW, 1300 kW and 2000 kW) and operated at different hub heights (50 m, 80m, 100m and 120m) integrated with two different solar panels (Panasonic-330W and Kyocera-315W) considered for electricity production. In addition, the electrolyzers having different rated power (48 kWx18, 215 kwx4, 430 kWx2 ve 860 kWx1) are added to the the solar/PV hybrid system in order to investigate the hydrogen production potential. For all considered cases, the cost of electricity and hydrogen production are calculated. The obtained results bring out that Basra has the remarkable electricity and hydrogen prodution potential between the selected cities in Iraq.

Keywords: Solar Energy, Wind Energy, Hydrogen Production, Electrolysis

IRAKTA GÜNEŞ/RÜZGAR HİBRİD SİSTEMLERİ İLE ELEKTRİK VE HİDROJEN ÜRETİM POTANSİYELİNİN ARAŞTIRILMASI

Masad Mezher HASAN

Erciyes Üniversitesi, Fen Bilimleri Enstitüsü

Yüksek Lisans Tezi, Mart 2017

Danışman: Doç. Dr. Gamze GENÇ

ÖZET

Artan enerji talebi ve fosil kökenli mevcut enerji kaynaklarının çevreye ve insan verdiğe zarardan dolayı çevre dostu ve tükenmez enerji kaynaklarını aramak zorunluluk haline geliyor. Özellikle son yıllarda çevre kirliliği, toksik emisyon, küresel ısınma sorunlarını aşmak ve fosil yakıt bağımlılığını azaltmak için yenilenebilir enerji kaynaklarına olan ilgi oldukça arttı.

Bu çalışmada, Irak'ta yer alan Basra, Wasit ve Anbar şehirleri için güneş/rüzgar hibrit enerji sistemi ile elektrik üretim ve hidrojen üretim potansiyelleri araştırıldı. Bu amaç doğrultusunda, elektrik üretimi için farklı hub yüksekliklerinde (50 m, 80m, 100m ve 120m) farklı güçlerde (500 kW, 900 kW, 1300 kW ve 2000 kW) çalışan rüzgar türbinleri ile farklı iki güneş pilinden (Panasonic-330W ve Kyocera-315W) oluşan hibrit sistem incelendi. Daha sonra, hidrojen üretim potansiyeli araştırmak için güneş/rüzgar hibrit sistemine farklı güçlere sahip elektrolizör (48 kWx18, 215 kwx4, 430 kWx2 ve 860 kWx1) entegre edildiği düşünülerek her bir durumdaki hidrojen üretim miktarları araştırılmıştır. Ayrıca, ele alınan her bir durum için üretim maliyetleri de araştırılmıştır. Elde edilen sonuçlara göre, ele alınan şehirler içinde Basra şehrinin en yüksek elektrik enerjisi ve hidrojen üretim potansiyeline sahip olduğu bulunmuştur.

Anahtar Kelimeler: Güneş enerjisi, Rüzgar enerjisi, Hidrojen üretimi, Elektroliz.

TABLE OF CONTENTS

INVESTIGATION OF ELECTRICITY AND HYDROGEN PRODUCTION POTENTIAL FROM SOLAR/WIND HYBRID SYSTEM IN IRAQ

CHAPTER 2

HYDROGEN ENERGY

CHAPTER 5

HYDROGEN PRODUCTION POTENTIAL FROM WIND/SOLAR HYBRID SYSTEM IN IRAQ

CHAPTER 6

CONCLUSIONS AND RECOMMENDATIONS

NOMENCLATURE AND ABBREVIATIONS

Symbol	Description	Units
IG	Induction Generator	-
WRIG	Wound Rotor Induction Generator	-
SCIG	Squirrel Cage Induction Generator	-
DFIG	Doubly Fed Induction Generator	-
WRSG	Wound Rotor Synchronous Generator	-
PMSG	Permanent Magnet Synchronous Generator	-
DC	Direct Current	A
AC	Alternative Current	A
SRGs	switched reluctance generators	-
E	Kinetic Energy	$Kg.m^2/s^2$
m	Mass	kg
V	Wind Speed	m/s
ρ	Density	kg/m^3
A	The Area	m^2
Δt	Finite Time Interval	s
P	Wind Power Density	W/m^2
C_p	Power Coefficient of Wind Turbine	-
λ	Tip-speed ratio	-
β	Blade pitch angle	Degree
R	Radius of Turbine Blades	m
w_m	The Angular Speed of The Rotor Turbine	radians/s
$f(v)$	Weibull distribution probability density function	
K	Weibull Shape Parameter	-
c	Weibull Scale Parameter	m/s
MLE	Maximum Likelihood estimation	-
MPS	Maximum Product of Spacing	-
w-MLE	Weighted Maximum Likelihood estimation	-
MoM	Method of Moments	-
$f(x)$	Rayleigh distribution probability density function	-

b	Scale Parameter of Rayleigh distribution probability density function	m/s
$G(x;b)$	Cumulative Distribution Function	-
CSP	Concentrating Solar Power	-
MBE	Mean Bias Error	-
RMSE	Root Mean Square Error	-
HOMER	Hybrid Optimization of Multiple Energy Resources	-
CCS	Capture and Storage	-
SMR	Steam Methane Reforming	-
POX	Partial Oxidation	-
ATR	Autothermal Reforming	-
wt%	Gravimetric Energy Density	
MOFs	Metal Oxide Frameworks	-
PEM	Proton Exchange Membrane	-
DCO	Direct Connection Optimization	-
GHG	Greenhouse Gases	-
PECs	Photoelectrochemical cells	-
CPO	Catalytic Partial Oxidation	-
HRI	Hydrogen Research Institute	-
HHV	Higher Heating Value	Btu
AI	Artificial Intelligence	-
IO	Input-Output	-
LP	Linear Programming	-
CGE	Computable General Equilibrium	-
BHIRES	Bio-Hydrogen Integrated Renewable Energy System	-
WT	Wind Turbine	-
PV	Photovoltaic Panels	-
DRI	Direct Reduction Iron	-
HTGR	High temperature gas-cooled nuclear reactor	-
IEA	International Energy Agent	-
Mt	Million tons	
$\bar{v}$	Mean Wind Speed	m/s

σ	The Standard Deviation	
n	Number of Hours of Specific Period	-
z	Height	m
z_0	Anemometer Height	m
v_0	The Wind Speed that Recorded at Anemometer Height	m/s
z_s	The Surface Rugosity Scale	
H_0	Daily Extraterrestrial Radiation	MJ/m^2.day
I_{gs}	Solar Constant	W/m^2
δ	Solar Declination Angle	rad
f	The Inverse Relative Distance Earth-Sun	rad
ω_s	Sunset Hour Angle	rad
N	Daylight Hours	hour
φ	The Latitude for the Location	rad
H_{cal}	Calculated Global solar radiation	MJ/m^2.day
a_s, b_s	Regression Constant for Angstrom	-
n	Actual Duration of Sunshine	hour
$\frac{n}{N}$	Relative Sunshine Duration	-
H_T	Total Solar Radiation on Tilted Surface	MJ/m^2.day
H_B	Beam Radiation Incident on Tilted Surface	MJ/m^2.day
H_D	Diffuse Radiation Incident on Tilted Surface	MJ/m^2.day
H_R	Reflected Radiation Incident on Tilted Surface	MJ/m^2.day
H	Monthly Mean Daily Global Radiation	MJ/m^2
H_d	Diffuse Radiation Fraction	MJ/m^2
R_b	The Ratio of Daily Average Beam Radiation	-
K_T	Clear sky Index	-
ρ_r	Ground Reflectivity	
$P_i(v)$	The Output Power of Wind Turbine at Specific Wind Speed	W
P_R	Rated Power of the Wind Turbine	W

v_{ci}	Cut-in Wind Speed	m/s
v_R	Rated Wind Speed	m/s
v_{co}	Cut-out Wind Speed	m/s
LCOE	Levelized Cost of Electricity	$/kWh
$LCOE_{WT}$	Levelized Cost of Electricity for Wind Turbine	$/kWh
C_{WT}	Capital Cost of Wind Turbine	$
C_{aux}	Capital Cost of Auxiliary Equipment	$
C_{ci}	The Civil Work and Installation Cost	$
$C_{(om)esc}$	Cost of Operation and Maintenance	$
E_{WT}	The Annual Power Generation from Wind Turbine	kWh/year
CRF	Capital Recovery Factor	
i	Discount Rate	%
l	System Lifetime	year
C_{om}	Cost of Operation and Maintenance for The First Year	$
e	Escalation Rate	%
C_f	Capacity Factor	%
E_R	The Annual Rated Electrical Power	kWh/year
E_{PV}	The Annual Power Generation from Photovoltaic Module	kWh/year
N_P	Photovoltaic Module Efficiency	%
N_D	Performance Ratio	%
G	Average Solar Radiation That Incident on Tilt Photovoltaic Module	kWh/m^2
G_m	The Distance Between the Rows of Photovoltaic Module	m
β	The Tilt Angle	degree
L	The Length of The Photovoltaic Module	m
$LCOE_{pv}$	Levelized Cost of Electricity for Photovoltaic Module	$/kWh
C_{pv}	The Capital Cost of Photovoltaic Modules	$
E_{pv}	The Annual Power Generation from Photovoltaic Modules	kWh/year
$LCOE_{hybrid}$	Levelized Cost of Electricity for Solar/Wind Hybrid System	$/kWh

E_{total}	The Annual Power Generation from Solar/Wind Hybrid System	kWh/year
LCOH	Levelized cost of hydrogen	$/kWh
$LCOH_1$	Levelized cost of hydrogen Without Sale of Excess Power	$/kWh
$LCOH_2$	Levelized cost of hydrogen With Sale of Excess Power	$/kWh
m_{H_2}	Annual Hydrogen Production	m^3H_2/year
C^*_{EZ}	Annual Cost of Electrolyzer	$
C_{EZ}	The Cost of Electrolyzer	$
$C^*_{0,m}$	The Operation and Maintenance Cost of The Electrolyzer	$
$C_{electric}$	Annual Cost of Electric Energy	$/year
C_{Grid}	Excess Energy from The Electrolyzer	kWh/year
P_{EZ}	The Power of Electrolyzer	kWh/h

LIST OF TABLES

LIST OF FIGURES

INTRODUCTION

Fossil fuel has become the main sources of energy in the recent decades, especially in countries where this fuel is available, such as Iraq. However, it has been found that these traditional energy sources are being depleted, and also there are regular fluctuations in the prices of these fuels, especially the prices of oil. On the other hand, there are negative impacts of the fossil fuel on the environment and human health. The most serious impacts caused by the consumption of fossil fuel are air pollution, acid precipitation, and greenhouse gases emissions of the most prominent gases are sulfur dioxide, nitrogen oxides, and carbon dioxide which is the main cause of global warming. To reduce this phenomenon and to limit the effect of climate change, Paris agreement (Paris climate conference) was held that required the participating countries to intensify the efforts to decrease the Earth's temperature to two degree Celsius. This meant reducing greenhouse gas emissions since fossil fuels are the reason behind the emission of greenhouse gases. So the agreement directed the counties to look for alternative sources such as clean energy resources instead of contaminated energy resources such as oil and gas. In recent years, most researches trend to search for new, clean and sustainable sources of energy to reduce dependency on fossil fuels and seek to develop the use of these renewable energies. There are different types of renewable energies such as solar, wind, geothermal, hydropower, green power, bioenergy, and hydrogen energy.

The field of renewable energies is very important and is in continuous growth and will continue to grow in the future to occupy the place of conventional energy sources. Countries and companies around the world are showing interest to raise investment in renewable energies which is becoming more economic and environmental necessity. And because of population growth and increase in the demand for energy, it needs to be developed to meet the demands and for sustainable economic growth.

Because of all the above mentioned reasons, the aim of this thesis is to simulate and design an operating system to estimate the amount of electrical power that can be obtained from a hybrid renewable energy system consisting of wind power source and solar energy source. This will also investigate the potential to produce hydrogen from this obtained power in three different areas in Iraq.

CHAPTER 1

WIND AND SOLAR ENERGY

Using renewable energy is very important in view of reducing greenhouse gas emissions as well as meeting the energy demand and comsumption all over the world. Therefore, the energy systems based on renewable energy sources such as solar, wind, geothermal and tidal energy has been becoming more popular and efficient. However, wind and solar energy between all renewable energy sources will never run out since they are constantly regenerated.

1.1. Background of Wind Energy

Wind is the movement of air horizontally on the surface of the earth. It is essentially an indirect form of solar energy. One of the reasons for the formation of wind is the uneven heating of the atmosphere by the sun, where the rise in ground temperature makes the air near the surface more light blowing upward and replaced with cold air comes from air layers located above it. Otherwise, be caused by spatial variations atmospheric pressure where the wind is moving from areas of high pressure to low pressure areas based on the intensity of pressure. Other reasons are the infractions of the earth's surface, and rotation of the earth.

Wind energy is one of the oldest sources of energy used by human being. Ancient cultures used wind energy to drive the sailing ships. There are references to windmills belonging to a Persia in 644 AD and another windmills relating to 915 AD [1]. In eighteenth century, in The Netherlands, the use of windmills spread in 1750 AD and there were about 8-6 thousand Windmills. In the nineteenth century, fans with multiple blade were built, with about twenty blades, which were used mostly for irrigation purposes in the USA, while in Germany there were around eighteen thousand windmills in 1895 AD [2]. Windmill converts kinetic energy of the wind into mechanical power.

These Windmills were used basically for irrigation purposes and grinding grains. In 1897, 89 Watt wind turbine was used for the first time to produce electricity. Wind flow, can be exploited by converting this kinetic energy to mechanical power with its ability to move the blades of wind turbines, and convert this mechanical power into electricity power via generator.

In Denmark, between the period of 1940 and 1950, an engineering company produced wind turbine with two and three blades. In 1950, the first wind turbine was developed which worked with alternative current (AC). While the developed wind turbine provides 55 watts of electricity in 1980, 5 MW of electricity was provided in 2006 [3]. For present time, wind energy has evolved to the level where it is accepted as one of the promising and utility technologies.

Until 2008, the top five countries in terms of capacity of installed wind turbine were Germany, Spain, USA, China, and India. Recently, the growth rate in the wind energy sector has been most phenomenal among the other renewable energy sources. It is considered as the most cost-effective form of renewable source of energy with an annual growth rate of 40.5% in 2005 [4].

The development of wind energy technology has been featured after the oil crisis in the seventies of the last century and after the worries about the environmental effects of conventional energies. CO_2 gas emission from combustion of fossil fuels to generate electricity is one of the biggest contribution causes of pollution. The concerns about the climate change caused by greenhouse gases have driven the competent institutions to minimize the emission of the CO_2 and to look for more green alternative energy sources for electricity generation. Wind energy seems to be the least expensive energy source among the renewable energy alternatives [5].

The wind power has developed dramatically, especially during last 20 years. In 2015, more than 432000 MW of global annual cumulative wind capacity was obtained as shown in Figure 1.1. China has become the largest wind power market where overtook both Europe and the United States, as shown in Figure 1.2.

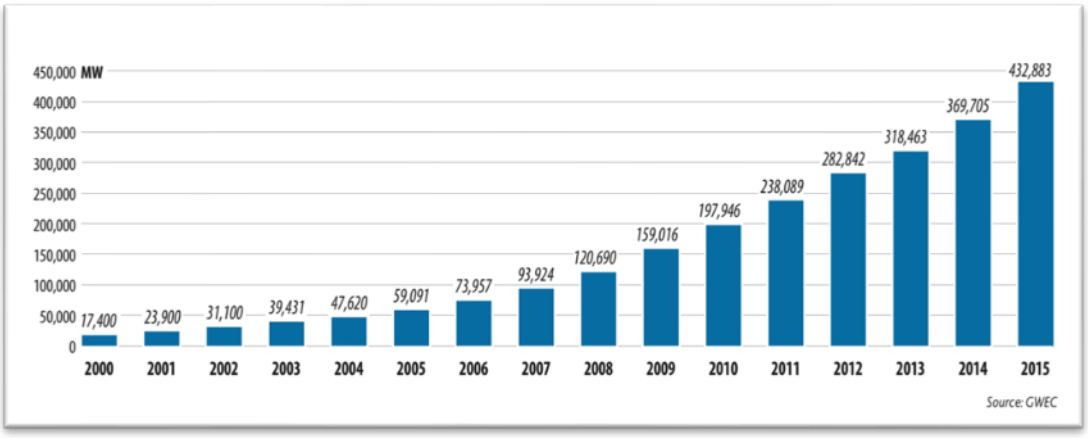

Figure 1.1 Global Annual Cumulative Wind Capacities between 2000-2015 [6]

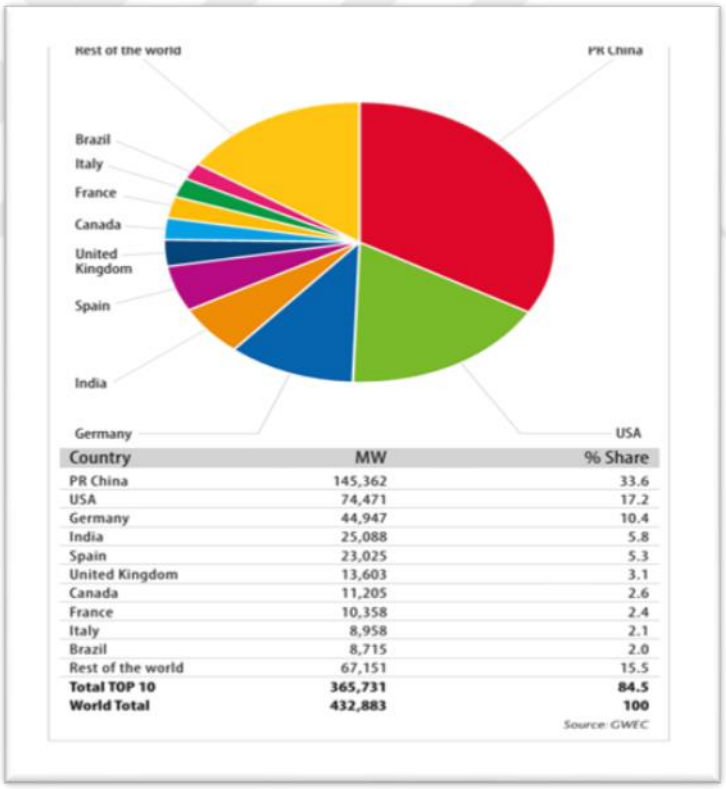

Country	MW	% Share
PR China	145,362	33.6
USA	74,471	17.2
Germany	44,947	10.4
India	25,088	5.8
Spain	23,025	5.3
United Kingdom	13,603	3.1
Canada	11,205	2.6
France	10,358	2.4
Italy	8,958	2.1
Brazil	8,715	2.0
Rest of the world	67,151	15.5
Total TOP 10	**365,731**	**84.5**
World Total	**432,883**	**100**

Source: GWEC

Figure 1.2 Top 10 Countries in view of Wind Power [6]

1.2. Wind Turbines

Wind turbine is a machine designed to extract energy from the wind. Several types of wind turbine designs exist; the most common classification is two categories: horizontal wind turbine and vertical wind turbine shown in Figure 1.3-a and Figure 1.3-b [7]. Now, the most common used wind turbine is the horizontal axis propeller type, having two or three blades installed on the top of a tower, while the three blades wind turbine is more common in the market. Although wind turbine with two blades has an advantage that the weight of the top tower is lighter than the with three blades; this could make the cost lower, but the rotor moment of inertia of the three blades wind turbine easier to understand and this kind has less noise than the two blades wind turbine [8].

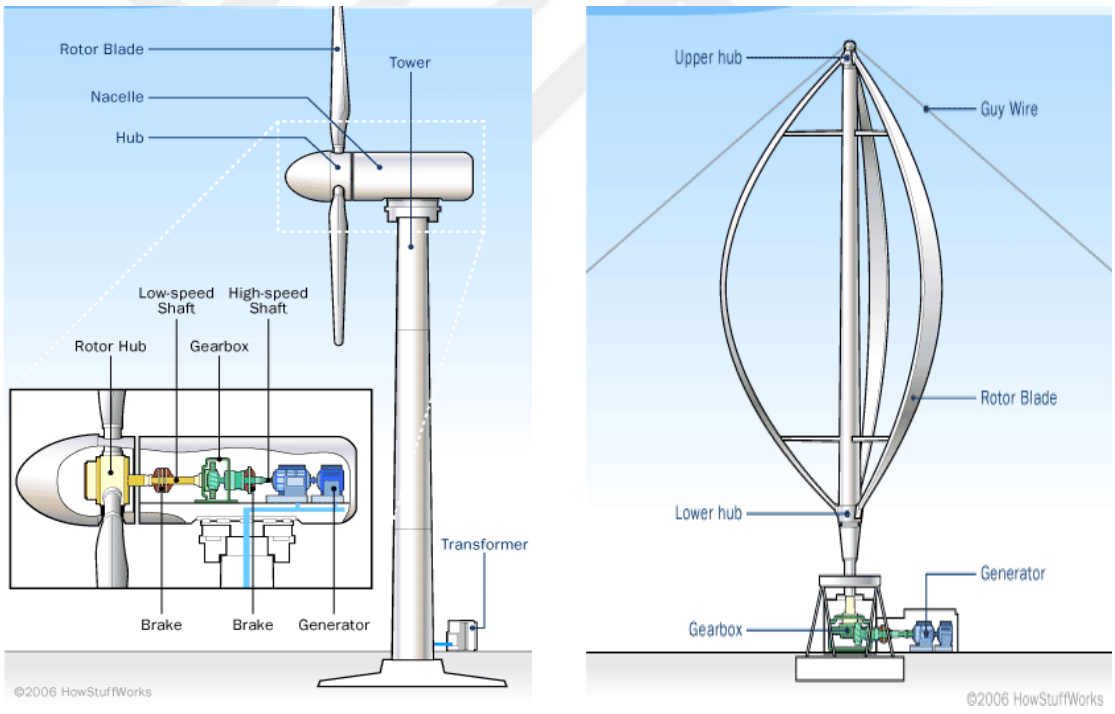

(a) **(b)**

Figure 1.3 (a) Horizontal-Axis Wind Turbine, (b) Vertical-Axis Wind Turbine

The wind turbine system could be classified depending on the operation speed into two types: constant speed constant frequency (CSCF) and variable speed constant frequency (VSCF). The VSCF wind turbine system is better than the CSCF wind turbine system because it works at a specific speed range, which can cause a decline in the overall power coefficient. While the VSCF wind turbine system is able to control the rotor speed according to the wind speed, makes it able to obtain maximum power [9]. The wind turbines are managed to operate at specific speed range by what is known as cut-out speed and cut-in speed. Figure 1.4 shows the curve of wind speed power, when the wind speed low, the power that can be generated in wind turbine very low to be exploited, due to the necessity to overcome the various types of losses. When the wind speed reaches 3 or 4 m/s the wind turbines start working, this is known as the cut-in wind speed which is the minimum wind speed that wind turbine starts to produce useful power. The power of wind turbine increases with the increasing of wind speed. At wind speed range from 12 m/s up to around 20-25 m/s, where the maximum output power can produce from the generator that denoted as the rated wind speed. When the wind speed surpasses 20 or 25 m/s, the wind turbines are usually directed to the standstill to avoid high loads on the turbine components. This wind speed is known as cut-out wind speed [10].

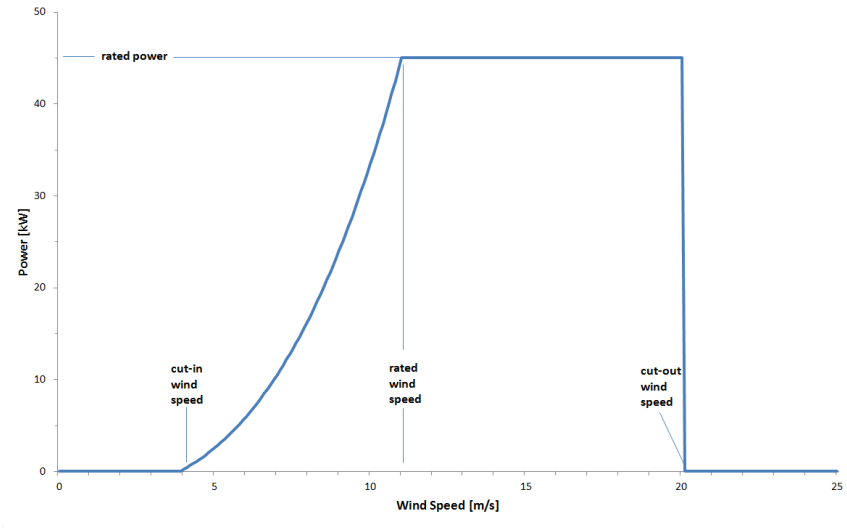

Figure 1.4 Wind Turbine Power Curve [11]

1.2.1. System Components of Wind Turbine

The wind turbine consists of the fundamental components to capture the wind energy and additional components to control the work of the turbine. The principle of power generation via a wind turbine is the conversion of the kinetic energy of the wind into mechanical energy by rotating the turbine blades. Wind energy that captured through wind turbine blades then moved through a gearbox. The gearbox and the rotor hub transferred to the mechanical energy in a shaft. And obtained mechanical energy is converted to electrical energy by a generator [12].

The components of a wind turbine are shown in Figure 1.5. The major components of wind-turbine-driven gearbox are as follows: Blades, generator (GEN), gearbox (GBX), inverter, electronics, and control (ELE).

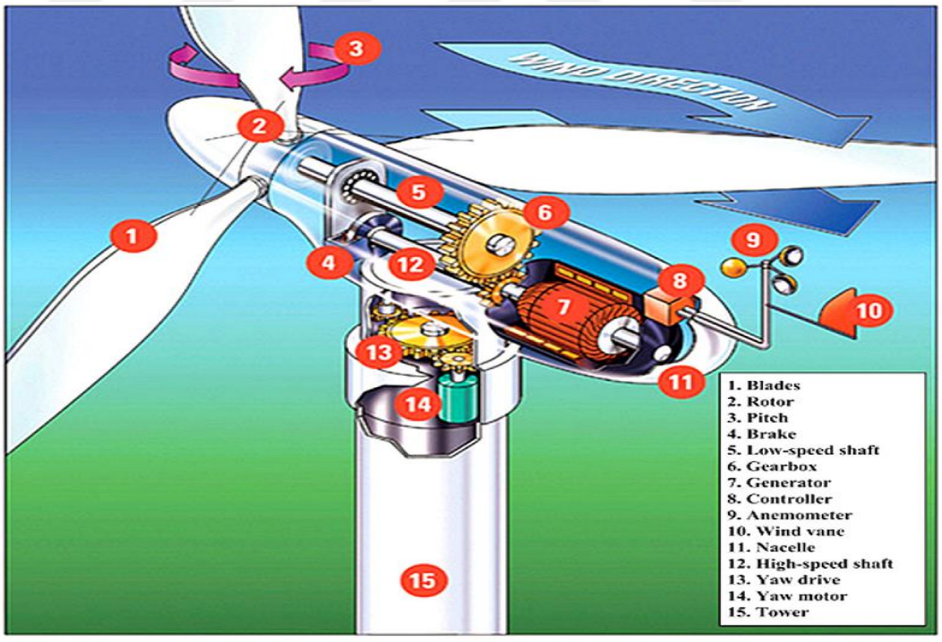

Figure 1.5 Major Components of A Typical Horizontal Axis [13]

The blade is one of the major components that work to pick up the wind energy. It must be with high specifications to ensure the safe operation of the wind turbine system and withstand operating conditions that persist for a long time. The blade material must be resistant to weather conditions, and it must be light to reduce the total weight of the

turbine at the same time. Glass fiber and carbon fiber are the most common materials that used in the manufacture of blades, but these types of materials have high-cost and harmful to the environment. The search for alternative materials has found that bamboo is a promising material for the manufacture of wind turbine blades because it's cheap and friendly to the environment [9].

The generator is an essential element for a wind turbine. The mechanical energy that available at the shaft is converted into electrical energy via a generator. Based on the electrical and mechanical construction of the generators, it could be classified into two principal categories: induction generator (IG) and a synchronous generator. The induction generators divided into three main types as follow: wound rotor induction generator (WRIG), squirrel cage induction generator (SCIG), and doubly fed induction generator (DFIG). The synchronous generators could divide into a wound rotor synchronous generator (WRSG), permanent magnet synchronous generator (PMSG), and salient pole synchronous generator, other generator types are known as DC generators and switched reluctance generators (SRGs) [14]. The DFIG wind turbine system is a preferable option and has more attention from other types of wind turbines because of its technological maturity and high efficiency. Another classification of wind generators based on the type of operation is as follows: direct drive generators, fixed speed generators, and variable speed generators.

Gear located in the nacelle connect the low-speed shaft to the high-speed shaft and this part increase the rotational speeds. A design which doesn’t use a gearbox in the wind turbine because of its high cost and heavy weight is called as direct drive generator, where the rotor shaft connects directly to the generator.

The control system includes the power amplifiers, sensors, actuators, controllers, and intelligence.

1.2.2. On-shore and Offshore Wind Turbines

The wind speed increases over the high regions, because of that the on-shore wind turbines installed in nearly high areas from ground to exploit the wind speed on these locations. The most prominent countries that exploit from the wind energy are USA,

China, Germany, Spain, and India. The largest on-shore wind turbine farms are in the USA and China.

The wind turbines are constructed on offshore to exploit wind energy where the offshore wind speed is more powerful than the wind speed on the ground. Some of the largest offshore wind farms are constructed in the UK such as London Array Offshore Wind Farm, which is the largest offshore wind farm in the world with a capacity of 630 MW, and wind turbines have a height reach to 87 m above sea level. Germany, Denmark and Belgium are the other countries that containing the top 10 largest offshore wind farms in the world. Nevertheless, this type is facing many challenges; as it is more expensive than on-shore, or there are a lot of countries not having the area to devote to wind turbines, on the other side difficulties in laying cables inside the sea because of fishing activities and anchors. However, future of offshore wind farms in countries that have potential are expected to be construct in the depth of the sea far from shore and have larger capacities than present day.

1.2.3. On-grid and Off-grid of Wind Turbines

The mean of grid connection or on-grid is that the wind turbine is connecting to the power network through transmission lines for supplying the grid. Stand-alone or the off-grid systems are usually used to supply power to remote regions or for technical applications. In technical applications, the wind turbine capacities can differ from a few watts to about 50 watts. For the rural or remote regions, the capacity is up to 300 kilowatts, sometimes wind turbines combination with generators and sometimes use a storage system like battery system [8]. This stand-alone system is also used to provide power for pumping oil or water and for irrigation water.

1.3. Wind Power Potential

In the wind, the kinetic energy of air estimate by [15]:

$$E = \frac{1}{2} m v^2 \tag{1.1}$$

where v is the wind speed (m/s) and m is the total mass of the air (kg) calculated from Eq. 1.2.

$$m = \rho A v \Delta t \tag{1.2}$$

where ρ is the air density (1.225 kg/m^3). By writing the Eq. (1.2) into the Eq. (1.1),

$$E = \frac{1}{2}\rho A v^3 \Delta t \tag{1.3}$$

Therefore, the wind power can expressed as:

$$P = \frac{E}{\Delta t} = \frac{1}{2}\rho A v^3 \ \ [W] \quad \text{or} \quad P = \frac{1}{2}\rho v^3 \ \ [W/m^2] \tag{1.4}$$

The maximum power output is calculated from the following equation [14]:

$$P_m = \frac{1}{2}\rho A v^3 C_p(\lambda, \beta) \tag{1.5}$$

where A is the area swept by the rotor blades (m^2), C_p is the power coefficient of the wind turbine, λ tip-speed ratio, β is the blade pitch angle.

The power coefficient of wind turbine (C_p) and tip-speed ratio (λ) are given in Eq. 1.6 and Eq. 1.7, respectively:

$$C_p(\lambda, \beta) = \frac{1}{2}\left(\frac{98}{\lambda_i} - 0.4\beta - 5\right) exp\left(\frac{-16.5}{\lambda_i}\right) \tag{1.6}$$

$$\lambda_i = \left[\frac{1}{(\lambda + 0.089)} - \frac{0.035}{(\beta^3 + 1)}\right]^{-1} \tag{1.7}$$

$$\lambda = \frac{R\, w_m}{v} \tag{1.8}$$

where R is the radius of turbine blades, w_m is the angular speed of the rotor turbine.

Before starting the implementation of any project depends on the wind energy, the measured wind data must be analyzed because the wind speed density is vary from one region to another. In order to determine the wind speed probability distribution, there are several methods. Two analytical models which are commonly used are Weibull distribution and Rayleigh distribution.

Weibull distribution which is invented by Waloddi Weibull in 1939 is a continuous probability distribution. This distribution is commonly used in reliability engineering. The most general form to express of Weibull probability density distribution function is given by the two-parameter, which can be expressed as [16]:

$$f(v) = \left(\frac{k}{c}\right)\left(\frac{v}{c}\right)^{k-1}\exp\left[-\left(\frac{v}{c}\right)^{k}\right] \qquad \text{For } k>0 \qquad (1.9)$$

where f(v) represents the probability of a wind speed, k is the Weibull shape parameter (dimensionless), c is the Weibull scale parameter (m/s), and v is the wind speed (m/s).

Also, there are two forms of the Weibull distribution known as the three-parameter Weibull distribution and one-parameter Weibull distribution. For the form with the three-parameter, there is a parameter known as location parameter but it does not use and it's value usually equal to zero. For the form with the one-parameter, it takes the same form of the two-parameter Weibull distribution unless the shape parameter is known before and there is no need to be estimated. However, the studies prove that the two-parameter Weibull distribution gives the best fit for estimated probability distribution than the other methods and gives the nearest values of data when compared with the experimental data.

To calculate the cumulative distribution function by taking the natural logarithm of Equation (1.9) twice gives [16]:

$$F(v) = 1 - \exp\left[-\frac{v}{c}\right]^{k} \qquad (1.10)$$

To calculate Weibull parameters, four methods can be used which are Maximum Likelihood estimation (MLE), Maximum Product of Spacing (MPS), Weighted Maximum Likelihood estimation (w-MLE), and the method of moments (MoM). The most used method is Maximum Likelihood estimation, although the method does not give the best results to estimate the parameters of Weibull distribution when comparing it with other methods, it has given the best fitting parameters when the value of the shape parameter equal to one or more [17].

Rayleigh distribution is a continuous probability distribution for random variables and it is used for the life testing studies and the communication engineering. Rayleigh distribution probability density function can be expressed by the following equation [18]:

$$f(x) = \frac{x}{b^2} \exp[-\left(\frac{x^2}{2b^2}\right)] \qquad \text{For x >= 0, b > 0} \tag{1.11}$$

which (b) is the scale parameter.

The cumulative distribution function can be given by [19]:

$$G(x;b) = 1 - \exp(-\frac{x^2}{2b^2}) \tag{1.12}$$

1.4. Potential of Wind Energy in Iraq and Worldwide

Iraq has a high potential of wind energy, but the research and exploitation of this renewable and clean source still substandard. Iraq depends on fossil fuels to produce energy due to the availability and low price of this resource. While there is no interest to exploit abundant renewable energies that exist in Iraq except for some researches and experimentations to highlight this clean energy.

Iraq can be divided into three regions according to the wind speed probability. The first region represents 48% of Iraq that has wind speeds vary between 2-3 m/s, the second region represents 44%, which has wind speeds vary between 3.1- 4.9 m/s, and the third region represents 8% of Iraq, has relatively high wind speeds of more than 5 m/s [20].

Worldwide wind energy is distributed uniformly over the earth, as in Figure1.6 that shows an annual average of wind speed at 100 m height during 2007-2008. In general, the strongest wind found over ocean water in both hemispheres, significantly over the Southern Ocean, the North Atlantic, and the Gulf of Alaska. On the land, the Sahara desert, the southern tip of South America, the Himalayas, and central regions in North America are the regions with high wind speed. Wind speeds vary according to the seasons, for example in the Pacific and the Atlantic oceans because of low-pressure wind velocities are increased in winter to more than 12 m/s, while in the summer is much less [21].

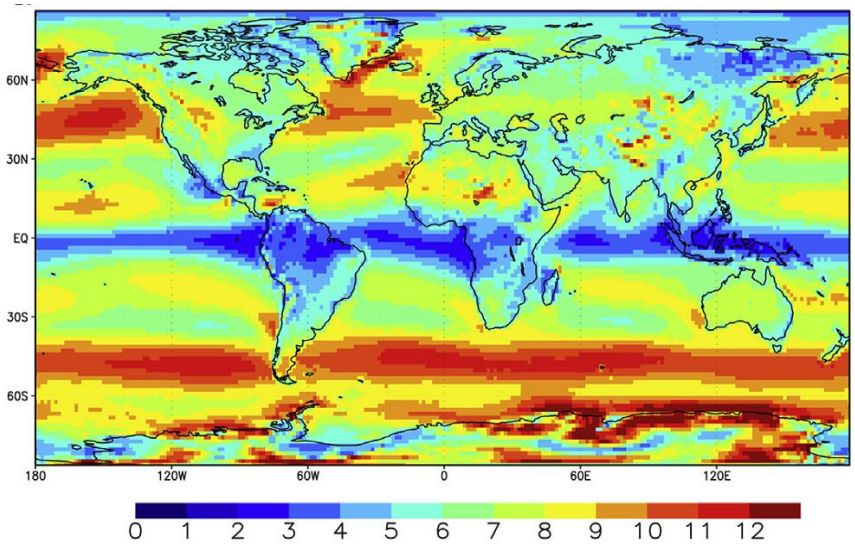

Figure 1.6 Distributions of Yearly Average Wind Speed (m/s) at 100 m in 2007-2008 [21]

At the last decades, the use of wind capacity has spread. The power capacity from wind energy source is growing continuously. For example, global wind-power capacity was 282 gigawatts (GW) at the end of 2012, and by the end of 2014 wind farms were operating producing more than 370 GW around the world; this rate has been increased to reach about 433 GW by the end of 2015. This rate of growth is expected to continue, the capacity expected to increase to about 537 GW by 2017, as shown in Figure 1.7. By the end of 2015, more than eighty countries have seen the wind activity commercially. The countries with more than 1000 MW installed capacity were 26 country including 17 country in Europe where four from them had more than 10000 MW [Germany with capacity of 44947 MW, Spain with 23025 MW, UK with 13603 MW, and France with 10358 MW], 4 countries in Asia [China with 145362 MW, India with 25088 MW, Japan, and Australia], 3 country in North America [US with 74471 MW, Canada with 11205 MW, Mexico], 1 country in Latin America which is Brazil, and 1 country in Africa which is South Africa [6].

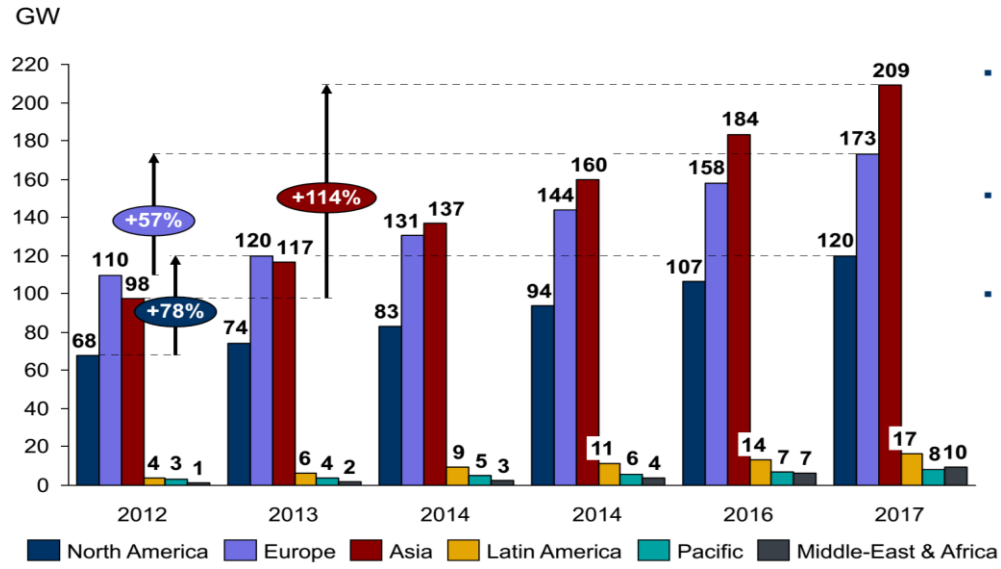

Figure 1.7 Projected Installed Wind Capacities by Regions (2012-2017) [11]

1.5. Background of Solar Energy

Solar energy which is a clean and the most abundant energy source for the Earth is transferred from the sun through space in the form of electromagnetic waves in straight lines. The rate at which solar energy reaches a unit area of the Earth called the "solar irradiance" or "insolation". The units of measure for irradiance are watts per square meter (W/m^2). Every day solar irradiance falls on the surface of the Earth and the amount of solar irradiance that received varies from location to another depend on: i) the time of day where the maximum radiation occurred at noon and less at the rest time of the day, ii) the season which depends on the location of the Earth of the Sun, iii) weather conditions, and iv) geographical location.

Where the spherical shape of the Earth makes the distribution of the incoming solar radiation not equal, the total daily radiation is maximum at the equator and decrease at the poles; that is why the Earth is warmer at the equator more than the poles. The atmosphere that surrounding Earth reduces the ratio of solar radiation that passes through it to the Earth by about 30% on a clear day to approximately 90% on a very cloudy day. The solar radiation that reaches the earth's surface is measured to about 1000 W/m^2 at sea level and is considered as a standard measure. The solar irradiance received by the Earth's surface divided into two types: solar irradiance, which reaches the Earth's surface directly without being diffused known as a beam or direct solar

irradiance, and a diffuse solar irradiance that could be absorbed, scattered or reflected because of the different weather factors. The sum of these two types, diffuse and direct solar radiation, is called global solar radiation.

Since BC, the solar energy has been used by utilizing glass and mirrors to concentrating the sun's heat for igniting fires. The first solar collector in the world invented by Horace - Swiss scientist - in 1767, he designed a rectangular box placed inside it smaller boxes which been isolated and the top of the boxes covered with glass to exposed to the sun, noticed the temperature increased significantly inside the boxes. In 1816, Robert Stirling built a heat engine that used later in the dish/Stirling system, depending on a concept of a solar thermal electric technology that concentrates the thermal of solar energy to produce power. Between 1860 and 1880, August Mouchet and Abel Pifre constructed the first solar-powered engines and used them for several applications. In 1876, William Grylls Adams and Richard Evans Day discovered that selenium had the ability to produce electricity when exposed to light. In 1891, Baltimore invented the first solar water heater used later for cooking or heating water. In 1908, William J. Bailley patented a solar collector with an insulated box, which can be used in the day and night for heating water. In 1947, the urgent need for energy during World War II in the United States made the passive solar buildings in demand. In 1955, Frank Bridgers designed commercial office which was the first commercial building in the world used passive design and solar water heating [22]. After the oil crisis in 1973, efforts seriously turned to find alternative energy sources, at the end of the 1970s; photovoltaic solar panels were producing more than 500 kW. In the early 1980s, developing countries began to finance solar energy programs and encourage the citizens to use rooftop solar systems in their homes, wherein 1983, photovoltaic production exceeded 21.3 MW.

Over the last thirty years, the industry of solar-cell has grown significantly. Today, needing energy in remote regions, make solar cells an effective solution and an alternative source of energy. There are several ways to harness solar energy: photovoltaic solar panels (PV) or called solar electric, solar heating and cooling, passive solar, and concentrating solar power (CSP). These technologies use the solar energy to provide electricity, heat, light, hot water, and cooling for homes, businesses, and industry.

1.6. Solar Photovoltaic

We can benefit from the sunlight to produce electricity via photovoltaic panels. Photovoltaic panels are devices that contain number of solar cells can absorb the sunlight and convert this light into electricity causing phenomenon known as photoelectric effect by using N-type and P-type semiconductor materials (like silicon). In 1839, Edmund Becquerel, a French scientist, invented the first photovoltaic cell when he observed production of a current and a voltage from a silver chloride electrode immersed in an electrolytic solution and connected to a metal electrode which exposed to sunlight [23]. In 1954, Photovoltaic technology known in the United States when Daryl Chapin, Calvin Fuller, and Gerald Pearson managed to develop the silicon photovoltaic cell, with 4% efficiency and later achieved 11% efficiency. Until the 1970s, solar cells manufacturing costs too expensive developed a design of thin-film photovoltaic cell with 15.9% efficiency made of cadmium telluride. In 1999, cumulative worldwide installed photovoltaic capacity reached to about 1000 megawatts [24]. For the present time, the biggest photovoltaic power station produces 579 MW installed in California.

1.6.1. Photovoltaic Systems

When PV cells are interconnected together, it forms PV modules with a power capacity up to several hundred watts. Modules consist of solar cells placed between two pieces of glass and framed. The module protects cells from damage, the environmental conditions, and makes handling with it easy, also provides a strong unit that can easily connect to other modules. When modules are interconnected together, constitute a system called array. The array, in conjunction with electrical equipment (like inverter, charge controller, battery bank, etc.), constitutes a photovoltaic system shown in Figure 1.8. It can be used to provide power for water treatment, water pumping, and electrical demand load for the user. There are several types of PV vary depending on the material that manufactured from it, as shown in Figure 1.9, the main formats commercially available are (1) flat-plate crystalline Silicon (C-Si) panels, (2) thin film and (3) CPV (concentrated photovoltaic). C-Si PV is prevailing technology in the markets today, most PV projects still dependent on this type despite the appearance of thin-film and other technologies. Best and most used types of C-Si PV are monocrystalline and

polycrystalline, where the efficiency of these types 13-19% and 11-15% respectively [25].

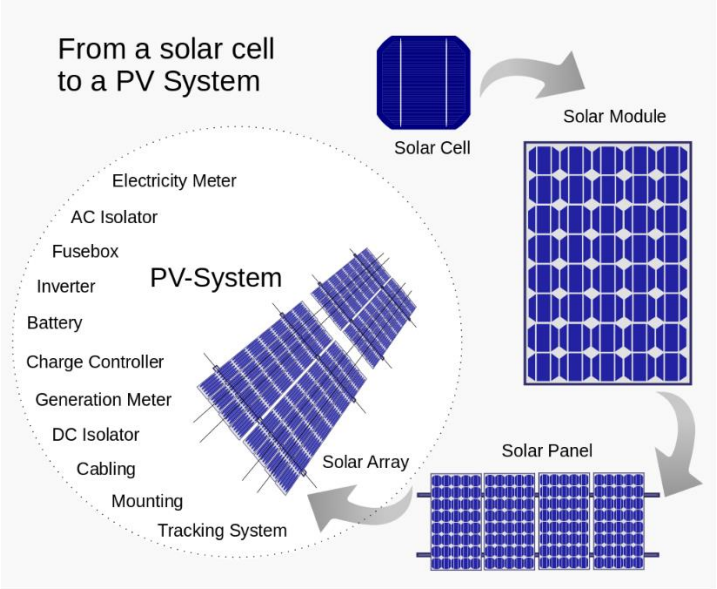

Figure 1.8. A solar cell and a PV system [26]

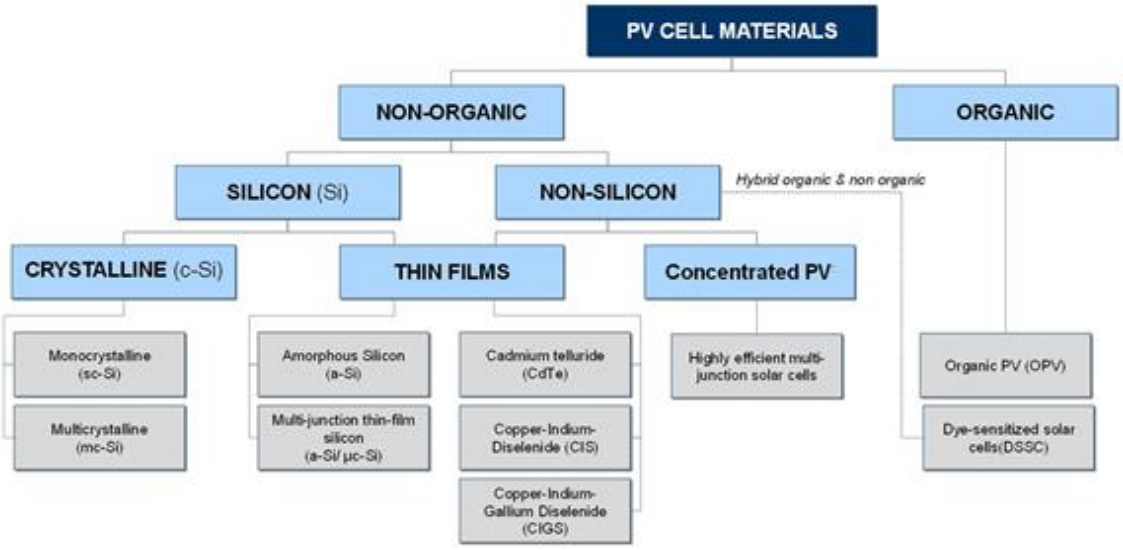

Figure 1.9. PV Cell Materials [27]

In terms of the operation of the solar panel system, PV systems can divide into two major categories: grid-connected systems, and stand-alone systems. The grid-connected systems that linked to the electric network are consisted from the PV array; inverter, distribution panel, and AC load. The excess of the energy goes to the electricity grid; these kinds of PV systems are using in residential, commercial, and industrial fields. The stand-alone PV systems or known as off-grid PV system that is work independent with no connecting to the electric grid. These systems can directly be coupled with loads of DC type to provide a current directly without a need to inverter or batteries, which mean this kind of system can operate during the sunlight hours only. Other systems that have a battery that acts as an energy store, charge controllers, inverter, and distribution panel, this kind can be powering DC and AC loads. These PV systems used to supplying electricity to rural and remote communities, in space, passive houses, and utilities.

For carrying photovoltaic arrays, there are different types of solar panel carriers, divided mainly into fixed carriers and movable carriers to track the movement of the sun such as (1) fixed PV mounting structures, (2) adjustable tilt angle, (3) horizontal single axis tracking, (4) vertical single axis tracking, (5) inclined single axis tracking, and (6) dual axis tracking. Research has shown that the sun tracking system is better than the fixed photovoltaic system, because of the marked increase in the output power of the sun tracking system.

1.6.2. Electricity Generation from Solar Photovoltaic Cells

The structure of PV cells composed of two layers; the first layer that carries a positive charge has a high concentration of hole or electron deficiency this layer is known as p-type, and the second layer that carries a negative charge has a high concentration of electron which known as n-type. These two layers placed together, n-type must be the top layer to expose to sunlight and the boundary between these two layers known as a P-N junction as shown in Figure 1.10. The materials that PV cells manufacture from must be semiconductor material and must be contaminated (doped), the most common material that used is Silicon which has a valence number of 4 and doped with chemical elements with a valence of 3 and 5, whereas p-type doped with boron and n-type doped with phosphorus.

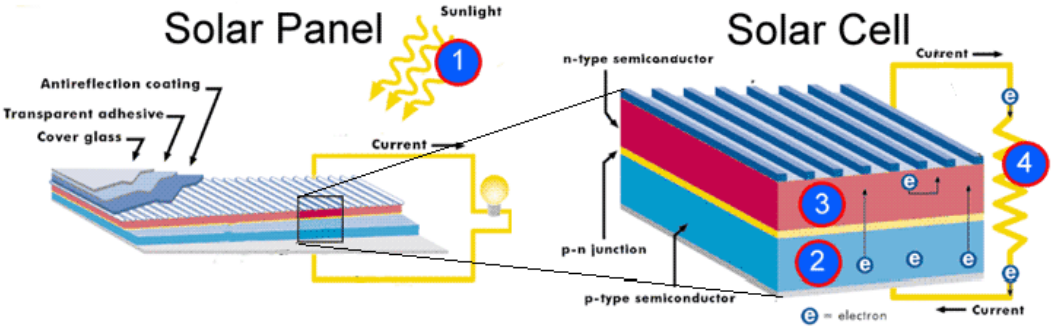

Figure 1.10. Composite of solar cell [28]

The sunlight falls on the cell, the incident photon excites an electron from n-type which diffuse the hole of p-type in the same time the excess hole in p-type diffused with the electron of n-type, electron will moves to the p-type zone and leaves positive ion cores in the n-type zone, while hole will moves to the n-type side and leaves negative ion cores in the p-type zone, this movement forming depletion region at the junction zone between n-type and p-type, then an electric field develops at this zone, this an electric field will make the charge carriers in opposite directions which cause an electric current. The electric current can be harvested when an external circuit interfaced to the semiconductor. The process of converting sunlight (photons) to electricity is known as the photovoltaic effect. At the current time, photovoltaic solar panels can convert the visible light spectrum and almost half of the ultraviolet and infrared light to usable energy.

1.6.3. Advantages and Disadvantages of Solar PVs

The first advantage of PV systems is that they can be used for a variety of requirements and applications, and they can be used by either connecting to the grid or stand-alone. PV systems are modules, easily expandable so that we can increase the size of the system (increasing the number of solar panels) according to need. They are safe to use, do not cause pollution and do not make noise during operating. The fuel is in abundance and free which is the sunlight. PV systems have long lifetimes and there is need to minimal maintenance if designed and installed properly. In addition, it creates independence in the energy field and do not cause harm to the environment making them attractive systems. On the other hand, the disadvantages of the PV systems are that

high cost of PV systems comparing with conventional energy sources and the efficiency of the system is affected by several factors (number of hours of sun brightness and weather conditions) where cloudy and dusty weather reduce the efficiency as well as cannot produce power during the night, and PV arrays require large surface area which may be an obstacle.

1.7. Solar Energy Potential in Iraq and Worldwide

Abundant sunshine and the existence of the open lands make that Iraq is one of the best locations for exploiting solar energy. But as a result of the wars, the energy sector has been destroyed in Iraq, and the government suffers from lack of investment. Because of these reasons, there is no project to take advantage of this vast energy.

While solar radiation changes throughout the year varying from 13 MJ/m^2 in December and January to 27 MJ/ m^2 in June and July, respectively, in the southern territories, it changes from 7 MJ/m^2 in December and January to 23 MJ/m^2 in June the northern territories [20]. Also, the yearly average of changes between the northern and southern territories can be considered as the average of changes in the central territory. Periods of sunshine varies from 2800 to 3300 hours per year that ensures to provide large amounts of solar energy, and the direct normal irradiation is ranges from 1800 to 2390 kWh/m^2/year as shown in Figure 1.11 [29].

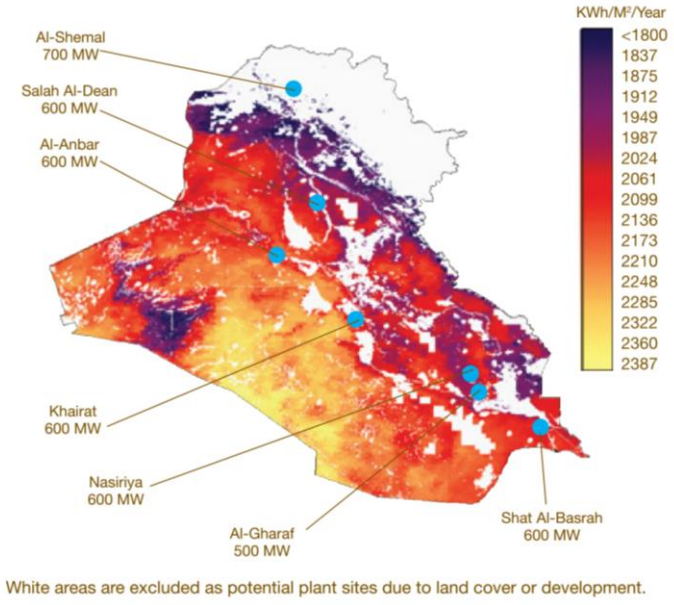

Figure 1.11. Iraq's Solar Irradiation [29]

These values give Iraq the qualifications to exploit the solar energy in several territories of its lands. Based on these values, most lands receive sufficient solar radiation, and the highest value is in Anbar which receives 2310 kWh/m^2/year. According to an analysis based on NASA data, using hybrid system which consists of solar plant and fossil fuel plants could reduce the emissions of carbon dioxide. For example if using 50 MW of concentrating solar plant with 300 MW fossil plants would reduce about 40000 metric tons of carbon dioxide emissions per year, compared with just 50 MW expansion of fossil fuel capacity.

Worldwide, solar PV development has begun in the 1970s, and in the beginning it was just spread in a few of countries. In 2001, the electricity that is produced from solar energy used to provide about 0.1% of the world's electricity. But since 2010 the capacity of photovoltaic cells around the world has been doubled from previous decades, and PV share of global electricity reached 11% in 2010, and it expected to rising up to reach 16% by 2050. In 2014, the total global capacity has grown at an average rate of 51% reaching more than 150 GW, which is expected to rise to about 230 GW by 2017. The largest photovoltaic power stations in the world as of 2015 are USA, China, and India, where the largest solar plants in the world are located in United States. The combined Solar Energy Generating Systems in California’s Mojave Desert has a capacity of 579 MW. Currently, China, Japan, and the United States are considered as the top three installers around the world. The U.S. is currently the third-largest solar market in the world. The amount of solar power installed in the U.S. has increased more than 23 times over the past eight years from 1.2 GW in 2008 to an estimated 27.4 GW at the end of 2015. Few countries in Europe have also constructed large PV systems of which Germany is the first and then comes Italy. In Asia, the most significant growth was in India (added 1.1 GW), followed by South Korea (0.4 GW) and Thailand (0.3 GW). Beyond Asia, about 16.7 GW was added worldwide, primarily in the EU (about 10.4 GW) and North America (5.4 GW), according to the "global status report 2014" of Renewable Energy Policy Network.

1.8. Literature Review of Iraq Renewable Energy System

AL-Riahi, et al. [30] presented a model of beam transmittance of the atmosphere to assess the direct solar transmittance for a clear day by applied the methodology using a

daily global radiation data for five years between (1991-1995) at Baghdad, Iraq. The statistical tests that used to evaluated the direct normal radiation and global radiation values were MBE (Mean Bias Error) and RMSE (Root Mean Square Error). By comparison, between measured and modeled values found that the difference does not exceed 5%.

AL-Riahi and AL-Kayssi [31] studied the mean of annual, monthly and daily global and diffuse radiation for Baghdad, Iraq. The maximum values of global radiation occur noon at peak point vary from more than 400 Wh/m^2 during the winter months to more than 800 Wh/m^2 during the summer months, the yearly cumulative global radiation was (2160–7000) MJ/m^2 per year. The annual total of daily diffuse radiation was about (600–700) MJ/m^2, while 2825 MJ h/m^2 is the highest of UV radiation that received during June and July and the lowest is received in December of 920 MJ h/m^2. This value of radiation constitutes 3.25% of the global radiation.

Al-Karaghouli and Kazmerski [32] designed a small project to using a photovoltaic solar system instead of a diesel generator to supply power to a remote health clinic in the south of Iraq by using the HOMER program to determine the best economic system for this clinic that has a daily load of 31.6 KWh. The best economic system to provide the required load consists of 6 kW photovoltaic panels, 3 kW inverter, and 80 batteries, with the cost of electricity $ 0.238 /kWh. The analysis showed that the price of electricity produced from the photovoltaic system was four times less than that produced by the diesel generator, besides the advantage of reducing the release of CO_2 and other toxic gases, which could prevent the release of 14927 kg/year, and 399.88 kg/year respectively.

Dihrab and K. Sopian [33] analyzed the potential of solar and wind energy in three cities in Iraq; Baghdad, Basra and Mosul. A hybrid renewable energy system connected to grid and consists of 5 MW of photovoltaic panels and 1 MW of wind turbines was assumed. System simulated by using Matlab and the results of this work showed that it is possible to use this renewable energy system to generate power for supply about 750 house in the rural or remote area with 30 kWh/day per house. The results demonstrated that the power output from PV modules was highest in Basra and followed by Mosul

and Baghdad. For the wind turbines power, it was highest in Basra, followed by Baghdad and then Mosul.

Kazem and Chaichan [34] analyzed and studied the situation of renewable energy in Iraq. The employments of renewable energy sources have reviewed, like wind, solar, and biomass. This paper provided recommendations for the utilization of these energy sources and found that the solar energy density in Iraq among the highest potential in the world, where the hourly solar intensity varied between 833 W/m^2 in June to 416 W/m^2 in January. Furthermore, they analyzed 23 stations to investigate the potential of wind energy and found that there is significant wind energy potential in several areas in Iraq where the approximate average energy per 24 hours of the day of 287.2 W/m^2. On the other hand, Iraq is rich in biomass, but the government has not paid attention in this sector.

Amori and Al-Najjar [35] designed a model of photovoltaic/thermal air collector, where a theoretical investigated of the thermal and electrical performance was applied. Matlab program used to simulate the model, which applied in two days; a wintry day for Baghdad province and a summery day for Fallujah province in Iraq. The results were 12.3% electrical efficiency, 19.4% thermal efficiency, and overall collector efficiency was 53.6% in the wintry day, while it was 9%, 22.8% and 47.8% respectively in the summer day.

Noaman Hussein et al. [36] presented a programming of PVSD (Off-Grid Photovoltaic System Design Software) by using Visual Basic program that works under Iraq conditions, verified with real data from solar power system which is off-grid photovoltaic system has been designed, installed and tested in Ministry of Science and Technology. The program can do the calculations of loads, photovoltaic modules, battery, and wiring, and it can analyze the output as an average energy generated per day and draw a graph for it.

Ali and Salih [37] developed a simple and friendly tool in Visual Basic Programming language V6.0 that can use to designing and sizing a stand-alone photovoltaic system, this tool defined as an execuTable Graphic User Interface bundle. This tool was developed to design photovoltaic systems in Iraq, and it has a feature that easily to use by persons who does not have an engineering or technical experience. Sizing the system

depending on the city specification and meet the requirements of the loads. The program proved its accuracy and effectiveness.

Mahdi et al. [38] designed 1.1 kW of a solar photovoltaic system with battery storage. The system has put under monitoring for nine months, calculated the average solar irradiance by using hourly data of 5.6 kWh/m^2/day, and the average power generated of 8 kWh/day.

In the study of Al-Hilphy [39], a comparison between incidence theoretical and practical solar radiation intensity during the years 2006 and 2011 at Basra province was studied. Solar radiation has been calculated on a horizontal surface and another case with tilt 30 degrees with the horizontal. The maximum intensity of solar radiation was 740 W/m^2. From the results, it can concluded that the solar radiation falling on the inclined surface is higher than falling on a horizontal surface, and the values of the intensity of solar radiation in 2011 were highest from those in 2006.

The aim of the study presented by Hiba A. Hasan [40] was to simulate and design an operating system to control the electrical loads depending on the amount of electrical power that obtained from renewable energy sources (the wind and solar), with the availability of grid power and batteries as backup sources. Furthermore, nominate each load with its turn-on to optimize the minimum cost of the total load consumption.

Mustafa J. Kadhim [41] brought out the study of renewable energy resources (solar and wind) in Basrah city in the south of Iraq, and creating a tool to construct the optimal design of a system mainly depending on these resources with its economic feasibility.

Abed et al. [42] presented a review of the renewable energy, energy status, and the possibility of using solar energy to the power supply in Iraq. Found that the net solar radiation in the south about 3-9 MJ/m^2.day, in the middle 2.8-8.5 MJ/m^2.day, while in the north about 3.5-8.25 MJ/m^2.day. They concluded that the criteria of using solar energy were the best solution for investment in a renewable power system, and it best than investing a lot of money in both oil and gas power generation.

Kazem et al. [43] reviewed the Iraq geography characteristics. Besides, a review of the causes of increased desertification that leads to increased sand and dust storms in the

country, focus on the study of causes dust, and its specifications, also analyzing the dust impacts on PV systems performance.

Jawad Khadim et al. [44] detected the monthly and yearly optimum tilts angle for fixed photovoltaic solar panel for each province in Iraq by using google earth program to determine the locations and a program in NASA website to calculate the tilt angles. Noticed that the tilt angle was changed from month to another varying from 1-8 degrees, and noted that the difference between the optimum yearly tilt angle for each province and the latitude of this province was between 2-3 degrees.

In the study performed by A.Hunaish [45], the sun tracking system has designed and experimentally implemented to follow the sun and maintain the Photovoltaic (PV) panel facing the sun all the time. The maximum power point tracking techniques that proposed have tested experimentally; the obtained results showed that the controller had a good response.

1.9. Literature Review of Solar-Wind Power Systems

A hybrid renewable energy system (HRES) is an application in which two or more of different renewable energy sources like (solar-thermal, solar photovoltaic, wind, biomass, hydropower, etc.) are integrated to supply electricity or heat, or both of them, increase system efficiency, and reduce the intermittency in supplied energy. The most utilized hybrid system is the hybrid that consists of photovoltaic panels and wind turbines, by integration these two energy sources in a proper combination for utilizing the capability of one source to overcome the shortcoming of the other. The utilization of different energy sources allows enhancing the efficiency of the system and reliability of the energy compared with systems involving only a single renewable energy source. Turbines with solar panels comprise an efficient hybrid system for extract energy from the wind and from the sunlight too. These renewable resources would supply power to remote regions and residential regions, and it can be used to produce hydrogen by using electrolyzers powered from the excess energy. Then hydrogen can be stored or used to run a fuel cell and other applications. The costs of these hybrid systems that based on electrolysis are still high but are expected to be reduced to the half in the next years [46]. Besides that, the costs of storage and transport could be avoided because of the hydrogen can be produced on-site [46].

A photovoltaic panels /wind turbine /fuel cell grid connected hybrid energy system was designed by Das et al. [47] with a dc-dc converter for maximum power point tracking MPPT and maximum power extraction from the hybrid system. 15 kW of a photovoltaic array and 20 kW of a wind turbine as primary energy sources designed to generate power and to avoid that power fluctuating in different weather conditions, while a 10 kW of a fuel cell has used as a secondary source. The maximum power that system can generate was 35 kW, while the minimum power was 10 kW. For simulated this system PSIM software program was using.

Ahmed et al. [48] designed a stand-alone hybrid energy system consists of photovoltaic solar panels, wind turbines, a fuel cell, where 1 kW of a wind turbine and 1 kW of photovoltaic solar panels was used as a primary energy system to produce electricity and 1.25 kW of a fuel cell as a backup system. The PSIM software program has been used to simulation the system, and the results were good as well as expected for the system performance.

Zhou et al. [49] described a stand-alone hybrid system consists of solar and wind energy with a battery bank. This system was compared with the photovoltaic system alone and wind turbines system alone, where found that the hybrid system is the best option for power supply. In addition, the study reviews optimum sizing, simulation, and control technologies for the system. Several types of optimization technologies have been discussed and have found that the artificial intelligence method can help operators, as part of the energy system, to reduce the cost of the system.

F. Caballero et al. [50] designed a hybrid energy system consists of photovoltaic panels and wind turbine to generate electricity in a remote region, this region depends on diesel generators to produce electricity which it needs for 2.26 million liters of diesel per year, where it cost a lot. The hybrid system assumed to connect to the grid (on-grid) without energy storage. The optimal sizing of this system was obtained by using HOMER software, where the initial cost of photovoltaic panels $ 4.07/kW and the initial cost of wind turbines $ 2.8/kW. Also, other cases have been investigated that study the feasibility of selling the excess power from the hybrid system to the grid, use it in other operations, or net metering where delivered the excess power to the grid and deduct the amount of energy that delivered from consumer bills.

Maouedj et al. [51] presented photovoltaic/wind turbines/battery hybrid system consists of 600W of PV, 1kW wind turbine, and 24V/1600Ah battery bank. This study discussed the measured data from PV modules subsystem, wind turbine subsystem, and from the load profiles. The system power has used for the operation of street lamps at night from 20:00 to 08:00 am, where found that the system needs to 2640 Wh per day to run the lights.

A simple sun-wind tracker hybrid system has designed by Rahimi et al. [52]. This hybrid tracker system is tracking the sun by using a system of two axes type, also using a wind tracker that exploits the wind potential for cooling the solar panels by using wind vane. This study compared the performance of the PV with/without sun tracker and wind tracker, it was evident that the output power with tracking system higher than the fixed system. The two-axis sun tracker system increased the amount of power generation 39.43% in a day when comparing with a fixed system. The amount of energy that collected from hybrid tracking system increasing by 49.83% compared with a fixed system, while the amount of energy in the hybrid tracking system increased 7.4% when it compared with sun tracker system.

Nguyen et al. [53] discussed how to minimize the cost of a hybrid system that consists of 1.8 kW solar photovoltaic panels and 15 kW of DFIG (Doubly Fed Induction Generator) wind turbine. This system has simulated via Matlab/Simulink program to find out the feasibility of running the hybrid system. The system uses sensorless Maximum Power Point Tracking (MPPT) for photovoltaic panels, where substituted the sensor of a turbine instead of the photovoltaic sensor to estimate the photovoltaic power, also eliminated the inverter of photovoltaic and compensated by using the inverter of the wind turbine. In this way, the power loss and the overall cost has reduced, besides of reducing the maintenance cost of this system due to using less number of converters and sensors.

Al Busaidi et al. [54] reviewed various photovoltaic/wind hybrid systems that used to generate electric power and verification of the best approach of the hybrid system by comparing the cost of the power output. Moreover, reviews the sizing techniques of the photovoltaic/wind hybrid system and the optimum methods that can be used to improve the system at the lowest possible cost. Found that both of Iterative and Artificial

Intelligence optimization techniques offer more precision and fast estimation comparing with the other methods. The study compared two cases to investigate the potential of hybrid renewable energy systems in Oman and found that the cost of energy (CoE) was 0.182 $/kW and 0.222 $/kW, which showed that the renewable energy systems are promising in this country

CHAPTER 2

HYDROGEN ENERGY

2.1. Introduction

At a time when countries of the world are seeking to reduce reliance on the use of petroleum as fuel, attention directed to other sustainable and less harmful sources such as hydrogen. Unlike Fossil Fuel, Hydrogen does not produce toxic emissions from the combustion that harm the environment on the contrary; the combustion products like water and heat are actually useful.

Hydrogen is the most abundant gas in the universe and in the earth’s crust. Free hydrogen exists in the solar atmosphere, stars, and in gas giant planets. But in the atmosphere of the earth its presence in free form is scarce, only 1 ppm (volumetric ratio), because of that hydrogen could not be found in its elemental form on earth but is combined with other elements as a component of raw materials, it can be found in the composition of water and organic materials like oil and wood. The proportion of its presence in the Earth's crust is about 0.9%.

2.2. The History of Hydrogen

Before the official discovery of hydrogen by Henry Cavendish in 1766, both Paracelsus (1500) and Robert Boyle (1671) had noted that when dissolving iron filings in dilute acid the resulting bubbles from this reaction were flammable, whereas Cavendish has gathered these bubbles resulting from the same reaction and discovered that it was a discrete material different from the rest of the gases calling it "inflammable air" [55]. Later he found that the result of combustion gas was water. In 1783, Antonio Lavoisier gave the name 'hydrogen' for the gas when he and Pierre-Simon Laplace confirmed Cavendish's finding that hydrogen produces water when burned. The name comes from the Greek origin 'hydro' meaning water and 'genes' meaning former. Together they mean

'water forming'. In 1898, James Dewar managed to liquefy hydrogen and produce solid hydrogen. In 1931, Harold Urey detected a second form of hydrogen named deuterium (symbol D or 2H) which is a hydrogen isotope that has a mass twice as that of ordinary hydrogen, it is used in the production of heavy water and can be involved in nuclear reactions which is why it is expected to be used in the future to generate clean nuclear power. In 1934, Ernest Rutherford, Mark Oliphant, and Paul Harteck managed to prepare tritium; another isotope of hydrogen, also known as hydrogen-3 (symbol T or 3H), It can be used in luminous paint, nuclear fusion reactions, chemical and biological labeling experiments due to its radiation activity [56].

After the industrial revolution in the nineteenth century, also known as the technological revolution, the world has seen rapid industrial development and the reliance was on fossil fuels as an energy source. After the oil crisis in the early seventies of the last century, governments and communities realized the importance of searching for alternative sources of energy. This triggered the spread of awareness campaigns encouraging the use of renewable energy.

The increase in population density around the world and the growing sophistication of technology causes an increase in energy demand. Burning billions of tons of fossil fuels whether from power plants or industrial facilities or transport leads to accumulation of the greenhouse gas (GHG) in the atmosphere such as carbon oxides CO and nitrogen oxides NOx and these gases are continuously causing global warming, The International Energy Agency (IEA) expected that in 2035 Gas emission will reach more than 37 GT of CO_2 gas which will result in Global warming of about 3.6 degree.

The 21st century has witnessed more reliance on renewable energies and growth of sustainable economy, in the near future global energy systems will depend on the gases in general and particularly on hydrogen as shown in Figure 2.1 [57].

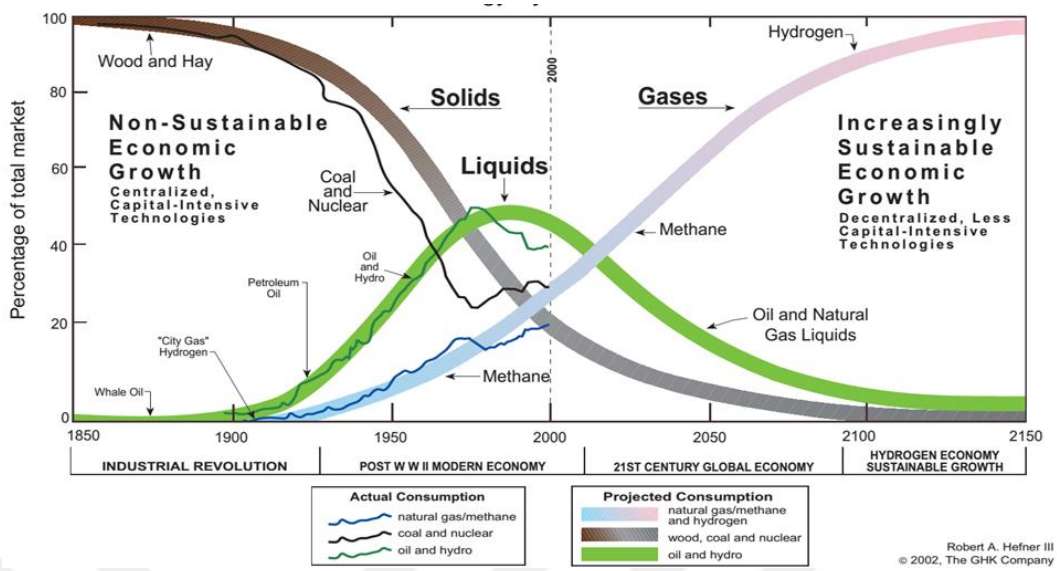

Figure 2.1 The Age of Energy Gases

2.3. Hydrogen Energy

Hydrogen is considered an energy carrier, it is a secondary energy source, which means it can be used to store, move and deliver energy. Hydrogen can be produced from primary energy sources using different methods, the produced energy can be used to generate electricity, heat, and as fuel to run machines like combustion engines and other applications. The energy yield by hydrogen combustion is about 120 kJ/g and this is considered 2.7 times greater than conventional fuels as shown in Table 2.1, where hydrogen has the highest value among the other various fuels [57].

For the near future, Hydrogen is a promising fuel, renewable, clean without toxic gases emissions. Thus, if its production costs can be reduced it is expected to become an attractive alternative source of energy, especially if produced from renewable energy sources like solar and wind energy, which will make it a competitor for fossil fuels.

Table 2.1 Higher and Lower Heating Value for Some Fuels [57]

Fuel	Higher heating value	Lower heating value
Hydrogen	141.8 kJ/g	119.9 kJ/g
Gasoline	47.5 kJ/g	44.5kJ/g
Diesel	47.5kJ/g	42.5 kJ/g
Methane	55.5 kJ/g	50.0 kJ/g

2.4. The Properties of Hydrogen

Hydrogen is the first chemical element in the Mendeleev periodic Table that has the chemist symbol H and its atomic number is one. Hydrogen is a diatomic molecule, colorless, odorless, univalent, and under standard conditions of temperature and pressure, it has a gaseous status. As an element, hydrogen structure consists of one proton and one electron and is considered as the simplest and lightest element. In this composition, it resembles the alkali metals containing one electron in orbit S, it also resembles the halogens that need one electron to reach the rare gas structure, which is helium, and thus constitutes a negative hydride anion. For this reason, in the periodic Table it was placed in two different groups at the same time, the first group for its similarity with the alkali metals, and in the seventh group containing halogens such as chlorine and bromine.

Hydrogen is lighter than air by 14.4 times, causes it to leak out of the atmosphere which why it is not present in pure form on earth, instead it is found only combined with other elements. As shown in Table 2.2 [58], hydrogen is non-poisonous, flammable within a wide range and has high explosion limits comparing with other fuels, its enthalpy of combustion is about -286 kJ/mol. Hydrogen has a density of 0.089 g/liter at 0º C and 1 atm in a gaseous status, and a molecular weight of 2.01594 g. Hydrogen has the lowest melting and boiling point, where liquefying at 252.77°C and solidifies at -259.2°C., as shown in Tables 2.3 and 2.4 [59].

Hydrogen is not reactive at normal temperature and it needs to stimulate by a proper catalyser. But it's highly reactive at high temperatures.

Table 2.2 Compare values of combustion limits between hydrogen and other common fuels

	Hydrogen	**Natural Gas**	**Gasoline Vapor**
Flammability limits	4-74%	5.3-15%	1.4-7.6%
Explosion limits	18.3-59%	5.7-14%	1.1-3.3%
Ignition energy (mJ)	0.02	0.29	0.20
Flame temperature (°C)	2045	1875	2197
Stoichiometric Mixture	29%	9%	2%

Table 2.3 The basic properties of hydrogen

Atomic number	**1**
Atomic mass	1.007825 $g.mol^{-1}$
Electronegativity	2.1
Vander Waals radius	0.12 nm
Energy of first ionization	1311 $kJ.mol^{-1}$
Group, period, block	1, 1, s
Electronic shell	$1s^1$
Ionic radius	0.208 (-1) nm

Table 2.4 The physical properties of hydrogen

Density (gaseous state)	**0.089 g/liter**
Molecular weight	2.02
melting point	-259.14 °C
boiling point	-252.87 °C
Auto ignition temperature	500-585°C
Flame temperature in air	2045°C
Internal Energy at NTP*	2648.3 kJ/kg
Specific volume at NTP	11.94 m^3/kg
Thermal conductivity at NTP	0.1825 W/mK
Viscosity at NTP	8.813E-5 g/cm-sec

* NTP: normal temperature and pressure 20°C, and 1 atm.

2.5. Hydrogen Production

Hydrogen is not available in a free form in nature, because of that we need production methods to manufacture it. Hydrogen can be produced from non-sustainable resources such as coal and natural gas, also from renewable resources such as water with power input from renewable energy sources like wind and sunlight.

2.5.1. Hydrogen Production from Fossil Fuel

Hydrogen is considered as an alternative energy option and a crossing towards a sustainable energy for the near future. Hydrogen can be produced by the most of the fossil fuels yet it is not renewable and produces almost the same quantity of CO_2 that is produced from direct combustion of the conventional fuel. All processes of H_2 production from this resource leads to the release of CO_2; as a result, CO_2 must be captured and stored (CCS) to obtain a sustainable production of hydrogen with zero-emission, which is needed for more energy. About 96% of the hydrogen produced is obtained from fossil fuels, as example natural gas reforming, while 4% of hydrogen is produced via water electrolysis [60].

The most common methods of producing hydrogen from fossil fuels are the reforming of natural gas and the gasification of coal. It can also be produced as a by-product from various processes such as catalytic reforming, and in petrochemical plants through off-gas reforming, from coke oven gas, and from ethylene crackers.

2.5.1.1. Hydrogen Production from Natural Gas

In the present time, hydrogen can be produced from natural gas by the following chemical processes: steam methane reforming (SMR), partial oxidation (POX), and autothermal reforming (ATR).

Hydrogen production via steam reforming methane (SMR) is the most economical and widespread technique among the present commercial processes. SMR is an endothermic reaction that involves reacting methane (CH_4) with water vapor and producing syngas, which is a mix of hydrogen (H_2) and carbon monoxide (CO). The heat is mostly provided by the combustion of some of the feed gas (CH_4). The chemical process typically happens at temperatures of 700 to 850 °C and pressures of 3 to 25 bar. The product gas contains about 12 % CO, which can be further converted, through the water-gas shift reaction, into H_2 and CO_2 as in equations 2.1, 2.2. The efficiency of SMR is around 80%- 85% for large-scale units and the cost of hydrogen from this process is between \$10-\$15/GJH_2, whereas for small units the efficiency is lower than 75% and the cost may exceed \$50/GJ[61].

$$CH_4 + H_2O + \text{heat} \rightarrow CO + 3H_2 \quad (2.1)$$

$$CO + H_2O \rightarrow CO2 + H_2 + \text{heat} \quad (2.2)$$

Partial oxidation (POX) of CH_4 is the process whereby CH_4 reacts with pure O_2 through the partial combustion to yield H_2 and CO. There is no need for external heat because the reaction is an exothermic as in equation 2.3. CO can be further shifted into H_2 and CO_2 through the water-gas shift reaction.

$$CH_4 + 1/2O_2 \rightarrow CO + 2H_2 + \text{heat} \quad (2.3)$$

Autothermal reforming (ATR) is a combination of both SMR and POX, The reaction is exothermic, the outlet temperature is around 950 to 1100 °C, and the gas pressure may reach to 100 bar. Also in this process, the CO produced is converted to H_2.

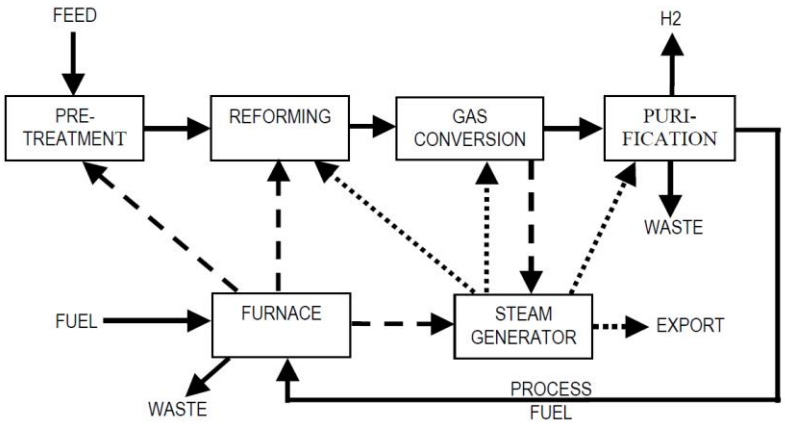

Figure 2.2 Schematic of SMR Process [62]

2.5.1.2. Hydrogen Production from Coal

Hydrogen can be obtained from coal through a number of gasification processes, such as: fixed bed, entrained flow or fluidised bed. Coal gasification process produces H_2, CO_2, CO, and CH_4. CO can be shifted to additional H_2 and CO_2 via water-gas shift reaction as in equations 2.4, 2.2. This reaction is endothermic, so it is needed for additional heat. The process preferred carried out under high temperatures in order to avoid formation of phenols, char, and tars.

$$C(s) + H_2O + heat \rightarrow CO + H_2 \qquad (2.4)$$

Coal gasification is more costly than the reforming of natural gas and it is more complex. But due to the availability of coal in many regions of the world, it makes attractive and motivates developed technologies to use it.

2.5.2. Hydrogen Production from Renewable Energy

The concern of using fossil fuel for producing hydrogen is the emitting of CO_2 and other emissions; this has a negative impact on the environment. Because of that, the

renewable energy resources are more tempting for hydrogen production. Hydrogen can be produced from biomass or from the splitting of water via various technologies such as water electrolysis, thermo-chemical water splitting, photo-electrolysis, high-temperature water decomposition, and photo-biological production.

2.5.2.1. Hydrogen Production from Water Electrolysis

Electrolysis is an electro-chemical process that separates water into its basic components H_2 and O_2 by using electricity. There are different types of electrolyzers depending on the material of electrolyte that can be used. Currently, electrolyzer concepts work on the same principle of fuel cells but in reverse mode. The main types of fuel cell are proton exchange membrane fuel cell (PEM or PEMFC) which works at (50°C-100°C, 15 bar) and has an efficiency that ranges from 30% to 50% , alkaline fuel cell (AFC) works at 70°C-100°C, and has an efficiency of around 60%-70%, phosphoric acid fuel cell (PAFC) works at 150°C-220°C, and has an efficiency of around 40%-55%, direct methanol or ethanol fuel cells (DMFC and DEFC, respectively) have the same conditions 90°C-120°C and a 20%-30% efficiency percentage, the high-temperature molten carbonate (MCFC) works at 650°C-700°C, and has an efficiency of around 50%-60%, and solid oxide fuel cells (SOFC) works at 800°C-1000°C, and has an efficiency of around 50%-60% [63].

The key parameters for electrolysis are efficiency and cost. According to IEA, electrolysis costs are above $\$30/GJH_2$ and is expected to drop under $\$20/GJH_2$ (including pressurization process) in the near future, assuming the cost of electricity at \$35/MWh and an 80% efficiency of the process.

In alkaline water electrolyzers, the electrolyte uses 20-30%wt of aqueous potassium hydroxide (KOH) solution. The typical operating conditions of these electrolyzers are temperatures about 70 to 100 ℃ and pressures in the range of 1 to 30 bar. The principle of the alkaline electrolyzer is shown in Figure 2.3, electricity passes through a cell and causes the decomposition of water to H_2 on the cathode and O_2 on the anode as we can see in the equations below.

Electrolyte: $2H_2O \rightarrow 2H^+ + 2OH^-$ (2.5)

Cathode: $2H^+ + 2e^- \rightarrow H_2$ (2.6)

Anode: $2OH^- \rightarrow 1/2O_2 + H_2O + 2e^-$ (2.7)

Total reaction: $H_2O \rightarrow 1/2O_2 + H_2$ (2.8)

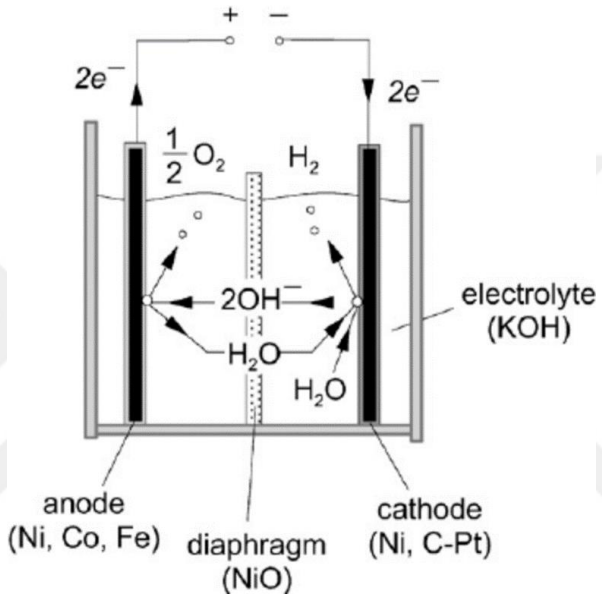

Figure 2.3 Principle of Alkaline Electrolyzer [63]

PEM water electrolysis is a promising technology. The principle of PEM electrolysis is shown in equations 2.8 and 2.9. PEM electrolyzers use iridium oxide or ruthenium oxide catalyst at the anode and platinum at the cathode, the electrodes separated by electrolyte uses a solid acidic polymer membrane. The membrane is so thin it allows high pressure to operate, and its solid nature makes the design simpler than alkaline electrolyzers. PEM works at a high current density, which reduces the costs of the operation and produces high purity hydrogen gas. The disadvantages of this kind are the short lifetime of the membrane, low capacity, and high cost [64].

Anode: $H_2O \rightarrow 1/2O_2 + 2\,H^+ + 2e^-$ (2.9)

Cathode: $2H^+ + 2e^- \rightarrow H_2$ (2.10)

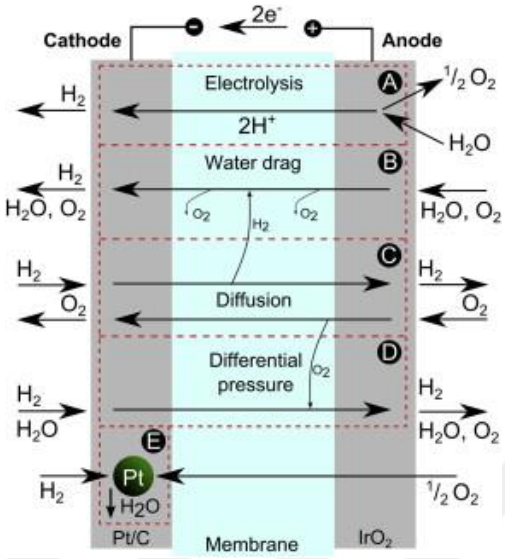

Figure 2.4 Principle of PEM Electrolyzer [64]

The oxide electrolyzer cell (SOEC) has the same principle of the solid oxide fuel cell (SOFC) which depends on high-temperature fuel cell technology but works in reverse mode as shown in Figure 2.3. SOEC operates at a range of temperature around 700 to 1000 ^{0}C and uses solid oxide at electrolyte to produce H_2 by splitting the steam water. Because of the high temperatures, SOEC can achieve high efficiency [65].

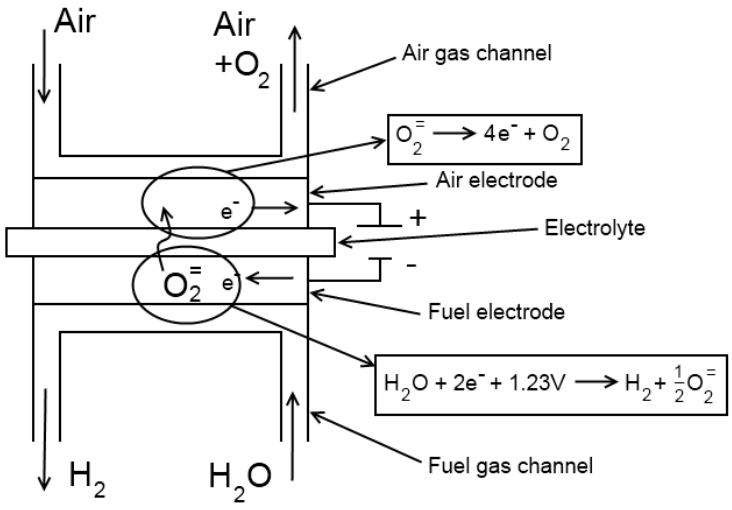

Figure 2.5 The Principle Work of Solid Oxide Electrolyzer Cell [65]

Photo-electrolysis (photolysis) is the combination of photovoltaic panels system with electrolysis system in a monolithic single device. This system requires a semiconductor with a specific bang gap to be able to extract the electrons from water and decompose water directly into H_2 and O_2, without having to resort to further steps for electrolytic process, which is lead to reduce the cost of hydrogen production and raising the efficiency. The process requires the photo-catalysts to motivate the reaction. There are some technical challenges in this method such as the stability of the semiconductors, and their band gaps, which should be above 1.6-1.7 eV and not exceed 2.2 eV [66].

Photo-biological production is an appealing method to produce H_2. It is a process of growing microorganisms under exposition to sunlight, there are types of these photosynthesis organisms that have the ability to use the energy of photons harvested from sunlight to move electrons from water and produce H_2, a few examples are encaryotic algae, photosynthetic-bacteria, and cyanobacteria (blue-green algae). Photosynthetic-bacteria show a promising applied system for the near term. This method needs more research to understand the metabolic and genetic properties of H_2 production; on the other side, it offers a promising solution for H_2 production from renewable resources. As in equation 2.11, the first step of process is photosynthesis and the second step is H_2 production, which the reaction can catalyze by, hydrogenises or nitrogenises as shown in equation 2.12.

Photosynthesis: $2H_2O \rightarrow 4H^+ + 4e^- + O_2$ (2.11)

Hydrogen Production $4H^+ + 4e^- \rightarrow 2H_2$ (2.12)

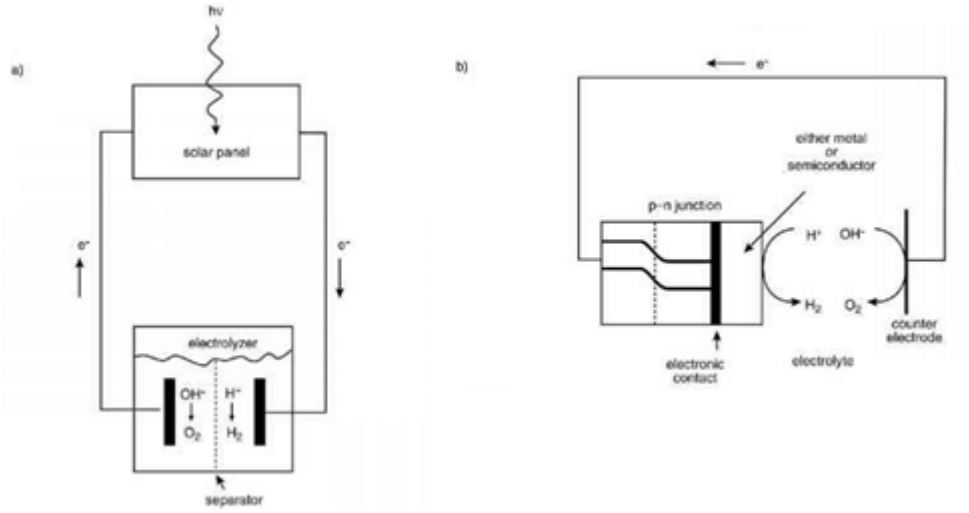

Figure 2.6 Photo-Electrolysis Configuration [66]

High-temperature decomposition: a high-temperature used for decomposing water into H_2 and O_2, the reaction occurs at temperatures around 3000°C, a small percentage of water splitting to H_2 and the rest could be recycled. The process is endothermic; the required heat can be supplied from solar energy or nuclear energy. This process has a high efficiency of above 50% and may contribute to reducing the costs of H_2 production. But there are technical challenges like corrosion due to high temperatures, separation process, heat storage, and heat exchangers.

The thermo-chemical splitting is a chemical reaction driven thermally to split water to H_2 and O_2. Thermal-chemical cycles occur at temperatures above 2200°C, This process can achieve low costs and high efficiency for H_2 production. The obstacles that face this method are the high temperature required which in its turn makes separating H_2 from O_2 difficult, in addition to corrosion problems.

This method is suitable as long as the heat is supplied from renewable sources such as solar energy or from nuclear energy, corrosion-resistant materials can also be used. The common cycles are magnesium chloride (Mg-Cl), bromine-calcium (Br-Ca), copper-chlorine (Cu-Cl), and sulphur-iodine (S-I) which is considered the most promising process, they can occur at temperatures under 950°C as described in equations 2.13, 2.14, 2.15.

(850 °C): $H_2SO_4 \rightarrow SO_2 + H_2O + 1/2O_2$ (2.13)

(120 °C): $I_2 + SO_2 + 2H_2O \rightarrow H_2SO_4 + 2HI$ (2.14)

(450 °C): $2HI \rightarrow I_2 + H_2$ (2.15)

Total: $H_2O \rightarrow H_2 + 1/2O_2$

2.5.2.2. Hydrogen Production from Biomass

Biomass can be exploited to produce H_2 by using energy and water. There are two common methods to produce H_2, gasification and pyrolysis of biomass.

Gasification of biomass is a mature technique. It is similar to the coal gasification but, this method does not increase CO_2 in the atmosphere like the gasification of coal. The process occurs at relatively high temperatures of around 727°C, and partial oxidation occurs to biomass particles producing gas and charcoal, then from this charcoal, we can produce H_2, CO, CO_2, and CH_4 as in equation 2.16. Biomass absorbs CO_2 during the growth and releases it through the gasification, thus, the CO_2 capture and storage must be applied. Large-scale plants can be installed to reduce CO_2 concentration. Currently, small-scale plants have been installed for H_2 production and its efficiency is about 50-60%.

Biomass + heat + steam $\rightarrow H_2 + CO + CO_2 + CH_4$ + light and heavy hydrocarbons + char (2.16)

For increased H_2 production, steam reformed applied on the gasses that produced, and water-gas shift can be applied to shift CO into CO_2. For minimizing tar that formed during the process, there are three methods: proper operation and control, a favorable design of gasifier, and using additives and catalysts [67].

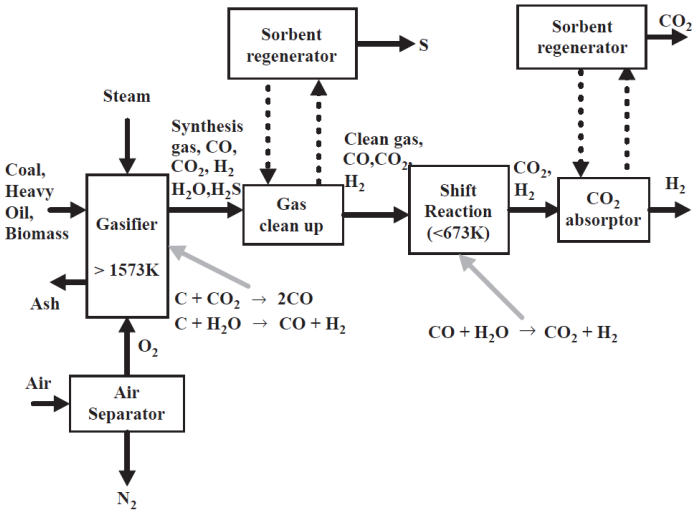

Figure 2.7 The Process of Biomass Gasification [67]

A new gasification method is known as "Hydrogen Production by Reaction Integrated Novel Gasification" (HyPr-RING), where a single reactor integrates water-H_2 reaction, water-gas shift reaction, and absorption pollutants [68] Figure 2.8. The reaction is exothermic and occurs at 650-700°C equation 2.17 describes the reaction.

$$C + 2H_2O + CaO \rightarrow CaCO_3 + 2H_2, \qquad \Delta H_{298} = -88 \text{ kJ/mol} \qquad (2.17)$$

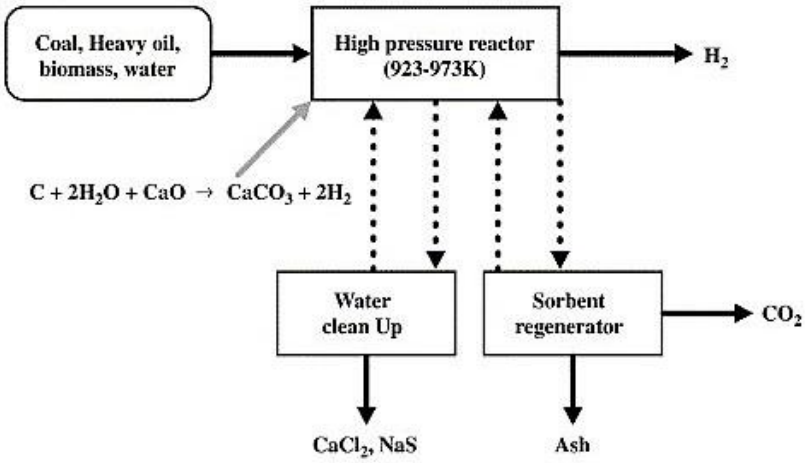

Figure 2.8 HyPr-RING Process [69]

Pyrolysis of biomass this reaction occurs at a temperature between 377-527 °C, a pressure of around 1-5 bar and in isolation from the air. The products are liquid oils, charcoal, solid and gaseous compounds. Steam reformed reaction and water-gas shift reaction applied on the gases to produce further H_2 and improved the process. When flash pyrolysis occurs in higher temperatures, H_2 could produce directly as in equations below:

$$\text{Biomass + heat} \rightarrow H_2 + CO + CH_4 + \text{other products} \quad (2.18)$$

$$CH_4 + H_2O \rightarrow CO + 3H_2 \quad (2.19)$$

$$CO + H_2O \rightarrow CO_2 + H_2 \quad (2.20)$$

Biomass gasification is more favorable than the pyrolysis method for hydrogen production. In addition, it is competitive with SMR from methane. According to the DOE if the prices of methane reach $10/GJ this will make biomass gasification less costly.

2.5.3. Hydrogen Storage

Hydrogen is presently a useful form that stores energy and can reuse or export it off-grid. The main challenge for using H_2 is the storage. Various storage techniques have been suggested, and a lot of researches and attempts underway to develop more economic hydrogen storage methods to achieve higher efficiency. Generally, hydrogen can be stored in three forms: gas, liquid, and solid [70,71].

Hydrogen in a gaseous form can be stored using high-pressure vessels such as composite storage tanks. It is a safe, available way, well designed and does not need a heat exchanger. The disadvantages of these tanks are the need of a high pressure of about 350-700 bar to compress H_2, high cost, and low H_2 density. Another way that is available to store H_2 is glass microspheres, H_2 fills up at high temperature (300 °C) and high pressure (350-700 bar), and has gravimetric energy density above 5 wt% H_2.

Liquid H_2 can be obtained via liquefying cooled H_2 to the cryogenic temperature (-253 °C) at an ambient pressure, then storing it in thermally insulated cryonic tanks.

Practically the gravimetric density for this process is 20 wt% H_2. The difficulties of this approach are the energy that is required for the liquefaction process, and the difficulty to keep H_2 in such a low temperature without risking evaporation or leak.

Another method to storage liquid H_2 is by constituting it in other solutions for example $NaBH_4$ solution as in equation 2.21, the gravimetric density is 10.9 wt% H_2, the challenges are the high cost of $NaBH_4$, and the reaction produced $NaBO_2$ which needs regeneration or removal. In addition, organic liquids that have the ability to recharge could store liquid H_2 in an indirect way. The first step is dehydrogenating organic liquid at temperatures 300-400 °C to produce H_2 then the second step is transportation, in third step liquid H_2 will be re-dehydrogenated. The gravimetric density of this method is 6.1 wt% H_2, and has disadvantages in its toxicity. It is also not safe during transport.

$$NaBH_4\ (l) + 2H_2O\ (l) \rightarrow 4H_2\ (g) + NaBO_2\ (s) \qquad (2.21)$$

For the solid H_2 form, H_2 can be stored in materials by contributing to their structure or can be adsorbed on the surface of the compound if it has a high surface area; it then becomes possible to release it at a specific temperature and low pressure. This technology is a promising method because of its safety and efficiency. Mainly the materials can be classified into carbon-based and other high surface area materials, chemical hydrides, and rechargeable hydrides.

Carbon-based high surface area materials are like activated charcoals, nanotubes, graphite nanofibers, and other high surface area materials are like metal oxide frameworks (MOFs), and clathrate hydrates. These materials are able to adsorb H_2 on their surface and then release it by adding heat. This method is still under research to understand the nature of the materials and improve the performance. The challenge that faced this method is the high temperature that is required to store and release H_2 from these materials, but MOFs prove their ability to store H_2 at low temperatures, which makes it a promising technology. Currently, the research seeks to increase the potential of H_2 storage capacity in these materials and release an adequate quantity of H_2 under reasonable operating conditions.

Chemical hydrides: in this technology, chemical reactions occur where H_2 is stored and released such as hydrolysis reactions, thermal reactions,

hydrogenation/dehydrogenation reactions, and alcoholysis reactions. Hydrolysis reaction occurs in H_2O-reactive chemical hydrides such as NaH, LiH, MgH_2, CaH_2, and $LiAlH_4$. For example the reaction of magnesium hydride (MgH_2) with water which forms magnesium hydroxide $Mg(OH)_2$ and H_2, whereas $Mg(OH)_2$ must be regenerated, this method has a storage density of about 5-8 wt% of H_2.

Rechargeable hydrides can store H_2 through absorption, where H_2 atoms can be incorporated into atoms in the compound, then by adding heat desorption process will occur where H_2 can be released. There are different types of rechargeable hydrides (alloys and intermetallic, nanocrystalline, and complex hydrides). The complex hydrides are the most promising technology for the future, such as borohydrides $(BH_4)^-$, alanates $(AlH_4)^-$ and amides $(NH_2)^-$. For example alkali metal aluminum hydrides (alanates) the most known compounds are ($NaAlH_4$, $LiAlH_4$, $Mg(AlH_4)$, and $Ca(AlH_4)$) which has light weight and high storage capacity, but the decomposition process needs high temperature and due to this high temperature it becomes difficult to rearrange the mechanism of the elements.

2.5.4. Hydrogen Applications

Hydrogen can be used as energy through fuel cells or as fuel by combustion in turbines and engines. By using hydrogen, we can run all the means of transport, the operation of plants, and heating instrumentation in buildings. Gaseous hydrogen can transmit energy efficiently over long distances through transport pipes, and hydrogen relying upon the fuel energy or machinery that supplies for electricity, and drinkable water [71]. Hydrogen has the highest specific energy content of all conventional fuels, and when it is used in different fields, the final output is almost pollution-free energy with water as the main by-product. In addition, H_2 has the advantage of being flexible as energy [72]. Hydrogen is currently regarded as one of the alternative energies for the 21st century. It will contribute considerably to the reduction of the environmental impact, the improvement in energy security, and a creation of new energy industries.

As a chemical element, H_2 has a variety of applications and uses. It can be used for the synthesis of ammonia and nitrogenated fertilizers, refining and desulphurization (hydrogenation reactions, hydrodesulphurization), hydrogenation of hazardous wastes (PCBs, dioxins), synthesis of methanol, ethanol, dimethyl, food preparation, chemical

plants, alternative fuels synthesis by Fischer–Tropsch (FT) synthesis, gas to liquid (GTL) synthesis technology [73].

2.6. Literature Review

2.6.1. Literature Review on Hydrogen Production from Wind Energy

Dutton et al. [74] presents a stand-alone wind-hydrogen energy system, using two types of electrolyzers for hydrogen production. Tests conducted on electrolyzers to determine permittivity volatile of energy inputs from wind turbines and the ability to smooth the output energy. The results showed no operating problems for electrolyzers when given the intermittent power. In addition, it found that wind turbine with 10 kW rated power and 10 kW electrolyzer rated power that is simulated for one year period can generate hydrogen volume of 8992 Nm^3 at wind speed 8 m/s.

Honnery and Moriarty [75] examined the use of wind as energy generator by locating a 2 MW wind turbine on each km^2 of land; wind can supply 516 EJ of energy annually and by constraining falls to 359 EJ. Total potential of annual energy EHT as hydrogen was 179 EJ for the constrained case. With comparing the wind energy with the energy utilizing from photovoltaic they found that peak energy intensity for wind turbines is more than twice that of solar PV and the energy generation costs for solar PV are higher than equivalent wind turbine systems.

Khan and Iqbal [76] this paper presented a stand-alone wind-hydrogen hybrid energy system. The simulations presented the system behavior by using Matlab, and the dynamic interaction between the components of the system has been considered. The wind energy conversion system WECS generated about 6.5 kW at high wind speed >12 m/s, excess energy goes directed toward the electrolyzer to produce hydrogen. At low winds, the polymer electrolyte membrane (PEM) fuel cell delivers the power in addition to the losses in the converters.

Zolezzi et al. [77] carried out a survey of the possibility of making use of the wind resource at Magellan, Chile. Then using that energy to produce hydrogen by means of electrolyzer, the hydrogen volume must be reduced by liquefaction for transportation and used in the various fields of energy and industrial applications in the center of the

country. The results showed that hydrogen could reach high competitiveness in the next years compared with fossil fuels.

Javier Pino et al. [78] in this article a wind-hydrogen system to produce electric and hydrogen was analyzed, which most of the models consider nominal operating conditions; this study analyzed the influence of using the real behavior of the equipment in location by analyzing the influence of the electrolyzer operating temperature and the wind turbine power curve in annual hydrogen production. It is showed that current simulation tools present significant errors in calculations when they are compared with simulation results using mathematical models, when real power curve for wind turbine was used the annual hydrogen production was 5046.3 kg, when the manufacturer power curve was used the annual hydrogen production was 6742.8 kg and for the power model curve the annual hydrogen production was 5385.3 kg.

The costs of hydrogen, hydrogen production quantities using wind energy conversion system (WECS) was investigated by Genc et al. [79] for five different locations in the central Anatolia in Turkey. Four different WECSs (300, 600, 1300 and 2300 kW) were considered and rated power at different hub height. The maximum value of hydrogen production was 6288.59 kg H_2/year, while the minimum value of hydrogen production was 1665.24 kg H_2/year. They found that electrolyzers with low rated power would be able to produce more hydrogen than the electrolyzer with higher rated power.

Genc et al. [80] investigated the hydrogen production potential and costs by using wind/electrolysis system in Pınarbaşı-Kayseri. Their results brought out that the electricity production costs are decreased with the increase of turbine hub height. And also, the maximum hydrogen production quantity was obtained 14192 kgH_2/year.

Zhang et al. [81] presented a model that aggregates electrolyzers within the wind turbine to produce hydrogen which is established from utilizing curtail wind energy was studied, the study found that the hydrogen price balance point is 0.29 \$/Nm^3 that is produced from this model, which is smaller than the cost of the second model that takes electricity directly from grid electricity which was 0.425 \$/Nm^3.

The study of Sarrias-Mena et al. [82] deals with four different electrolyzers models for hydrogen production, these models were integrated with a variable speed doubly-fed

induction generator (DFIG) wind turbine model. The simulation of these systems have been done by using Matlab/Simulink, the aim was to develop a comparative analysis of these electrolyzers models. The results have shown a satisfactory operation between the (DFIG) wind turbine and all the electrolyzer models.

Siyal et al. [83] have been made a preliminary assessment of hydrogen production potential from wind energy in each 1 km^2 grid cell through the land area of Sweden, which can be exploited to reduce the usage of gasoline fuel and carbon dioxide emissions in the transport sector of this country by 50%. Vestas-112 wind turbine, which has 3MW rated power and 90m hub height was used, they found that the total wind potential that can be achievable to hydrogen energy could be (860 TWh/year) and the hydrogen mass production is (25580 ktons/year).

The study prepared by Douak and Settou [84] considered four types of wind turbines with different output power to produce hydrogen, and the output energy of the wind turbines was estimated for three different regions in Algeria. The maximum hydrogen production was (113.99 tH_2/year), while the minimum production was (76.12 tH_2/year), but this value of production has achieved minimum cost of unit energy per kWh with 0.0132 $/kWh.

Valverde-Isorna et al. [85] highlighted the effectiveness of the use of hydrogen in the on-grid wind/hydrogen hybrid system to reduce wind intermittency. The researchers endeavored to develop a comprehensive mathematical model to present a real scale for wind/H_2 systems. The Hydrogen Office (HO) wind/hydrogen energy system had been chosen for modeling this system.

2.6.2. Literature Review on Hydrogen Production from Solar Energy

Hollmuller et al. [86] aimed to describe a manually controlled photovoltaic PV-hydrogen production and storage system for a residential home at Zollbrück in Switzerland. The study presented evaluation of the system's performance and simulate its potential for energy storage. The system comprises PV array consist of 162 solar panels connected in series with 7.4 kWp capacity, with hydrogen production 0.32-0.95 Nm^3/h. estimated percentage of PV power usable for energy storage was 43%, while

energy losses was 57% losing in control unit, auxiliary energy, electrolyzer, and purification.

Kazim and Veziroglu [87] suggested that the oil production will start to decline in the UAE in the future; causing a huge gap between production and the demand for energy and creating a serious problem by the middle of this century, this will impact on the economy which depends fundamentally on fossil fuels. To overcome this problem a solar-hydrogen energy system to produce hydrogen has been proposed. This study has provided economical and technical analysis for fossil fuel production, and the methods of replacing it by hydrogen, which is an efficient, cleaner, and renewable energy source.

Thomas and Kelly [88] tested a number of solar panel modules according to the different materials they are manufactured from, such as: monocrystalline, multicrystalline, layered amorphous silicon and crystalline silicon, and single-crystal silicon cells; they aimed to test the best productivity for solar hydrogen production. The modules have been connected to electrolyzers to produce hydrogen by splitting water, where two types of electrolyzer were tested: alkaline electrolyzer and proton exchange membrane (PEM) electrolyzer. The results found indicated found that the PEM electrolyzer was more efficient. In an effort to simplify the system and reduce the cost; the system connected in two methods: DC-DC converter (DDC) and direct connection optimization (DCO), where in this way converter DC-DC and inverter have been canceled and the electrolyzer connected directly with the PV modules. To overcome the problem of getting the voltage level that the electrolyzer needed without resorting to the use of a converter DC-DC when using the DCO method; PV modules were designed with the required number of solar cells to obtain the optimum voltage. As a result, the circuit resistance decreased and the efficiency of the system has increased.

Hua Li et al. [89] presented three different energy storage technologies used with three stand-alone photovoltaic power systems: single system comprising from photovoltaic and battery, single system consisting of photovoltaic and fuel cell, and a hybrid system comprising from photovoltaic, fuel cell, and battery. The work evaluated the storage capacity and the efficiency of the three systems, and found that the hybrid photovoltaic/fuel cell/battery system achieved higher efficiency and lower cost compared with other storage systems.

Amao et al. [90] performed an effort to produce low carbon fuel like hydrogen gas. This study seeks to develop an artificial leaf to produce hydrogen from solar energy based on artificial photosynthesis. The device consists of a chlorophyll derivative chlorin-e6 (Chl-e6) as a photosensitizer, platinum nanoparticle as a catalyst, and a viologen as an electron carrier molecule that is immobilized on a thin layer of silicone gel, in the existence of NADPH as electron donor. The results showed that hydrogen production increases with the increasing time of solar radiation, 6.8×10-8 mol were produced during three hours of exposure to the device to radiation.

A concentrated photovoltaic unit coupled to an electrolyzer has been used to estimate the potential of hydrogen production for different cities in Algeria in the study presented by Boudries [91]. Two types of concentrators were considered: a Fresnel mirrors-photovoltaic concentrator and a parabolic trough-photovoltaic concentrator. The results were about (0.14-0.19) kgH_2/m^2.day and (0.10-0.17) kgH_2/m^2.day for both types respectively, that makes the Fresnel reflector more important than parabolic trough reflector for hydrogen production in this system.

Boudries et al. [92] determined the optimal design of PV energy system for powering a CEVITAL hydrogen production unit, which is at the floating glass-manufacturing unit by using HOMER software. Results had shown that the use of sun tracking for PV system could improve the viability of system and found that using a north/south tracking could reduce the cost of the system by 21%, while using a two-axis tracking could slash it by almost of 50%. In addition, the using of concentrated photovoltaic cells offer more viability for the system where it needs less land than conventional cells and provide large-scale production of hydrogen.

Zafar and Dincer [93] considered a hybrid energy system consists of photovoltaic/thermal-fuel cell (PV/T) to generate electricity, heat, and hydrogen. The electrical power goes directly for consumption while the excess electricity goes to operate the electrolyzer that produces hydrogen, and then the generated hydrogen is used as fuel to power fuel cells that can produce electrical power when there is a shortage of electric energy supply from the hybrid system, at the same time produces heat and drinkable water. This study indicates that using the emitted heat from the PV/T

system and emitted water from the fuel cell can improve the overall system energy efficiencies.

Giuseppe Mura et. al. [94] designed a house powered by photovoltaic cogeneration solar collectors; this system was intended to meet the electricity and thermal demands with using heat pump cycle for winter heating and summer cooling, electrolytic cell for the hydrogen production and fuel cell to produce electricity by using the accumulation of hydrogen in periods of low availability of solar energy. The analysis showed positive results but the cost was high.

Motalleb et al. [95] discussed the energy system in a passive house (a house building with passive solar technology materials that can absorb, release, and store the energy of the sun), the house is not connected to the grid. The design was simulated using Matlab/Simulink that completely depends on using solar and hydrogen energy. They found that the passive house provides energy by up to 90% compared to the existing houses and reduces carbon dioxide emissions by a range between 50-65%.

Jacobsson et al. [96] compared between different approaches of solar devices uses for hydrogen production which were: photoelectrochemical (PEC) cells and photovoltaic (PV) electolyzers in differences and similarities, the experimental investigation found that the concepts of these devices can be changed by a simple change in the physical device configuration, so it can consolidate the concept of the devices under the unified concept of photo driven catalysis (PDC-devices).

Yilmaz et al. [97] presented a review of the available technologies for hydrogen production from solar energy. The methods consist of photoelectricity, solar electricity, photobiological generation, concentrated solar thermal energy and thermochemical processes are discussed and compared with each other to determine their pros and cons. They found that the hydrogen production based on solar energy produces low emissions of GHG; because of that, it is one of the effective methods that are used to produce hydrogen.

The study of Sellami and Loudiyi [98] presents a practical study of hydrogen production using electrolyzers supplied with power by photovoltaic solar panel. The study included a comparison between two types of alkaline electrolyzers one with sodium hydroxide

(NaOH) electrolyte and the other with potassium hydroxide (KOH) with the same concentration (3M) and under the same conditions of temperature and pressure. The variables of temperature and pressure are the most effective on electric demand of electrolyzer and thus affect the efficiency of hydrogen production, at high temperature electrolyzer need fewer amounts of energy but at the same time the electrical efficiency will decrease, while at the high pressure the demand of energy decreases at temperatures between 25 and 90^0C. With watching the electrolyte behavior and its effect on the efficiency of hydrogen production found that the current of KOH electrolyzer is higher than in NaOH electrolyzer, that means the electrical resistance of KOH electrolyzer is lower than in NaOH electrolyzer, and the amount of hydrogen produced by the KOH cell is more than that produced by the NaOH cell.

Dalapati et al. [99] investigated the design of photoelectrochemical cells (PECs) for water splitting process and hydrogen gas evolution. Platinum is usually the metal that is used in the counter electrode, but in this study the researchers replaced it with earth-abundant in hydrogen evolution test, tungsten oxide (WO_3) and iron-oxide (Fe_2O_3) as electrodes and aluminum alloyed iron silicide (FeSi(Al)) as auxiliary electrode . The comparison of the results with commercial platinum electrode showed that the earth-abundant like iron-silicide have highly stability and durability as well as Platinum, furthermore the silicide materials have the potential for low cost PECs that are used in solar hydrogen unit, because of that it can be used instead of Platinum.

Bhattacharyya et al. [100] studied and analyzed the feasibility and performance of the electric system when combined with renewable energy sources; it presents a preliminary design of stand-alone solar photovoltaic energy system that provides the alkaline electrolyzer with necessary electricity to produce hydrogen. The results showed that theoretical cell potential increases with increasing pressure when the temperature is constant, while decreases with increasing temperature under known pressure. Hydrogen production rate is influenced by the variation of the solar radiation rate and temperature variation, the project is facing problems in terms of the cost needed to buy wide land for the project and the costs of installing solar photovoltaic panels.

2.6.3. Literature Review on Hydrogen Production from Hybrid Renewable Energy System

Agbossou et al. [101] investigated the the electricity generation via a hybrid renewable energy system of 10 kW wind turbine and a 1 kW photovoltaic solar array. Surplus energy from the hybrid system is used to produce hydrogen via electrolysis, hydrogen production rate was 1 Nm^3/h at 5 kW input for the electrolyzer. PEM fuel cell is used in this system to produce electricity; renewable energy was intermittent, by using produced hydrogen as fuel.

Gosselink [102] made a research on the production of sustainable energy. Shell discovered and developed an efficient and compact catalytic conversion technology CPO (catalytic partial oxidation) can convert gaseous hydrocarbons to synthesis gas (a mixture of carbon monoxide and hydrogen). It also discovered that liquid hydrocarbons could be converted by using CPO, followed by a number of other process, into hydrogen and CO_2. The CPO technology will enable the conversion of bio-fuel and conventional fuel to hydrogen that can be used for fuel cell applications.

Stojic et al. [103] experimentally tried to use ionic activators in the electrolytic of hydrogen production process in order to reduce the energy consumption in the electrolyzer, it has been using ethylenediamine complexes of cobalt, tris(trimethylenediamine) cobalt chloride complex, and tris(ethylenediamine) cobalt chloride complex as activators, it used it either single or combined with the Na-molybdate. It resulted reduce in consumption energy more than 10% for every mass unit of hydrogen.

Agbossou et al. [104] presented that the Hydrogen Research Institute (HRI) had developed a stand-alone renewable energy system based on hydrogen production and storage. It is a control system with power conditioning devices, consisting of a 10 kW wind turbine generator and 1 kW photovoltaic array. Hydrogen was produced in a 5 kW electrolyzer and the electricity was produced in a 5 kW fuel cell by using stored hydrogen. They also developed a renewable energy system that had a 10 kW programmable power, which was used to simulate the typical renewable energy patterns when there is insufficient power accessible from renewable energy sources.

Mills and Al-Hallaj [105] presented a hybrid system of photovoltaic/wind turbine working with diesel generator and testing to replace the diesel generator with fuel cell based on hydrogen and simulate the hybrid system to demonstrate its effectiveness. In this system, the fuel cell was utilized to provide energy when the renewable energy sources are not enough, and batteries were used as backup. In this study, the researchers used Hybrid2, which is a software program that is utilized to estimate long-term performances. The results demonstrate that energy produced from the system bypass the load by 160% during one year.

Ando and Tanaka [106] proposed a concept for hydrogen production, which was a simultaneous production system for hydrogen and hydrogen peroxide by using electrolysis; they discussed the possibility of obtaining electricity from solar energy and applying it to this system. In this process, the electrolyzer produces hydrogen gas on the cathode and hydrogen peroxide on the anode without any reaction that generates oxygen gas on both electrodes. The system has a possibility of producing the substances at lower cost than traditional production technique, but with low efficiency that needs to improve.

Levene et al. [107] presented an analysis to determine the potential of hydrogen production from solar and wind energy sources in the United States, supposing a system of photovoltaic/wind/electrolyzer will determine the amount of hydrogen that can be produced and if it is enough to meet the requirements of vehicle fueling. The results demonstrated that the highest potential of production was of 106000 million kg of H_2 in Texas, while the lowest potential of production was of 5 million kg of H_2 was in Washington D.C. The analysis includes the amount of electricity required to produce H_2 and showed that at 54-67 kWh/kg electrolyzer to get the hydrogen at a cost less than $ 3.00/kg the cost of electricity must be between $0.04 - $0.055 /kWh. The challenges still are to identify typical economical and technical systems to supply renewable energies to refuel stations.

Shakya et al. [108] presented a stand-alone photovoltaic/wind hybrid renewable system to produce electricity, and discussed the feasibility and cost of the production and storage of hydrogen via excess power from the system, they found that the storage of excess power in the form of H_2 instead of batteries is a better alternative. The system

used the stored hydrogen to produce electricity via diesel generators that having the ability for using H_2. The studied region (Cooma) has an average annual solar radiation of 1784 kWh/m^2 and wind energy of 932 kWh/m^2. The system has been simulated by using TRNSYS 15.2.10. The results showed that 52% of the cost of the system was for the electrolysis process. In addition, the lifecycle cost of photovoltaic/electrolyzer system of $382/GJ of H_2 was less than the cost of photovoltaic/wind hybrid system.

Meng Ni et al. [109] presented a review of recent hydrogen production methods and the useful renewable energies, and valuation of their integration for hydrogen production to supply energy in Hong Kong. This paper reviewed solar, wind, and biomass energy potential. They found that wind turbines and photovoltaic panels hybrid system connected with electrolyzers is a promising technology to produce hydrogen. Hydrogen production from biomass found that thermochemical processes are more appropriate than biological processes for the geographical lineaments of Hong Kong.

Wang et al. [110] simulated a stand-alone model of hybrid energy system by using MATLAB/Simulink, consisting of wind turbine, photovoltaic, fuel cell and electrolyzer. The PV panels and wind turbine are considered as primary sources to provide power and fuel cell with electrolyzer as a backup system. The system is designed to provide power to five houses and could be expanded where it could easily be integrated with other energy sources. In order to verify the performance of the system under different situations collected weather data and load profile for the allocated region were utilized.

Sopian et al. [111] used wind/photovoltaic PV hybrid energy system for hydrogen production and used HOMER software for estimating the optimal design of the system for an annual wind speed of 3 m/s and an annual average solar energy of 5.2 kWh/m^2/day. Twelve batteries were used to store the energy from the hybrid system then used to supply the power to 1 KW electrolyzer, while hydrogen produced was stored in the 60 kg storage tank. The optimum size integrated was 2 kW PV, 1kW wind turbine with electrolyzer and storage tank. The hydrogen annual average was 0.144 kg/day, and total hydrogen was about 53 kg/year with initial capital cost of 30000$.

Ratlamwala et al. [112] used solar energy combined with absorption cooling and electrolyzer for the production of hydrogen and cooling based on weather data for Abu Dhabi city. The highest value of rate of heat output was 14.8 kW and the rate of power

output 0.58 kW both for PV/thermal system area of 10 m^2, while the amount of hydrogen produced was about 7.8 kg -10.7 kg.

Calderon et al. [113] developed a test-bed stand-alone photovoltaic/wind turbine renewable energy system depending on the hydrogen storage. The excess energy that was produced from the hybrid system was used in the electrolyzer to produce hydrogen by water electrolysis; a metal hybrid system has been used for hydrogen storage. The stored hydrogen was used in a fuel cell to generate electricity. The energy efficiency and loss of the diverse components of the system has been determined.

A hybrid wind–photovoltaic system was accomplished for the aim of hydrogen production by using electrolyzer by Khalilnejad and Riahy [114]. Real data for solar irradiation, ambient temperature and wind speed at Sahand, Iran were taken to analyze this system in three various states by using just a wind turbine system, or just photovoltaic panels or a hybrid PV/wind as a power source, hydrogen was produced of 8297, 4592, and 10462 mol respectively; the results show that the hybrid system is more beneficial.

Posso and Zambrano [115] calculated the potential production of H_2 by water electrolysis supply with electricity from solar energy as a primary source or by using mini-hydroelectric and wind energy. The total H_2 that was produced could cover the energy requirements of the rural population of Venezuela. The calculation of the Higher Heating Value (HHV) used, gave a total production result of 2.073×10^{10} kg of H_2/year.

Two hybrid systems of a PV/wind/Battery-based hybrid system and a PV/wind/fuel cell FC-based hybrid system have been analyzed by Maleki and Askarzadeh [116]. For estimating an optimum sizing for the systems, four different types of artificial intelligence (AI) techniques were evaluated. The cost result showed that the PV/wind/FC system was lower than PV/FC or wind/FC systems.

2.6.4. Literature Review on Hydrogen Production from other Energy Sources

Duu-Hwa Lee [117] considered three energy models for hydrogen production: input-output (IO), linear programming (LP) and compuTable general equilibrium (CGE). The Taiwan general equilibrium model-clean energy (TAIGEM-CE) model is dynamic type

of CGE, which was used in this study for simulating the development of renewable energy sources for hydrogen production in Taiwan. TAIGEM-CE model take into account the price competition between conventional fuels and renewable energy sources. According to this study, the geometric annual rate of hydrogen by using wind energy will increase in 2040 by 15.14%, followed by bio-hydrogen by 14.29%, and solar energy by 13.79%.The competition between nuclear energy and renewable energy sources for hydrogen production found that nuclear energy is not competitive like the renewable energy sources.

Chang et al. [118] proposed two systems: an innovative Bio-Hydrogen Integrated Renewable Energy System (BHIRES) based on integration of biomass fermentation device and renewable energy consists of wind turbine WT, photovoltaic panels PV, electrolyzer, fuel cell (FC), control device, and storage device. BHIRES produced hydrogen, electricity, and heat. In this system, hydrogen was produced from biomass fermentation and water electrolysis, while FC supplied heat and power. The second system is a WT/PV/Hydrogen hybrid renewable energy system. They compared the energy use and the cost for these two systems also the capability of power provided and the cost of power production were investigated. This study showed that the BHIRES could provide energy at a lower cost than the WT/PV/Hydrogen hybrid renewable energy system.

Rahmouni et al. [119] investigated hydrogen production from the geothermal system by electricity production with capturing and storage of CO_2. The system consists of two subsystems: the first was the geothermal system for electricity production using CO_2 as a fluid that transmits heat; the second part was an electrolysis system. The annual electrical energy produced by the system was 8.5 GWh, and produced about 22 kg/h of electrolytic hydrogen. The costs of hydrogen production was 8.24 \$/kg H_2, while this costs will decrease to 3.85 \$/kg H_2 with imposed carbon tax, which means a decrease of 46% when environmental costs were included.

Yilmaz et al. [120] investigated a binary cycle geothermal power plant that provides energy to a PEM water electrolyzer for hydrogen production. Thermo-economic analysis, and the impact of geothermal water temperature on the electricity cost and cost of hydrogen production were investigated, the results showed that the costs increased

when geothermal water temperature increased. The rate of hydrogen production was 0.0253 kg/s, and the electricity cost and cost of hydrogen production were 0.0234 $/kWh and 2.366 $/kg H_2, respectively. The results can conclude that the geothermal water temperature as a renewable energy is a good option for producing hydrogen.

Klimova et al. [121] discussed the high temperature gas-cooled nuclear reactor (HTGR) and Direct Reduction Iron (DRI) technology with producing hydrogen accompanied with other gases. The secondary circuit of nuclear plant includes methane conversion to synthetic gas as a mixture of CO and H_2; they used a methane converter instead of electrolyzer for hydrogen production because of the high energy consumption of the electrolysis process.

CHAPTER 3

WIND AND SOLAR ENERGY POTENTIAL IN IRAQ

3.1. Introduction

Iraq has an enormous potential of energy, and it was one of the first Arab countries to research and study about sustainable energies such as wind and solar energy [122-125] to find out the potential of renewable energies. Researchers found that many of the regions have a good average of wind speed and high solar radiation, which is suitable to utilize for energy production.

In this thesis, three different cities are taken for the study of the potential of the wind and solar energy. Table 3.1 explains the geographical locations of the selected cities, which are meteorological stations. Wind speed and solar radiation data are obtained from the Ministry of Agriculture/Department of Agricultural Meteorology, consisting of daily data measurements in 5 years period from 2010 to 2014.

3.2. Geographical Location of Iraq

Iraq is one of the West Asian countries overlooking the Persian Gulf, bounded by Turkey in the north, Saudi Arabia and Kuwait in the south, the Islamic Republic of Iran in the east, and Jordan and Syria in the west. Iraq is located between the longitude 38° 45` and 48° 45` and between latitude 29° 50` and 37° 22`, and has an area of 438320 km^2. Iraq represents a diverse mixture of geography. It can be divided into four main territories: northeastern highlands representing 20% of the surface of Iraq, uplands region consisting of approximately 10%, alluvial plain which extends from Salah-ad-Din to the Persian Gulf and represents about 30%, and desert plateau which represents nearly 40% and extends to the west of the Euphrates River.

Iraq's climate is influenced by annual movements of the high pressure at subtropical zone and low pressure of mid-latitude zone, and by based on Köppen climate classification; there are three featured climate regions [126]:

- Subtropical Desert which is near to the subtropical high-pressure zone, extending from the Arabian Gulf coast far south at Basra to the desert of Syria.

- Subtropical Steppe represented in the upland area north of Baghdad.

- Dry Summer Subtropical, in the northern mountain areas.

The aim of this thesis is to study the potential of renewable energies in the different regions of Iraq for production of electricity and hydrogen. Stations that are selected for study are located in three different provinces: Basra in the southern, Wasit in the east and Anbar in the west of Iraq. Figure 3.1 shows the location of studied regions.

Figure 3.1 Map of Iraq

3.3. Energy Sources in Iraq

The energy sector in Iraq has a main role in the future and stability of the country. Iraq’s energy sector can be divided into three sections: oil, water resources, and electricity. Oil

considered as one of the most important energy resources in Iraq as more than 80% of the primary energy mixture is from oil. The rest depends on gas while a small percentage depends on water resources. Iraq is in third place in the world as oil exporter and in the fifth place as largest oil reserves. Also, it is in the thirteenth place for gas reserves. Currently, Iraq produces 3 million barrels of oil per day (bbl/d) and the country has plans to double its oil production by 2020 that will contribute to the prosperity of the national economy.

For water resources, 60% of it comes from outside of Iraq through Tigris and Euphrates rivers; Iraq is currently suffering from water scarcity due to upstream countries, the lack of rainfall, and poor quality of water infrastructures.

The electricity sector is not efficient in Iraq and is one of the main obstacles for the development of the country. The citizens are still suffering from the shortage of electricity. Electric stations depend on fossil fuels (oil and gas), and, even though fossil fuels are available but the country suffers from a lack of power because of the wars and conflicts. Energy sector was damaged heavily and suffered from disrepair over the decades since the Iraq-Iran war from 1980 to 1988 and the first Gulf war led by the United States in 1991 that led to a huge destruction of infrastructure. This continued with a period of international sanctions and then the second Gulf war in 2003 led by United States with coalition forces. At present, the electricity sector has seen some improvements but it is not significant. In 2011, only 60% of demand has been provided. While the peak demand is 15 GW, only 9 GW of net power was available.

To fill shortage of electricity, Iraqi families depend on diesel generators that are either private or through joint generators in the residential neighborhood. These generators play an important role to provide electricity even though they have high cost and are a source of air pollution.

The consumption of fossil fuels in energy production leads to increase pollution and increase greenhouse gas emissions. While CO_2 emission from the electricity sector was only 700 CO_2/kWh, the emissions from consumption fuel have tremendously increased in recent years according to the IEA. CO_2 emission has doubled as seen by the data. It was 72.9 million tons of CO_2 (Mt) in 2004 and it has risen to 141.0 Mt of CO_2 in 2014. Therefore, it is a necessity to transform fossil fuels to renewable or alternative energy

sources such as solar, wind, and biomass energy. The Iraq government must provide integrated energy strategy to increase oil production, develop renewable energy, and make use of new resources of water.

3.4. Wind Potential in Iraq

Wind energy is seen as an alternative source since it is more convenient and less costly for electricity production. Iraq is in seventh place of the wind speed rates in the Arab homeland. The geographical distribution of wind power in Iraq has varies according to time, locations, and speeds varying throughout the year between one the station and the other. Wind speed and direction is affected by many factors such as the geographical location of the country, water bodies, topography, air masses, and weather systems affecting the climate of Iraq. In general, the southern regions have higher wind speed than the rest of the regions.

The Weibull distribution function was given in Eq. 1.9. The two Weibull parameters of the wind speed distribution function, the scale parameter c and the shape parameter k are calculated from the wind speed data for the selected stations using the mean wind speed standard deviation method. They can be given as in Eqs. 3.1 and 3.2 [127]. Figure 3.2 shows the values of c and k and illustrates the Weibull distributions that are obtained.

$$c = \frac{\bar{v}}{\Gamma\left(1+\frac{1}{k}\right)} \tag{3.1}$$

$$k = \left(\frac{\sigma}{\bar{v}}\right)^{-1.086} \qquad (1 \leq k \leq 10) \tag{3.2}$$

where $\bar{v}$ is mean wind speed, σ is the standard deviation. They can be estimated by using Eqs. 3.3 and 3.4.

$$\bar{v} = \frac{1}{n}\left(\sum_{i-1}^{n} v_i\right) \tag{3.3}$$

$$\sigma = \left[\frac{1}{n-1}\sum_{i=1}^{n}(v_i - \bar{v})^2\right]^{0.5} \tag{3.4}$$

where n is the number of hours of specific period.

All data have been obtained at 3 m height above the ground level. The k values vary from 2.32 to 2.50, while the range of c is between 2.65 and 3.71 m/s. The average wind speed at the height of 3 m for the selected cities shows that while Basra has the highest value, Anbar has the lowest value.

For studied cities, wind speeds are calculated at different heights by using logarithmic law [128] as expressed in Eq. 3.5:

$$v = v_0 \left[\frac{\ln z/z_s}{\ln z_0/z_s}\right] \tag{3.5}$$

where v is the wind speed to be estimated at required height (z) (which is at height 50, 80, 100, and 120 m), v_0 is the wind speed that is recorded at anemometer height (z_0=3m), z_s is the surface rugosity scale which taken as 0.15 based on the terrain land in the studied cities.

Table3.1 Geographical Specification of Selected Cities in Iraq

City	**Latitude (N)**	**Longitude (E)**	**Altitude (m)**
Basra (Burjisiya station)	30° 29`	47° 06`	65
Wasit (Suwayra station)	33° 01`	44° 82`	27.74
Anbar (Dwar station)	33° 46`	43° 03`	58.33

Average wind speeds at different heights for studied cities are shown in Figures 3.3, 3.4, 3.5. Wind speed varies from one city to another. Basra has the highest values which reached to 15.758 m/s at 120 m height, while Wasit and Anbar have convergent averages that reached to 11 m/s at 120 m height for daily average wind speed as shown in table 3.2. The monthly average wind speed calculated for selected cities at four different height 50, 80, 100, and 120 m, showed that at 50 m, the estimated monthly average wind speed varies between 4.7 - 9.5 m/s in Basra, 4 - 6.68 m/s in Wasit, and 3.3 - 5.8 m/s in Anbar.

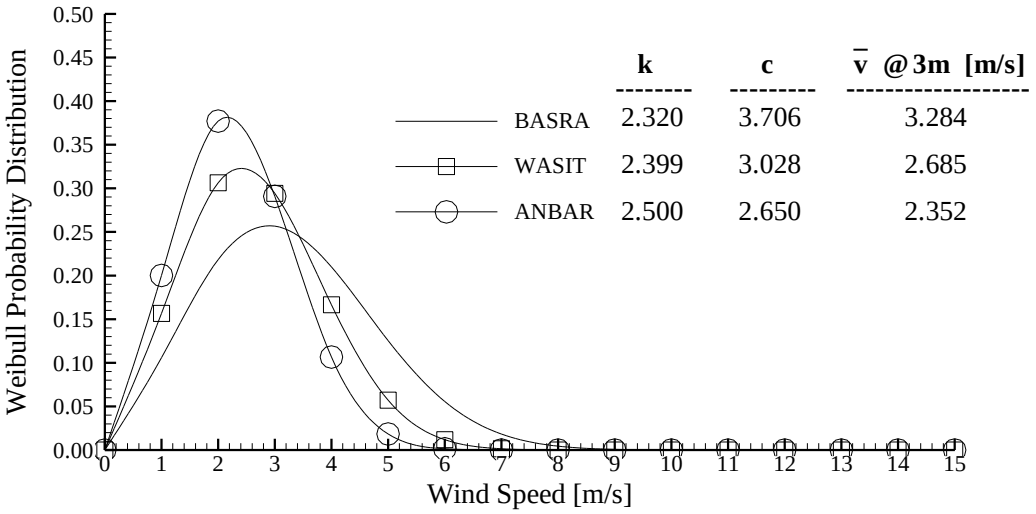

Figure 3.2 Annual Average Weibull Probability Distribution Function for the Period of 2010-2014 in Basrah, Wasit, and Anbar

Table 3.2 Maximum and Minimum Daily Average Wind Speed at Studied Cities

Height(m)	50		80		100		120	
Wind speed (m/s)	Min.	Max.	Min.	Max.	Min.	Max.	Min.	Max.
Basra	2	13.69	2.14	14.8	2.217	15.32	2.28	15.758
Wasit	2.11	9.56	2.278	10.33	2.359	10.7	2.42	11
Anbar	1.94	9.57	2.097	10.34	2.17	10.71	2.23	11.01

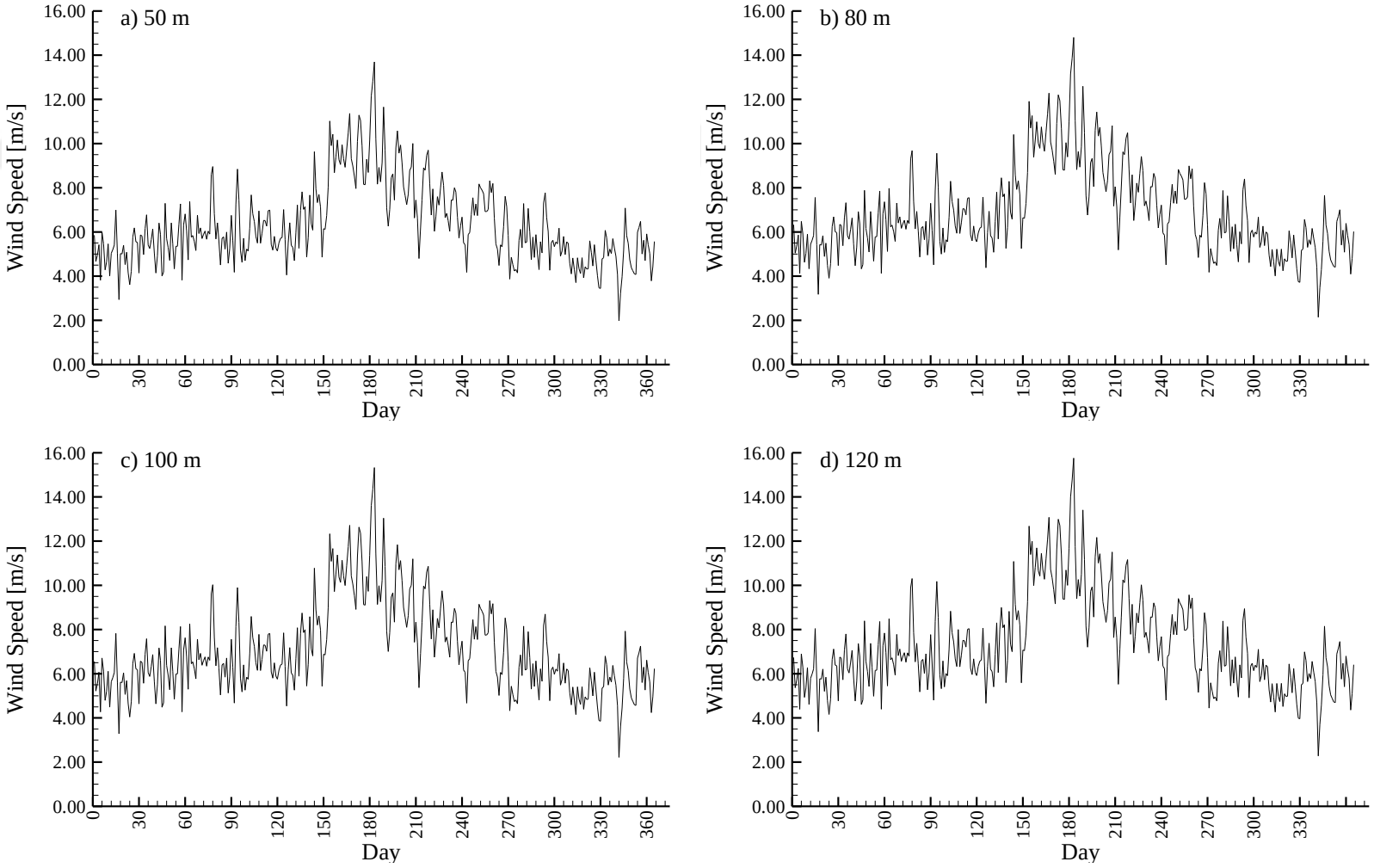

Figure 3.3 Variation of Wind Speed at Different Hub Heights in the city of Basra

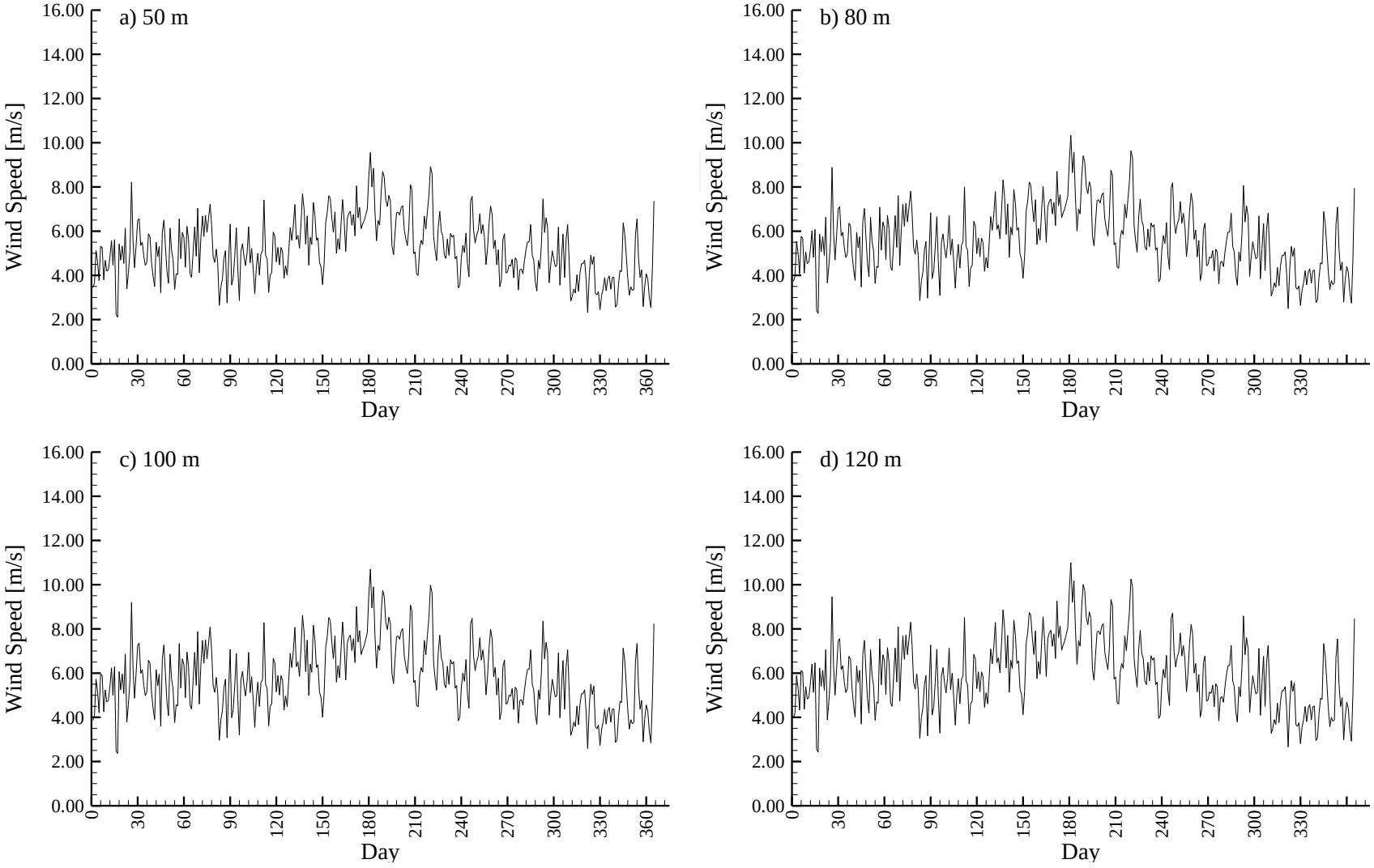

Figure 3.4 Variation of Wind Speed at Different Hub Heights in the city of Wasit

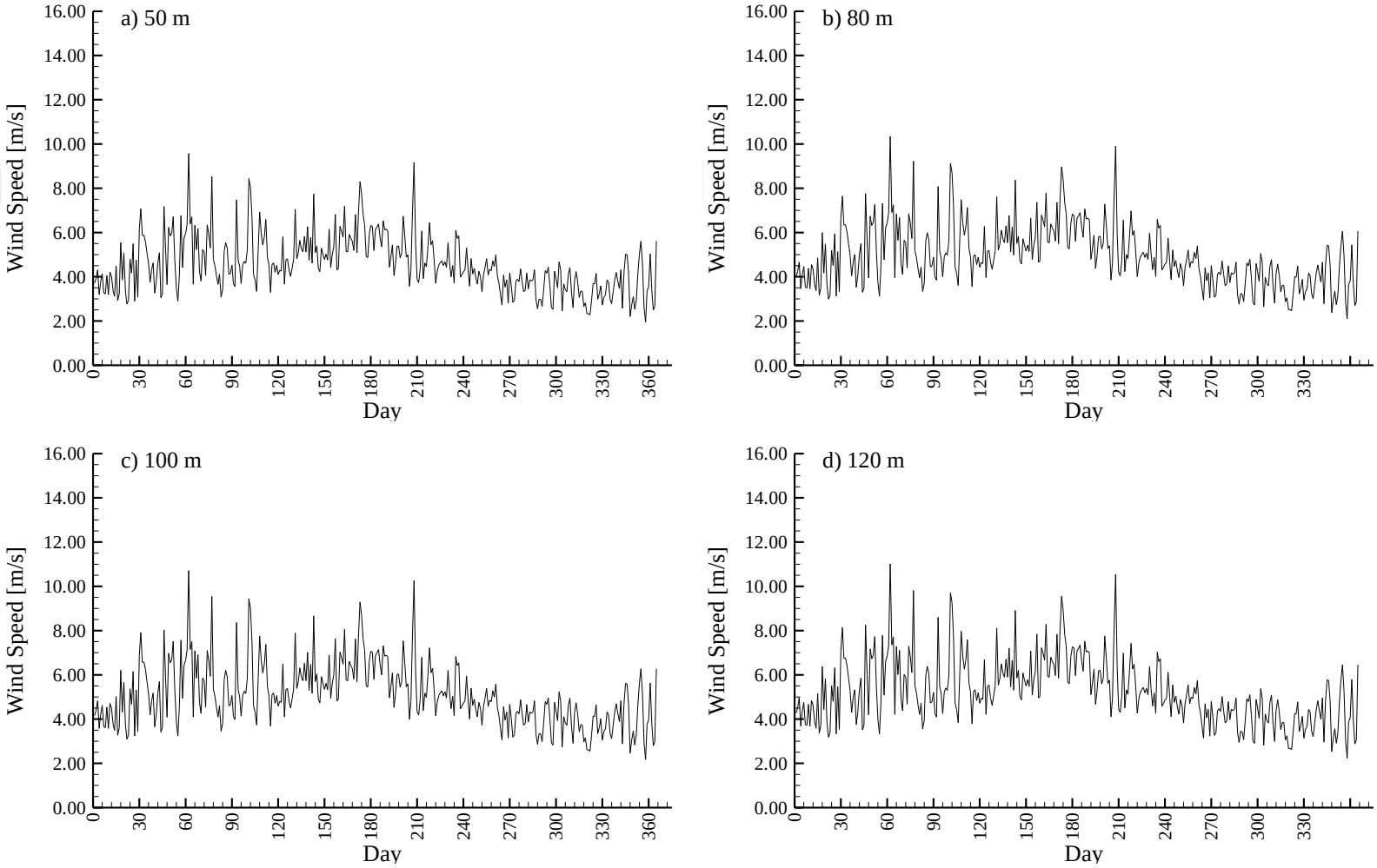

Figure 3.5 Variation of Wind Speed at Different Hub Heights in the city of Anbar

3.5. Solar Potential in Iraq

3.5.1. Solar Radiation on Horizontal Surface

The daily amount of total solar radiation outside the atmosphere is calculated. By using sunshine duration data taken from Iraqi agromet department, the monthly average of daily global radiation on the horizontal surface is estimated for three locations in Iraq, based on equations 3.6- 3.10 [129].

The value of solar radiation outside of the atmosphere H_0 (extraterrestrial radiation) can be calculated for each day and for different latitudes from the solar constant, and the solar declination using the following equation:

$$H_0 = \frac{24}{\pi} I_{gs} \cdot f(\cos\delta \cdot \cos\varphi \cdot \sin\omega_s + \frac{\pi}{180} \cdot \omega_s \cdot \sin\delta \cdot \sin\varphi) \quad (3.6)$$

where I_{gs} is solar constant ($I_{gs} = 1367\ W/m^2$), f is the inverse relative distance from Earth-Sun, and δ is solar declination angle (radian) which can be found from Eqs. 3.7 and 3.8.

$$f = 1 + 0.0333 \cdot \cos\frac{360 \cdot n}{365} \quad (3.7)$$

$$\delta = 23.45° \left[\sin\left(\frac{360 \cdot (n+284)}{365}\right)\right] \quad (3.8)$$

where, n is number of days. For January 1st, n=1 and for December 31st, n=365. δ varies between 23.45° ≥ δ ≥ -23.45°.

The sunset hour angle ω_s depends on the latitude and solar declination angle which is given by:

$$\omega_s = \cos^{-1}(-\tan\varphi \cdot \tan\delta) \quad (3.9)$$

where φ is the latitude for the location.

The daylight hours N is given by:

$$N = \frac{2}{15}\omega_s \tag{3.10}$$

Global solar radiation can be calculated from Eq. 3.11

$$H_{cal} = (a_s + b_s \frac{n}{N}) \cdot H_0 \tag{3.11}$$

where a_s and b_s are regression constant for Angstrom that are taken as 0.25 and 0.5, respectively [130], a_s regression constant expresses the fraction of H_0 reaching the earth on overclouded day (n =0), (a_s+b_s) gives the fraction of H_0 reaching the earth on clear day, n is actual duration of sunshine duration (hour), ($\frac{n}{N}$) is relative sunshine duration.

The study showed that the latitude has effects in determining solar incidence angle, the sum of solar radiation, and daylight hours. By analyzing the calculated data for the cities, it was found that the summer day is long by about 11-14 hours and winter day is shorter by approximately 10 hours from average day as shown in Table 3.3. While the annual average of day hours (N) hour/day is 4380 hours, the daily average global solar radiation H_{cal} is 19.1 MJ/m^2-day for Basra, 18.48 MJ/m^2-day for Wasit, and 18.02 MJ/m^2-day for Anbar, and the annual average of H_{cal} is 6975.6, 6743.7, 6578 MJ/m^2 for Basra, Wasit, and Anbar respectively. Through comparison between monthly average of daily measured values (H_{data}) and calculated values (H_{cal}), a very good congruence for all subject cities can be observed as shown in Figures 3.6. The maximum monthly average of H_{cal} values were in June and the minimum values were in December and January.

Table 3.3 Duration of Sunshine (Hours) for the Period of 2010-2014 in Basrah, Wasit, and Anbar

Month	Global sunshine duration					
	Basra		Wasit		Anbar	
	n*	N**	n	N	n	N
Jan	5.905	10.29	5.753	10.304	5.584	10.054
Feb	6.8512	10.945	7.17	10.948	6.7584	10.796
Mar	7.899	11.815	7.8	11.815	7.426	11.788
Apr	8.264	12.752	8.091	12.741	8.4136	12.849
May	9.182	13.531	9.045	13.515	9.014	13.737
Jun	11.46	13.92	10.845	13.899	10.386	14.18
Jul	11.261	13.735	10.994	13.718	10.289	13.972
Aug	10.413	13.059	10.807	13.049	9.887	13.202
Sep	9.865	12.154	9.977	12.154	8.925	12.176
Oct	8.138	11.221	7.502	11.229	8.033	11.118
Nov	6.345	10.446	6.422	10.463	6.789	10.238
Dec	6.347	10.077	5.967	10.098	6.084	9.817

* Actual duration of sunshine in day hour/day average for period 2010-2014

** Daylight hours hour/day average for period 2010-2014

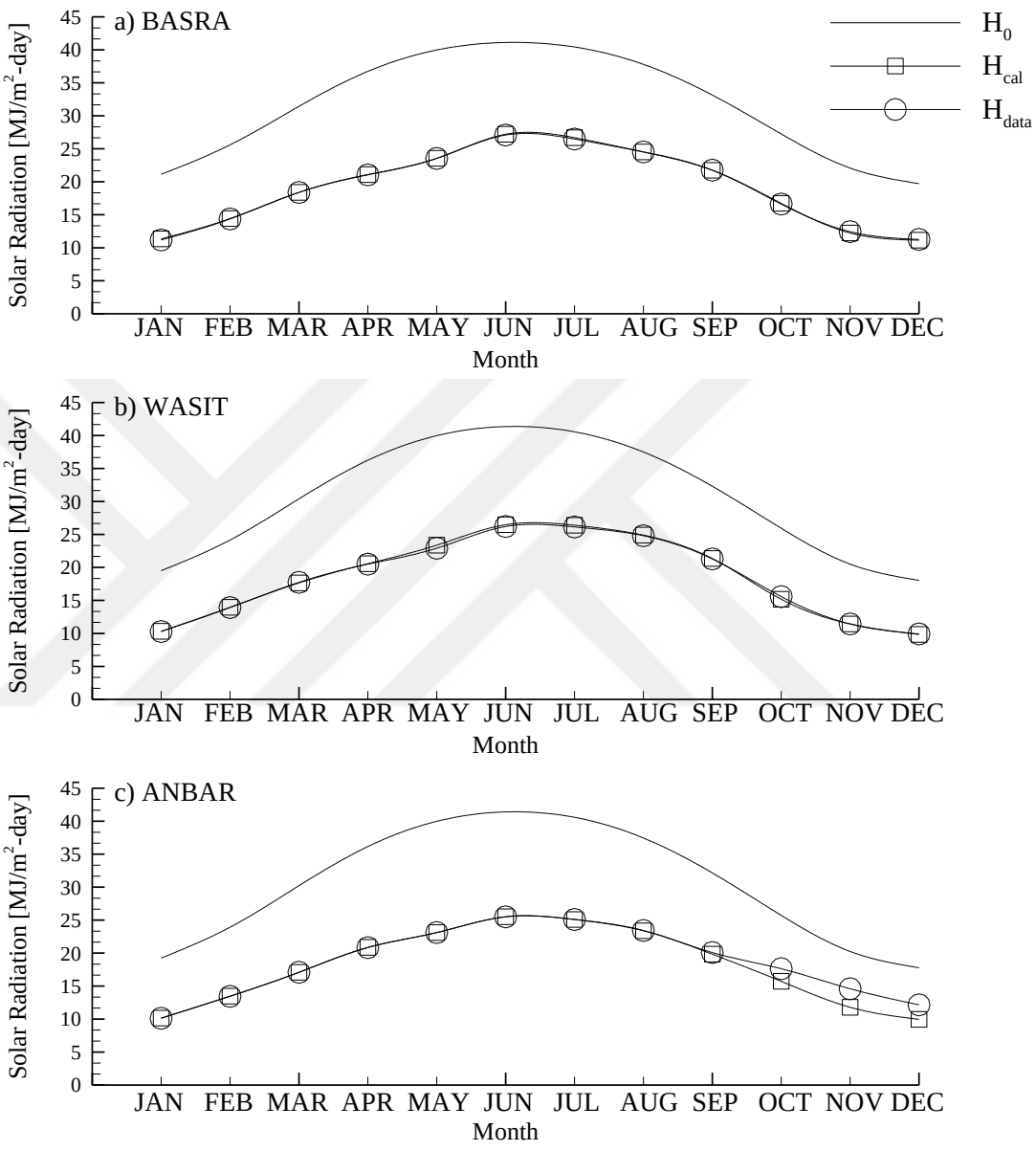

Figure 3.6. Solar Radiation on Horizontal Surface in the selected cities

3.5.2. Solar Radiation on Inclined Surface

The amount of solar radiation on tilted surfaces is estimated using the average radiation on horizontal surface, extraterrestrial radiation, beam radiation, diffuse and reflected radiation. The optimum tilt angle (β) can provide the maximum average radiation. In this research, two cases are discussed; one is for tilt angle equal to the latitude (β= φ) and the other is for tilt angle β which is obtained by subtracting the value of the solar declination angle from the value of the latitude (β= φ-δ). The tilt angle β is calculated for every day for the average period of the five years, and it was found that the tilt angle (β) estimated by the equation (β= φ-δ) achieves higher values than the values found with the estimation from the equation (β= φ).

The total global solar radiation on tilted surface is the sum of beamed, diffused, and reflected radiation.

$$H_T = H_B + H_D + H_R \tag{3.12}$$

where H_T is the total solar radiation on tilted surface, H_B is the beam or direct radiation, H_D is the diffuse radiation, and H_R is the reflected radiation.

$$H_B = (H - H_d) \cdot R_b \tag{3.13}$$

where H is monthly mean daily global radiation, H_d is monthly mean daily diffuse radiation, R_b is the ratio of daily average beam radiation on inclined surface to the average that on horizontal surface that can expressed in equation below:

$$R_b = \frac{\cos\delta \cdot \sin\omega_{sT} \cdot \cos(\varphi-\beta) + \frac{\pi}{180}\cdot\omega_{sT}\cdot\sin\delta\cdot\sin(\varphi-\beta)}{\frac{\pi}{180}\cdot\omega_s\cdot\sin\varphi\cdot\sin\delta + \cos\varphi\cdot\cos\delta\sin\omega_s} \tag{3.14}$$

where $\omega_{sT} = \min\{\omega_s, \cos^{-1}(-\tan(\varphi-\beta)\cdot\tan\delta)\}$

The ratio of monthly mean daily diffuse radiation to the monthly mean daily global radiation that can be expressed in equation below:

$$\frac{H_d}{H} = 1.311 - 3.022K_T + 3.427K_T^2 - 1.821K_T^3 \qquad \text{For } 0.3 \leq K_T \leq 0.8 \tag{3.15}$$

K_T is clearness index, which is the ratio of average global radiation to extraterrestrial radiation values, as expressed in Eq. 3.16 [131, 132]:

$$K_T = \frac{H}{H_o} \tag{3.16}$$

$$H_D = H_d \cdot R_d \tag{3.17}$$

$$R_d = \frac{1+\cos\beta}{2} \tag{3.18}$$

$$H_R = H \cdot R_r \tag{3.19}$$

$$R_r = \rho_r \frac{1-\cos\beta}{2} \tag{3.20}$$

where ρ is ground reflectivity and its value is 0.2.

According to the equations above, Eq. 3.12 can be rewritten as:

$$H_T = H\left(1 - \frac{H_d}{H}\right) + H_d \cdot R_d + R_r \tag{3.21}$$

The average radiation on horizontal surface and β are used as input parameters in Eqs. 3.15, 3.18 and 3.20. The calculated results of R_d, H_d and R_r were used in Eq. 3.21 to evaluate H_T. In addition to these, extraterrestrial radiation was used in Eq. 3.16 to calculate clearness index. The incident radiation intensity on tilted surface varies from one month to another due to difference of sun inclination with seasons.

Monthly average solar radiation on inclined surface at different tilt angels for the cities of Basra, Wasit and Anbar are plotted in Figures 3.7 and 3.8. The results indicate that the average of solar radiation intensity on tilted surface has increased significantly when compared to the intensity on horizontal surface. While Figure 3.7 is for the tilt angle of $\beta=\varphi$, Figure 3.8 is for $\beta=\varphi-\delta$. Although the highest values of H_T for Basra and Wasit occur

at September, it occurs at October for Anbar in the case of β=φ. In the case of β=φ-δ, the highest values of H_T for Basra, Wasit and Anbar can be seen at June.

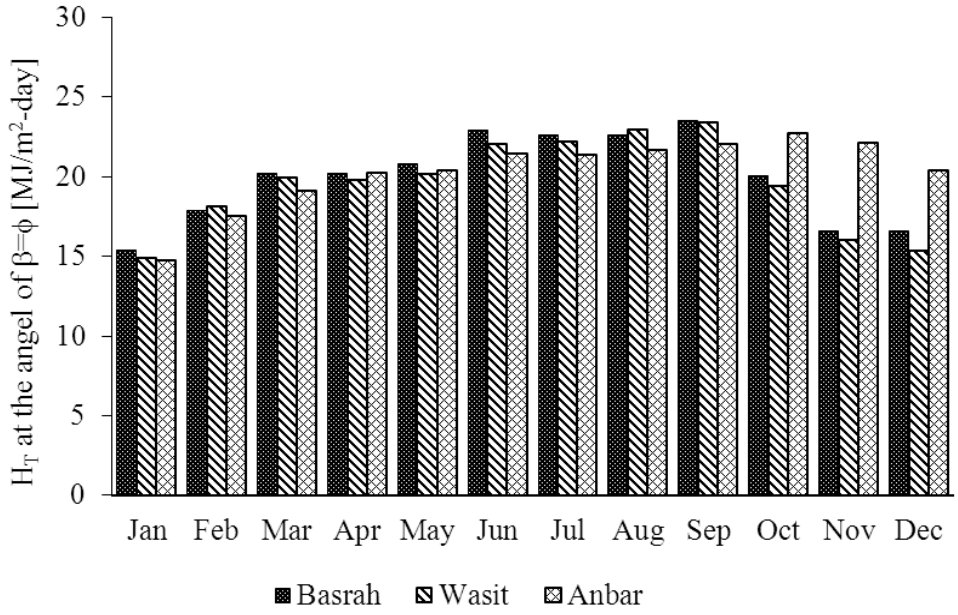

Figure 3.7. Global Solar Radiation on Inclined Surface (at β=ϕ) for the selected cities

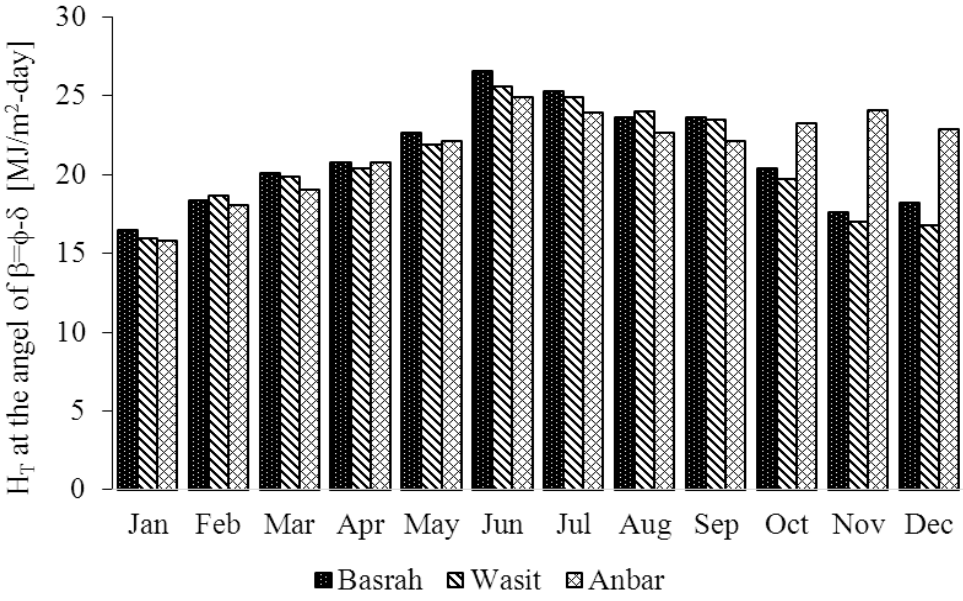

Figure 3.8. Global Solar Radiation on Inclined Surface (at β=ϕ-δ) for the selected cities

CHAPTER 4

ELECTICITY PRODUCTION FROM WIND AND SOLAR ENERGY IN IRAQ

4.1. Introduction

A hybrid system that consists of wind turbines and photovoltaic modules subsystems is proposed to investigate the potential to produce electricity, and the system is shown in Figure 4.1. Estimates and analyses of electricity production and costs in each system has provided for the three selected cities (Basra, Wasit, and Anbar).

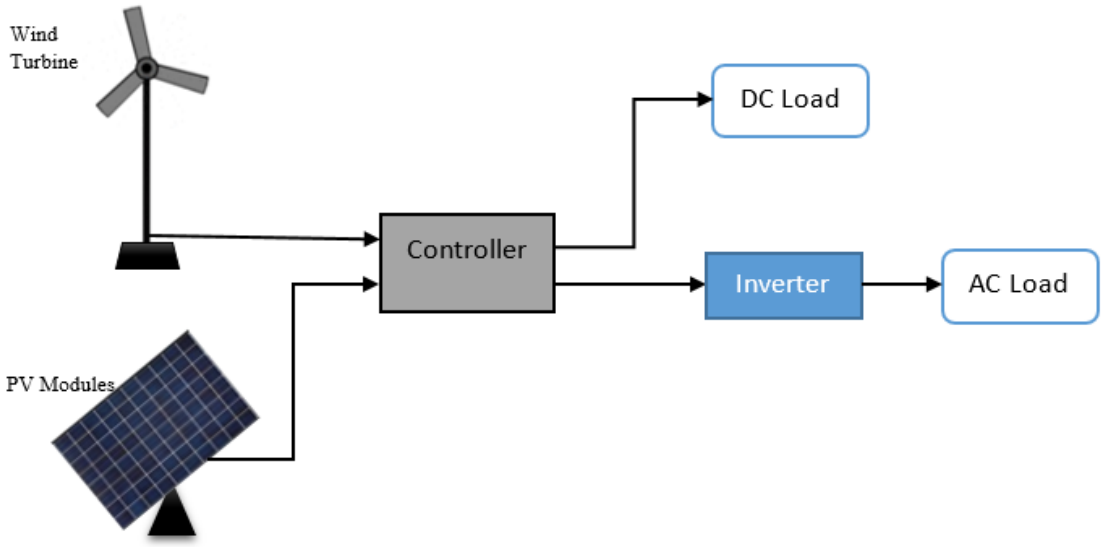

Figure 4.1. The Scheme of the Proposed Solar/Wind Hybrid Energy System

4.2. Electricity Production from Wind Energy

4.2.1. Mathematical Model of Wind Energy

A wind turbine is considered to produce electricity. The wind speeds measured at 3m were obtained from the Meteorological Department and these values were extrapolated to four different hub heights (50 m, 80 m, 100 m, and 120 m). In this chapter, to estimate the electrical energy, four different wind turbines (WTs) were selected: 500 kW, 900 kW, 1300 kW, and 2000 kW. Table 4.1 shows a review of the characteristics of the selected WTs. For each wind turbine, there is a different power output curve. Power curve depending on wind speed values can be given in Eq. 4.1 [133]. In this work, the power curve equation is obtained using methods of fitting curve as shown in Figure 4.2. This equation is used to estimate power generation at each calculated wind speed between cut-in and cut-out speeds for each WT.

Table 4.1. Characteristics of selected wind turbines

Characteristics	500 kW WT-1	900 kW WT-2	1300 kW WT-3	2000 kW WT-4
Type	EWT-DW 52/54	EWT-DW 52/54	Nordex-N60	Vestas-V100
Number of blades	3	3	3	3
Blade length (m)	N/A	N/A	29	49
Rotor diameter (m)	52 or 54	51.5 / 54	60	100
Variable Rotor Speed (rpm)	12 - 26	12 - 26	12.8 /19.2	N/A
Swept area (m^2)	N/A	N/A	2828	7854
Nominal Power Output (kW)	500	900	1300	2000
Cut-in wind speed (m/s)	2.5	3	4	3
Rated wind speed (m/s)	10	13	15	12
Cut-out wind speed (m/s)	25	25	25	22
Survival wind speed (m/s)	59.5	59.5 / 52.5	70	N/A
Price ($)*	100000[134]	900000	1300000	2000000

*The specific costs of wind turbines are taken as 1000 $/kW, except the wind turbine with rated power of 500 kW.

$$P_i(v) = \begin{cases} 0, & v < v_{ci} \\ (a_n v^n + a_{n-1} v^{n-1} + \cdots + a_1 v + a_0), & v_{ci} \le v < v_R \\ P_{R,} & v_R \le v < v_{co} \quad or \\ (a_n v^n + a_{n-1} v^{n-1} + \cdots + a_1 v + a_0), & v_{ci} \le v < v_R \\ 0, & v \ge v_{co} \end{cases} \tag{4.1}$$

where $P_i(v)$ is the output power of WT at specific wind speed, P_R is rated power of the WT, (v) is wind speed at the hub height, (a) is a regression constants, (v_{ci}) (v_R) (v_{co}) are cut-in, rated, and cut-out wind speeds, respectively.

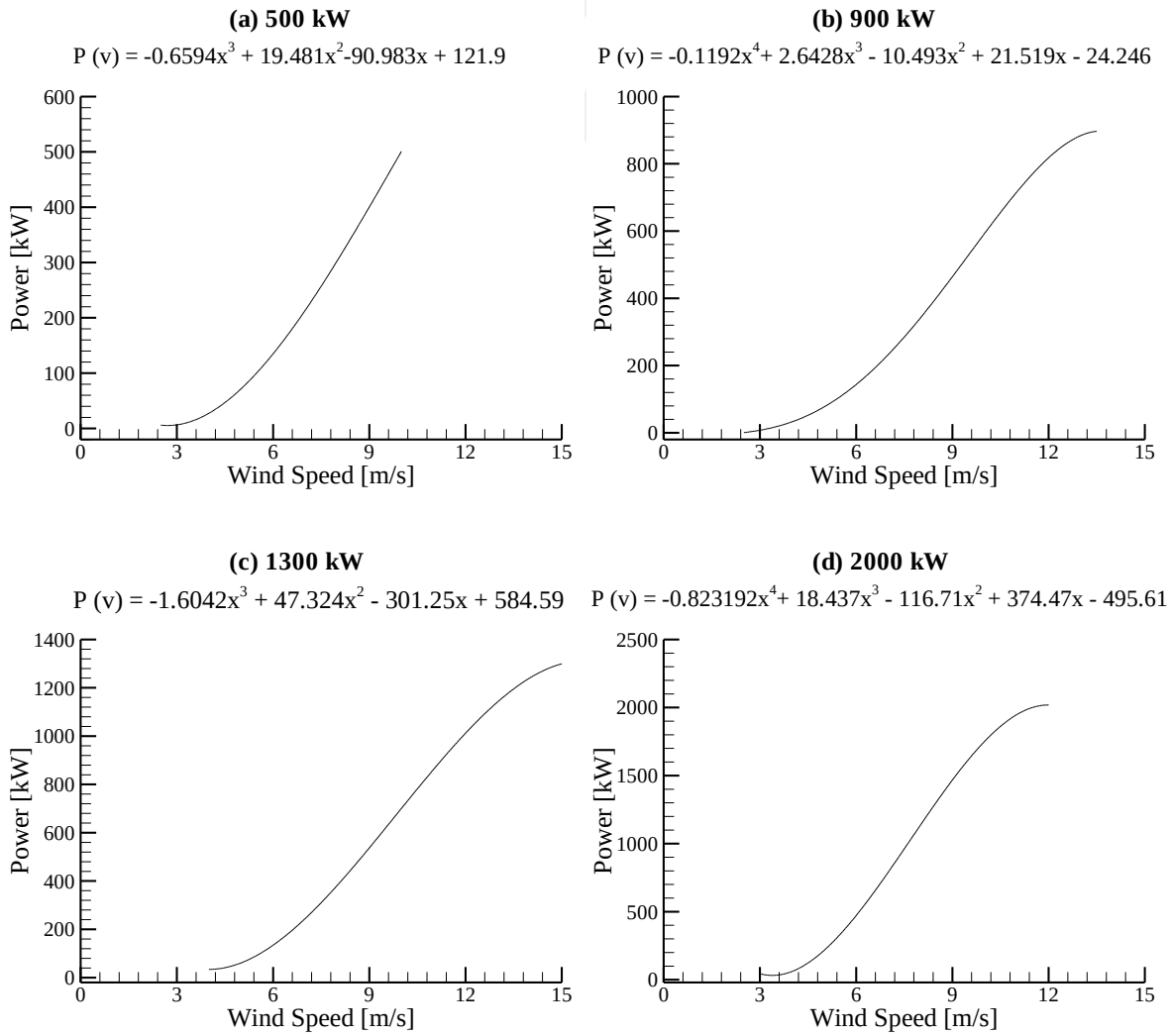

Figure 4.2. Power Curves of Selected Wind Turbines

It is supposed that both 1300 kW and 2000 kW WTs produce more energy than the other WTs, but the results obtained showed that 1300 kW WT has low values than expected; because the cut-in wind speed for this WT is greater than the rest of WTs. That means the average wind speed must be higher for 1300 kW WT to generate power efficiently.

The monthly average of daily power generation is calculated for each WT in different hub heights for Basra, Wasit, and Anbar as shown in Tables 4.2, 4.3, and 4.4. The results that are obtained show that Basra city has the highest values followed by Wasit while Anbar has the lowest values. For Basra, the highest power generation was in June while the lowest values were in December and January. In the case of Wasit, the highest values were in June and July while the lowest values were in November and December. For Anbar, the highest values were in June while the lowest values were in October and November.

Table 4.2 Monthly Average Power Production (kWh) in the Different Types of Wind Turbines for Calculated Speed with Different Hub Heights in the City of Basra

Mon.	500kW				900kW				1300kW				2000kW			
	50m	80m	100m	120m	50m	80m	100m	120m	50m	80m	100m	120m	50m	80m	100m	120m
Jan	1889	2467	2766	3020	2038	2655	2979	3259	1812	2445	2802	3119	6581	8596	9649	10556
Feb	2623	3353	3725	4039	2828	3634	4053	4412	2666	3578	4071	4500	9165	11777	13126	14276
Mar	3459	4346	4789	5142	3755	4760	5276	5714	3679	4889	5523	6067	12126	15308	16916	18268
April	3459	4343	4788	5147	3759	4766	5283	5722	3709	4915	5547	6090	12159	15361	16982	18344
May	4024	4966	5423	5807	4411	5543	6117	6603	4509	5886	6598	7203	14217	17748	19500	20953
Jun	10263	11157	11421	11582	12777	14952	15914	16650	15032	17931	19276	20348	38116	42295	43836	44808
Jul	8407	9432	9856	10141	10375	12171	13005	13672	12110	14545	15681	16596	30896	35287	37114	38458
Aug	5708	6887	7437	7862	6377	7876	8621	9241	6922	8799	9739	10525	20425	24895	27011	28707
Sep	4479	5528	6050	6485	4932	6178	6808	7339	5174	6698	7478	8138	15945	19849	21776	23368
Oct	2710	3457	3837	4158	2928	3755	4184	4551	2760	3703	4211	4652	9489	12154	13526	14694
Nov	1467	1954	2208	2426	1599	2106	2375	2607	1351	1868	2136	2381	5164	6822	7696	8452
Dec	1888	2459	2754	3005	2040	2653	2974	3251	1824	2458	2843	3156	6598	8593	9636	10532
Total/yr	50375	60349	65052	68814	57818	71048	77589	83020	61548	77716	85906	92777	180881	218686	236768	251415

Table 4.3 Monthly Average Power Production (kWh) in the Different Types of Wind Turbines for Calculated Speed with Different Hub Heights in the City of Wasit

Month	500kW				900kW				1300kW				2000kW			
	50m	80m	100m	120m	50m	80m	100m	120m	50m	80m	100m	120m	50m	80m	100m	120m
Jan	1774	2304	2576	2813	1938	2511	2810	3068	1780	2409	2727	3010	6254	8104	9061	9879
Feb	1818	2374	2661	2906	1967	2564	2877	3147	1738	2404	2772	3069	6350	8301	9321	10198
March	2286	2927	3255	3534	2469	3180	3551	3868	2319	3125	3547	3916	7982	10275	11472	12497
April	1606	2109	2370	2594	1751	2289	2571	2815	1558	2069	2424	2683	5635	7390	8308	9097
May	2642	3368	3737	4049	2862	3669	4088	4445	2745	3650	4139	4564	9272	11876	13215	14353
Jun	4609	5667	6177	6603	5048	6326	6973	7518	5239	6830	7644	8332	16281	20272	22245	23877
Jul	4595	5659	6186	6610	5077	6342	6980	7516	5354	6904	7694	8363	16378	20300	22220	23798
Aug	2999	3785	4182	4496	3273	4157	4611	4997	3182	4233	4774	5240	10552	13343	14753	15938
Sep	2543	3247	3605	3908	2758	3539	3945	4291	2629	3525	3992	4400	8932	11458	12758	13862
Oct	1748	2283	2560	2796	1909	2484	2786	3046	1754	2370	2683	2962	6161	8038	9014	9852
Nov	869	1177	1343	1484	968	1297	1472	1625	778	1168	1363	1547	3031	4135	4713	5212
Dec	1100	1443	1625	1782	1213	1599	1802	1977	1136	1574	1740	1925	3844	5102	5750	6314
Total/yr	28589	36342	40277	43573	31234	39958	44465	48314	30211	40261	45500	50012	100672	128595	142830	154877

Table 4.4 Monthly Average Power Production (kWh) in the Different Types of Wind Turbines for Calculated Speed with Different Hub Heights in the City of Anbar

Month	500kW				900kW				1300kW				2000kW			
	50m	80m	100m	120m	50m	80m	100m	120m	50m	80m	100m	120m	50m	80m	100m	120m
Jan	929	1240	1406	1551	1035	1379	1561	1719	888	1223	1484	1670	3214	4376	4990	5511
Feb	1857	2401	2682	2921	2017	2616	2929	3198	1857	2532	2898	3226	6481	8446	9464	10334
Mar	2390	3003	3300	3553	2640	3357	3724	4036	2617	3404	3812	4199	8450	10681	11798	12732
Apr	2178	2780	3088	3348	2408	3081	3429	3725	2380	3127	3498	3825	7760	9907	10995	11913
May	1965	2560	2866	3126	2134	2771	3103	3390	1919	2571	2937	3263	6911	8967	10038	10956
Jun	3165	3996	4416	4770	3430	4368	4851	5263	3330	4436	5021	5525	11108	14113	15646	16941
Jul	2552	3253	3590	3869	2779	3554	3955	4297	2674	3530	3994	4398	8960	11426	12684	13749
Aug	1583	2096	2362	2590	1726	2264	2548	2793	1538	2034	2325	2588	5583	7338	8260	9056
Sep	705	984	1135	1268	804	1096	1252	1389	753	912	1041	1138	2511	3484	4009	4461
Oct	508	720	835	937	583	811	934	1041	540	714	765	823	1770	2534	2926	3284
Nov	336	491	578	653	397	567	660	742	347	513	590	675	1123	1710	2022	2298
Dec	688	931	1061	1179	750	1018	1160	1285	603	891	993	1121	2315	3178	3639	4053
Total/yr	18856	24456	27320	29765	20703	26880	30105	32877	19446	25886	29360	32451	66186	86159	96471	105288

4.2.2. Cost Analysis for Wind Energy

Cost analyses are made for each scenario of WTs using Levelized Cost of Electricity (LCOE) method. LCOE is a detailed analysis method that predicts costs by assessing discount rate, escalation ratio, the cost of auxiliary equipment, the lifetime of the system. The following equations explain the mathematical calculations of cost analysis for WTs:

$$LCOE_{WT} = \frac{CRF_{WT} \cdot C_{WT} + CRF_{aux} \cdot C_{aux} + CRF_{ci} \cdot C_{ci} + C_{(om)esc}}{E_{WT}} \quad [\$/kWh] \qquad (4.2)$$

where C_{WT} is the capital cost of WT ($), C_{aux} is the capital cost of auxiliary equipment considering it 15%, C_{ci} is the civil work and installation cost which is considered being 10%, $C_{(om)esc}$ is cost of operation and maintenance, E_{WT} is the annual power generation (kWh/year) from WT. CRF is capital recovery factor that can be expressed as in equation 4.3 [135].

$$CRF = \frac{(i+1)^l \cdot i}{(i+1)^l - 1} \qquad (4.3)$$

where (i) is discount rate which considered being 10%, (l) is system lifetime which considered being 25 years.

The following equation can be used to estimate the cost of operation and maintenance for the whole lifetime of the system [135]:

$$C_{(om)esc} = \frac{C_{om}}{i-e}\left(1 - \frac{(1+e)^l}{(1+i)^l}\right) \qquad (4.4)$$

where (C_{om}) cost of operation and maintenance for the first year, (e) is escalation rate which considered being 4%.

For estimating the capacity factor (C_f) for each WT, which is the annual average power generated divided by the annual rated electrical power, can expressed as in the following formula:

$$C_f = \frac{E_{WT}}{E_R} \quad (4.5)$$

where E_{WT} is the annual generated power from WTs, E_R is the annual rated electrical power that can be expressed by:

$$E_R = \text{wind turbine rated power} \times 8670$$

The results of the analysis were shown in Tables 4.5, 4.6, and 4.7, where the electricity production, C_f of WTs, and LOCE were estimated. The maximum energy production obtained in Basra was 7.66 GW/year from 2000 kW WT at the hub height of 120 m, followed by Wasit with 4.72 GW/year at the hub height of 120 m from 2000 kW WT. The minimum value was in Anbar with 0.57 GW/year from 500 kW WT at the hub height of 50 m.

The highest values for the capacity factor C_f were 48%, 30%, 21% for Basra, Wasit, and Anbar respectively from WT that has 500kW rated power at the hub height 120m. The maximum cost of energy was in Anbar from 1300 kW WT at 50m hub height with 27.97 $/kWh, while the minimum cost was in Basra from 500 kW WT at 120m hub height with 0.606 $/kWh.

Table 4.5 Annual Energy Production, Capacity Factors and Levelized Cost of Electricity for Selected Wind Turbines at Different Hub Heights for Basra

WT	**500 kW**				**900 kW**				**1300 kW**				**2000 kW**			
Hub Height	**50m**	**80m**	**100m**	**120m**	**50m**	**80m**	**100m**	**120m**	**50m**	**80m**	**100m**	**120m**	**50m**	**80m**	**100m**	**120m**
Total P. [GW/yr]	1.53	1.84	1.98	2.10	1.76	2.16	2.36	2.53	1.87	2.37	2.62	2.83	5.51	6.66	7.21	7.66
C_f [%]	0.35	0.42	0.45	0.48	0.22	0.27	0.30	0.32	0.16	0.21	0.23	0.25	0.31	0.38	0.41	0.44
$C_{electric}$ [$/kWh]	0.828	0.691	0.641	0.606	6.493	5.284	4.839	4.523	8.809	6.977	6.312	5.845	4.612	3.815	3.524	3.319

Table 4.6 Annual Energy Production, Capacity Factors and Levelized Cost of Electricity for Selected Wind Turbines at Different Hub Heights for Wasit

WT	**500 kW**				**900 kW**				**1300 kW**				**2000 kW**			
Hub Height	**50m**	**80m**	**100m**	**120m**	**50m**	**80m**	**100m**	**120m**	**50m**	**80m**	**100m**	**120m**	**50m**	**80m**	**100m**	**120m**
Total P. [GW/yr]	0.87	1.11	1.23	1.33	0.95	1.22	1.35	1.47	0.92	1.23	1.39	1.52	3.07	3.92	4.35	4.72
C_f [%]	0.20	0.25	0.28	0.30	0.12	0.15	0.17	0.19	0.08	0.11	0.12	0.13	0.18	0.22	0.25	0.27
$C_{electric}$ [$/kWh]	1.458	1.147	1.035	0.957	12.012	9.390	8.439	7.767	17.929	13.456	11.909	10.835	8.282	6.484	5.838	5.385

Table 4.7 Annual Energy Production, Capacity Factors and Levelized Cost of Electricity for Selected Wind Turbines at Different Hub Heights for Anbar

WT	**500 kW**				**900 kW**				**1300 kW**				**2000 kW**			
Hub Height	**50m**	**80m**	**100m**	**120m**	**50m**	**80m**	**100m**	**120m**	**50m**	**80m**	**100m**	**120m**	**50m**	**80m**	**100m**	**120m**
Total P. [GW/yr]	0.57	0.74	0.83	0.90	0.63	0.82	0.91	1.00	0.59	0.79	0.89	0.99	2.01	2.62	2.93	3.20
C_f [%]	0.13	0.17	0.19	0.21	0.08	0.10	0.12	0.13	0.05	0.07	0.08	0.09	0.11	0.15	0.17	0.18
$C_{electric}$ [$/kWh]	2.219	1.711	1.531	1.405	18.185	14.006	12.505	11.451	27.969	21.014	18.528	16.764	12.642	9.711	8.673	7.946

4.3. Electricity Production from Solar Energy

4.3.1. Mathematical Model of Photovoltaic Panels

In this study, a system of PV modules is proposed to produce electricity. For installation of PV modules a land with an area of 10×100 m^2 for each selected city has been assumed. The PV modules must be facing the sun all the daytime to obtaine the maximum amount of solar incident radiation; because of that, the PV modules that installed on tilted surface or with tracking system received solar radiation more than that installed on a horizontal surface. Table 4.8 shows the monthly average of the tilt angle for the cities: Basra, Wasit, and Anbar. The tilt angle of the proposed system is calculated in the previous chapter for the selected cities.

Table 4.8 Monthly Average of Calculated Tilt Angle (Degree) of PV Module for Selected Cities in Basra, Wasit, and Anbar

Basrah ($\beta=\varphi-\delta$)	Wasit ($\beta=\varphi-\delta$)	Anbar ($\beta=\varphi-\delta$)
51.14	53.86	54.31
43.62	46.34	46.79
32.88	35.60	36.05
20.80	23.52	23.97
11.48	14.20	14.65
7.21	9.93	10.38
9.19	11.91	12.36
16.99	19.71	20.16
28.30	31.02	31.47
40.14	42.86	43.31
49.34	52.06	52.51
53.39	56.11	56.56

When installing the PV modules, there must be proper distance between the rows to avoid the fall of shadow over the adjacent PV modules. That mean shadow is another factor that has effects on the received solar radiation. Therefore, in our calculations, the shadow angle is estimated using Eq. 4.6.

$$G_m = \left(\cos\beta + \frac{\sin\beta}{\tan\alpha}\right) \cdot L \qquad (4.6)$$

where G_m is the distance between the rows, β is the tilt angle, L is the length of the module, and α=90- β.

Two different types of PV modules are selected. They are: the Panasonic-VBHN330SJ47 module with rated power 330W and Kyocera-KD315GX-LPB module with rated power 315W. Table 4.9 shows the specifications for both types. The number of each type of PV module, which can be installed on the chosen land, depends on the dimensions of the module, the dimensions of the land, tilt angle and angle of the shadow. From the calculations, the numbers of Panasonic modules (PV1) were 333, 306, 306 and the numbers of Kyocera modules (PV2) were 245, 231, 224 for Basra, Wasit, and Anbar respectively.

Table 4.9 Solar Modules Specifications

Specifications	Panasonic (PV1)	Kyocera (PV2)
Module type	VBHN330SJ47	KD315GX-LPB
Manufactured type	Monocrystalline	polycrystalline
Max. power (P_{max}) [W]	330	315
Max. power voltage (V_{oc}) [V]	69.7	49.2
Max. power current (I_{sc}) [A]	6.07	8.50
Open circuit voltage (V_{mp}) [V]	58	39.8
Short circuit current (I_{mp}) [A]	5.7	7.92
Length [mm]	1590	1662
Width [mm]	1053	1320
Depth [mm]	35	46
Weight [kg]	19	27.5
Efficiency [%]	19.7	16
Thermal Characteristics: Temp. Coefficient		
Voc [V/°C]	-0.174	-0.177
I sc [A/°C]	1.82×10^{-3}	5.10×10^{-3}
Price [$]	455 [136]	399 [137]

The power that can generated from the PV module can expressed as follow:

$$E_{PV} = N_P \cdot N_D \cdot A \cdot G \quad (4.7)$$

where N_P is PV module efficiency, N_D is the performance ratio of the system that is between (0.5-0.9), A is the module area (m^2), and G is average solar radiation that incident on tilt modules (kWh/m^2).

Table 4.10 shows the monthly average power from PV modules for the selected cities. The results showed that the Panasonic modules (PV1) have generated more power than Kyocera (PV2). The highest monthly average power generation values were in Basra. There was a

variation in generating power through the months. The maximum values were in June, while the minimum values were in January. It was observed that Anbar achieved high average power generation from June to December.

Table 4.10 Monthly Average Power Generation (kWh) from Photovoltaic Modules in Selected Cities

Month	Basra		Wasit		Anbar	
	PV1	PV2	PV1	PV2	PV1	PV2
Jan	452.04	353.94	401.72	322.74	398.85	310.72
Feb	503.88	394.53	470.58	378.06	454.30	353.92
Mar	554.30	434.01	504.43	405.25	483.41	376.60
Apr	570.36	446.59	513.66	412.67	523.68	407.96
May	620.53	485.87	552.49	443.87	558.21	434.87
Jun	729.39	571.10	645.17	518.32	627.41	488.77
Jul	692.81	542.46	627.31	503.97	603.39	470.07
Aug	647.85	507.26	605.60	486.53	571.46	445.19
Sep	647.56	507.03	592.22	475.78	557.81	434.56
Oct	559.39	437.99	497.07	399.34	586.60	456.98
Nov	482.68	377.94	428.50	344.25	606.40	472.41
Dec	499.53	391.12	423.16	339.96	576.41	449.05
Total/yr.	6960.32	5449.84	6261.93	5030.74	6547.92	5101.10

4.3.2. Cost Analysis for Solar Energy

Cost analyses are made for each type of PV modules using Levelized Cost of Electricity (LCOE) method. The following equations explain the mathematical calculations of cost analysis for PV modules:

$$LCOE_{PV} = \frac{CRF_{PV} \cdot C_{PV} + CRF_{aux} \cdot C_{aux} + CRF_{ci} \cdot C_{ci} + C_{(om)esc}}{E_{PV}} \quad [\$/kWh] \tag{4.8}$$

where C_{PV} is the capital cost of PV modules ($), C_{aux} is the capital cost of auxiliary equipment which considered being 15%, C_{ci} is the civil work and installation cost which considered being 10%, $C_{(om)esc}$ is cost of operation and maintenance, E_{PV} is the annual power generation (kWh/year) from PV modules, CRF is capital recovery factor and it can be calculated by using Eq. 4.3.

For estimating the cost of operation and maintenance for the lifetime of the PV system can be used the following equation [135]:

$$C_{(om)esc} = \frac{C_{om}}{i-e}\left(1 - \frac{(1+e)^l}{(1+i)^l}\right) \tag{4.9}$$

where C_{om}cost of operation and maintenance is for the first year, i is discount rate which considered being 10%, e is escalation rate which considered being 4%.

To estimate the capacity factor (C_f) for the PV modules, the annual average power generated divided by the annual rated electrical power, using the following formula:

$$C_f = \frac{E_{PV}}{E_R} \tag{4.10}$$

where E_{PV} is the annual average power generated from PV modules, E_R is the annual rated electrical power.

The results of the annualized cost analysis, as shown in Table 4.11 which includes the electricity production, C_f of PV modules and LOCE were estimated. The maximum energy production was obtained in Basra as compared with Wasit and Anbar, where the annual energy was 211.82 MW/year from Panasonic modules, followed by Anbar with 199.31 MW/year from Panasonic modules. The minimum value was in Wasit with 153.068 MW/year from Kyocera modules.

Table 4.11 Annual Energy Production, Capacity Factors and Levelized Cost of Electricity from Photovoltaic Modules for Selected Cities

Cities	**Basra**		**Wasit**		**Anbar**	
PV	**PV1**	**PV2**	**PV1**	**PV2**	**PV1**	**PV2**
E_{PV} [MW/year]	211.828	165.86	190.528	153.068	199.31	155.27
C_f [%]	0.220	0.172	0.198	0.159	0.207	0.161
$C_{electric}$ [$/kWh]	9.09	7.49	9.28	7.65	8.87	7.31

The highest values for the capacity factor C_f were 22%, 20.7%, 19.8% for Basra, Anbar, and Wasit from Panasonic modules, respectively. While the maximum cost of energy is occurred for Wasit in the case of Panasonic modules (9.28 $/kWh), the minimum one is for Anbar in the case of Kyocera modules (7.31 $/kWh).

4.4. Electricity Production from Wind/Solar Hybrid System

In this section, a hybrid system consisting of the PV modules subsystem and WTs subsystem is proposed with all suggested scenarios that are considered in previous sections. Performance predictions and economic evaluation for this hybrid system are analyzed.

4.4.1. Performance of Wind/Solar Hybrid System

Analyzing and comparing the PV/WT hybrid system with the WT system alone and the PV system alone found that there is a significant increase in the energy production in the hybrid system when compared with the alone system of WTs or PVs.

The results, as shown in Figures 4.3, 4.4 and 4.5, revealed that the maximum energy production was obtained in Basra as compared with Wasit and Anbar, where the annual energy was 7.8 GW/year from (2000kW WT at 120m +PV1), followed by Wasit with 4.9 GW/year from (2000kW WT at 120m +PV1). The minimum value was in Anbar with 0.72 GW/year from (500kW WT at 50m +PV2).

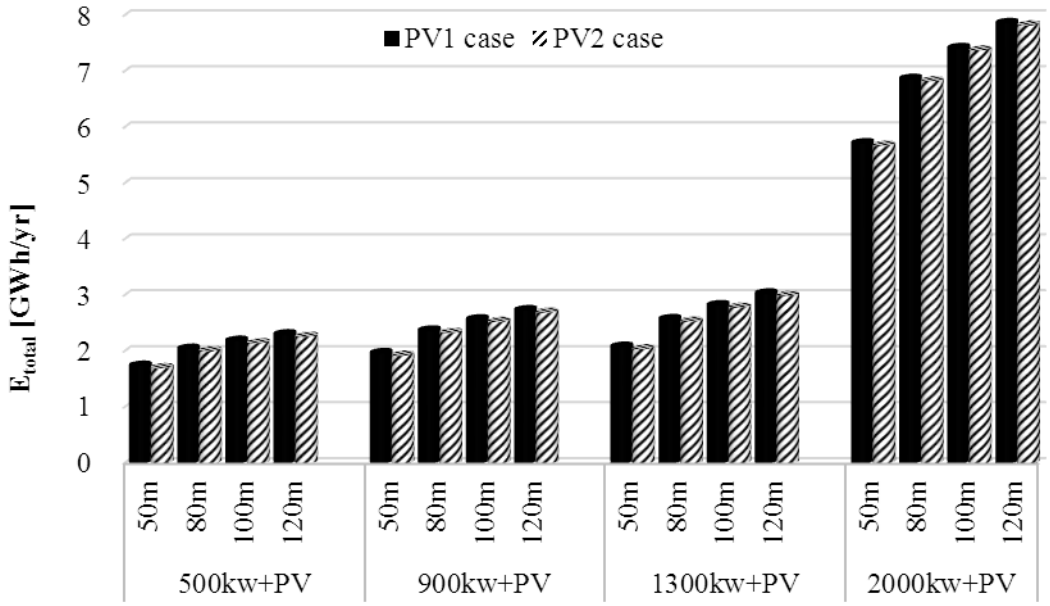

Figure 4.3 Total Power Production from Wind/Solar Hybrid System in Basra (PV1 case: Panasonic PV modules PV2 case: Kyocera PV modules)

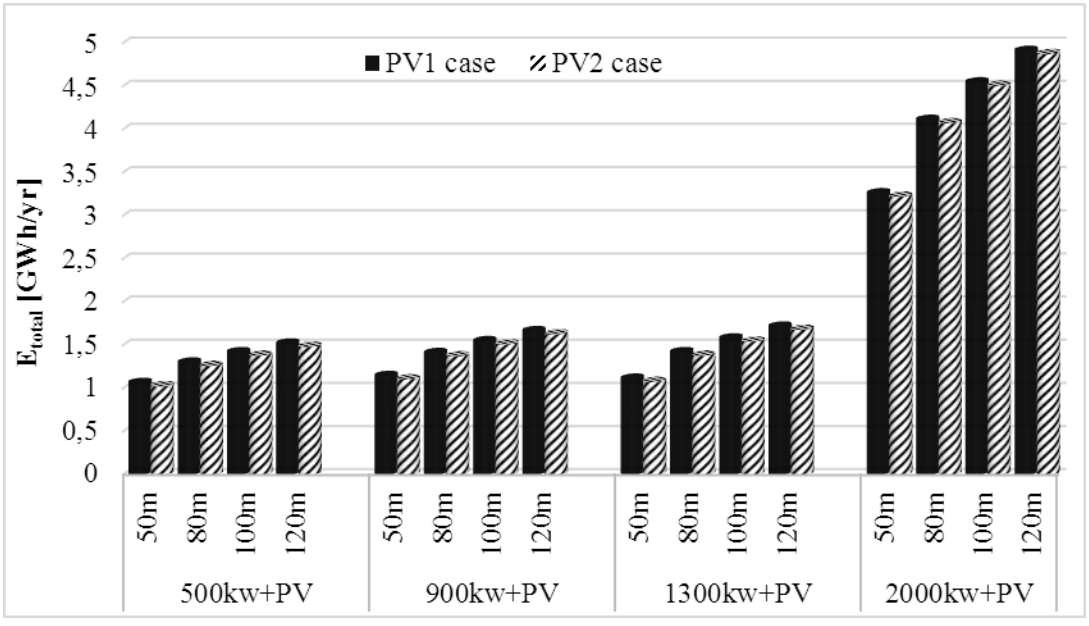

Figure 4.4 Total Power Production from Wind/Solar Hybrid System in Wasit (PV1 case: Panasonic PV modules PV2 case: Kyocera PV modules)

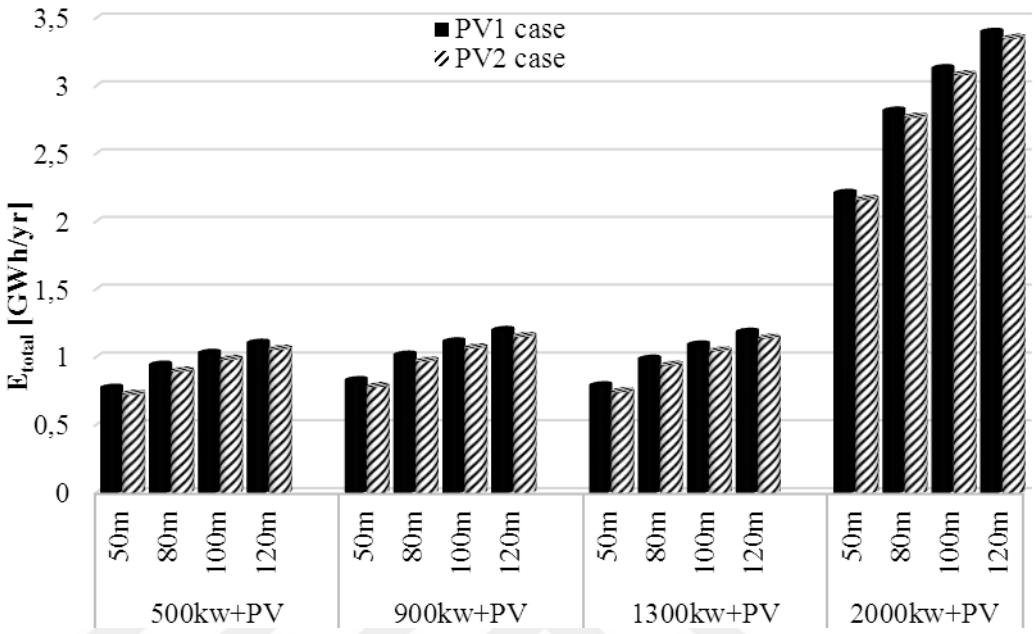

Figure 4.5 Total Power Production from Wind/Solar Hybrid System in Anbar (PV1 case: Panasonic PV modules PV2 case: Kyocera PV modules)

4.4.2. Cost Analysis for Wind/Solar Hybrid System

Cost analyses for PV/WT hybrid system were determined by using Levelized Cost of Electricity (LCOE) method. The following equations explain the mathematical calculations of cost analysis for the hybrid system:

$$LCOE_{hybrid} = \frac{CRF_{WT} \cdot C_{WT} + CRF_{PV} \cdot C_{PV} + CRF_{aux} \cdot C_{aux} + CRF_{ci} \cdot C_{ci} + C_{(om)esc}}{E_{total}} \quad [\$/kWh] \qquad (4.11)$$

where C_{aux} is the capital cost of auxiliary equipment that is considered being 15%, C_{ci} is the civil work and installation cost that is considered being 10%, $C_{(om)esc}$ is cost of operation and maintenance, E_{total} is the annual power generation (kWh/year) from PV/WT hybrid system, CRF is capital recovery factor that can be calculated by using Eq 4.3. For estimating the cost of operation and maintenance for the lifetime of the hybrid system the following equation can be used [135]:

$$C_{(om)esc} = \frac{C_{om}}{i-e}\left(1 - \frac{(1+e)^l}{(1+i)^l}\right) \quad (4.12)$$

where C_{om} is the cost of operation and maintenance for the first year, i is discount rate which is considered being 10%, e is escalation rate which considered being 4%.

The results, as shown in Tables 4.12, 4.13, 4.14, presented that the cost was getting between 0.02-0.43 $/kWh. The minimum cost of energy was in Basra from (500kW WT at 120m +PV2) with 0.02 $/kWh, while the maximum cost was in Anbar from (1300kW WT at 50m +PV2) with 0.43 $/kWh. The costs of the proposed renewable energy systems i.e. WTs and PVs modules systems were high. While the results of the PV/WT hybrid system was obviously competitive comparing with alone WTs system and PVs system. A hybrid system maximizes the power output and minimizes the costs of energy.

Table 4.12 Levelized Cost of Electricity for All Considered Cases in Basra

Hub Height	500kW WT		900kW WT		1300kW WT		2000kW WT	
	+PV1	+PV2	+PV1	+PV2	+PV1	+PV2	+PV1	+PV2
50m	0.033	0.027	0.124	0.120	0.161	0.159	0.087	0.086
80m	0.028	0.023	0.103	0.099	0.131	0.128	0.073	0.071
100m	0.027	0.021	0.095	0.092	0.119	0.117	0.067	0.066
120m	0.025	0.020	0.089	0.086	0.111	0.108	0.063	0.062

Table 4.13 Levelized Cost of Electricity for All Considered Cases in Wasit

Hub Height	500kW WT		900kW WT		1300kW WT		2000kW WT	
	+PV1	+PV2	+PV1	+PV2	+PV1	+PV2	+PV1	+PV2
50m	0.052	0.044	0.211	0.208	0.30	0.301	0.152	0.151
80m	0.043	0.035	0.171	0.168	0.235	0.234	0.121	0.119
100m	0.039	0.032	0.156	0.153	0.212	0.210	0.109	0.108
120m	0.037	0.030	0.145	0.142	0.195	0.193	0.101	0.10

Table 4.14 Levelized Cost of Electricity for All Considered Cases in Anbar

Hub Height	500 kW WT		900 kW WT		1300 kW WT		2000 kW WT	
	+PV1	+PV2	+PV1	+PV2	+PV1	+PV2	+PV1	+PV2
50m	0.072	0.06	0.291	0.293	0.423	0.432	0.225	0.224
80m	0.059	0.049	0.237	0.236	0.339	0.342	0.176	0.175
100m	0.054	0.045	0.216	0.215	0.306	0.308	0.159	0.157
120m	0.05	0.041	0.201	0.199	0.282	0.283	0.146	0.145

CHAPTER 5

HYDROGEN PRODUCTION POTENTIAL FROM WIND/SOLAR HYBRID SYSTEM IN IRAQ

5.1. Introduction

This chapter presents description the proposed hybrid system that consists of wind turbines subsystem, photovoltaic modules subsystem, and electrolyzers to investigate the potential of produced hydrogen as shown in Figure 5.1. Estimating and analyzing of hydrogen production and costs in each scenario of the hybrid system has provided for the three selected locations (Basra, Wasit, and Anbar).

5.2. Hydrogen Production from Solar/Wind Hybrid System

The electrolysis method is chosen to produce hydrogen. Electrolysis considered promising and an effective method to produce hydrogen from renewable sources, where using electricity for the separation of water molecules into hydrogen and oxygen. The reaction takes place in an electrolyzer unit as shown in Eqs. 5.1 and 5.2. The produced hydrogen must be stored.

Anode: $2H_2O \rightarrow O_2 + 4H^+ + 4e^-$ (5.1)

Cathode: $4H^+ + 4e^- \rightarrow 2H_2$ (5.2)

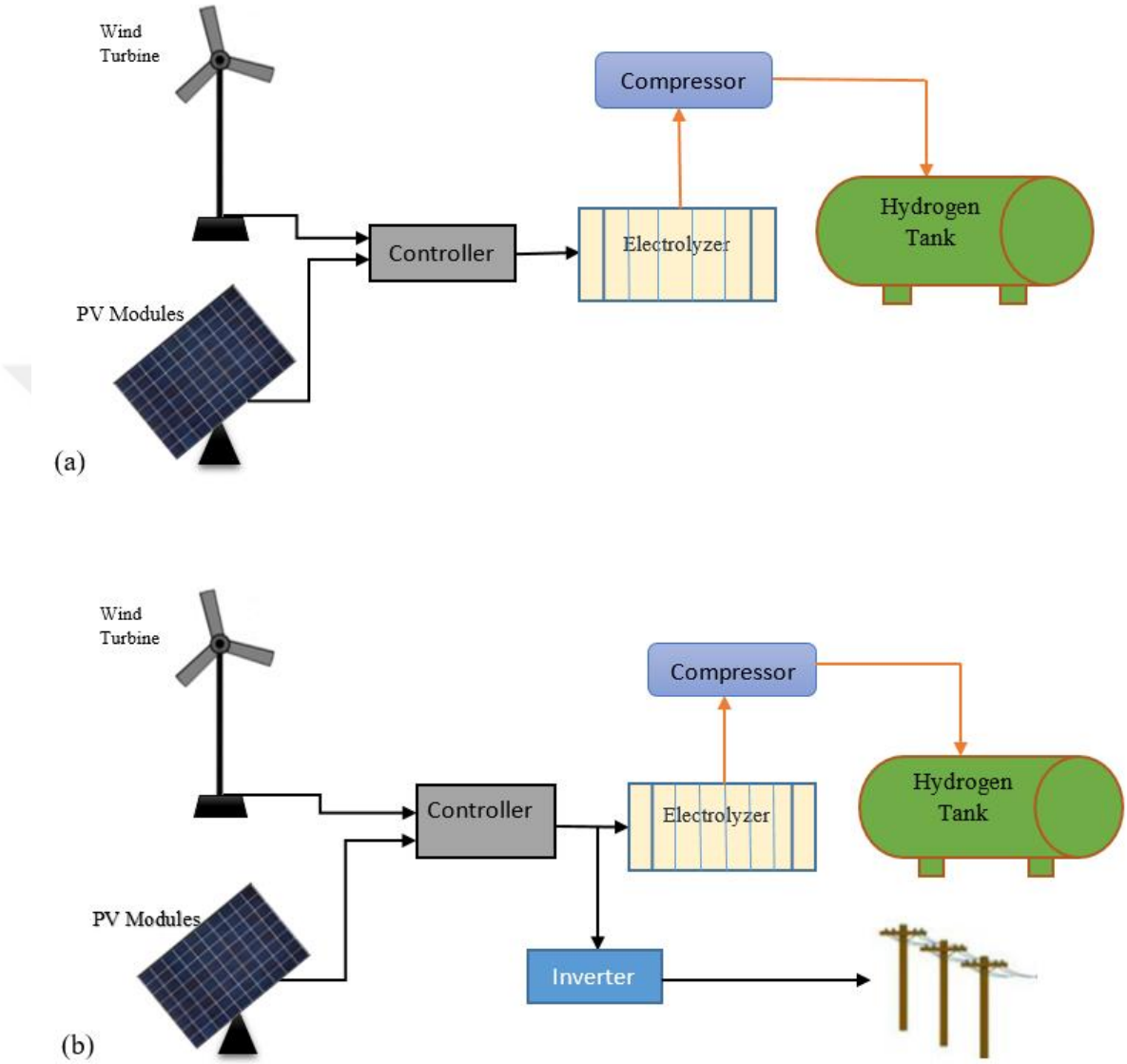

Figure 5.1 (a) the Scheme of the Proposed Stand-alone Solar/Wind Hybrid Energy System for Hydrogen Production (b) The Scheme of the Proposed Solar/Wind Hybrid Energy System for Hydrogen Production with Selling the Excess Energy to the Grid.

Proton exchange membrane (PEM) electrolyzer is selected to integrate with the hybrid system. Because of its operating at low temperature (50-80 ^{0}C), it has high current density, low ohmic losses although the high-pressure operation due to a very thin membrane of the electrolyte, high purity hydrogen production (99.999 %) due to the solid structure of polymer electrolyte membrane, and its ability to integrate directly with renewable sources such as solar and wind energy.

Four types of PEM electrolyzers with different rated power are selected. The numbers of units of each electrolyzer are selected where the overall rated power are being equal, i.e. one unit of electrolyzer with rated power of 860 kW (1×860 kW), two units of electrolyzer with rated power of 430 kW (2×430 kW), four units of electrolyzer with rated power of 215 kW (4×215 kW), and 18 units of electrolyzers with rated power of 48 kW (18×48 kW). Table 5.1 reviews the specifications of the selected electrolyzers.

Table 5.1. Specifications of Selected Electrolyzers

Electrolyzer	48 kW	215 kW	430 kW	860 kW
Model	ZDQ-10	HG-50	HG-100	HG-200
H_2O consumed [ml/hour]	N/A	41667	83334	166668
kWh consumed per hour	48	215	430	860
H_2 gas produced [m^3/hour]	10	50	100	200
Price [$]	198000 [138]	398995 [139]	598995 [139]	798995 [139]

The electric energy that was obtained from PV/WT hybrid system in the previous chapter is supplied to the electrolyzer to produce hydrogen. The PV/WT hybrid system is suggested to connect to electrolyzers in many cases as following:

- Hybrid system consists of 500 kW WT with different hub height (50 m, 80m, 100m, 120 m), PV1 (Panasonic 330W), and electrolyzers with rated power of (18×48 kW, 4×215 kW, 2×430 kW, 1×860 kW).
- Hybrid system consists of 500 kW WT with different hub height (50 m, 80m, 100m, 120 m), PV2 (Kyocera 315W), and electrolyzers with rated power of (18×48 kW, 4×215 kW, 2×430 kW, 1×860 kW).
- Hybrid system consists of 900 kW WT with different hub height (50 m, 80m, 100m, 120 m), PV1 (Panasonic 330W), and electrolyzers with rated power of (18×48 kW, 4×215 kW, 2×430 kW, 1×860 kW).
- Hybrid system consists of 900 kW WT with different hub height (50 m, 80m, 100m, 120 m), PV2 (Kyocera 315W), and electrolyzers with rated power of (18×48 kW, 4×215 kW, 2×430 kW, 1×860 kW).
- Hybrid system consists of 1300 kW WT with different hub height (50 m, 80m, 100m, 120 m), PV1 (Panasonic 330W), and electrolyzers with rated power of (18×48 kW, 4×215 kW, 2×430 kW, 1×860 kW).
- Hybrid system consists of 1300 kW WT with different hub height (50 m, 80m, 100m, 120 m), PV2 (Kyocera 315W), and electrolyzers with rated power of (18×48 kW, 4×215 kW, 2×430 kW, 1×860 kW).
- Hybrid system consists of 2000 kW WT with different hub height (50 m, 80m, 100m, 120 m), PV1 (Panasonic 330W), and electrolyzers with rated power of (18×48 kW, 4×215 kW, 2×430 kW, 1×860 kW).
- Hybrid system consists of 2000 kW WT with different hub height (50 m, 80m, 100m, 120 m), PV2 (Kyocera 315W), and electrolyzers with rated power of (18×48 kW, 4×215 kW, 2×430 kW, 1×860 kW).

The amount of hydrogen that was produced for each of the above cases with each hub height and every type of electrolyzer is calculated.

The monthly average of hydrogen production is evaluated for two different hub heights (50 m and 120 m) of considered lowest rated power turbine (500 kW) and highest rated power

turbine (2000 kW) of the hybrid system for each of the selected cities. For the proposed scenarios can be concluded the following:

1. For Basra, for the hybrid system that considered the scenario of [500 kW WT (50 m, 120 m) + PV1 + electrolyzer] found that the (18×48 kW) electrolyzer is produced hydrogen all months of the year, the highest amount of hydrogen was in the summer season, as shown in Figure 5.2a. At 120 m hub height, the production is increased due to increasing of power that received from the hybrid system. The maximum amount of hydrogen was in June with 91 m^3H_2, 105.33 m^3H_2 for 50 m and 120 m hub heights, respectively. For the (4×215 kW) electrolyzer that considered integrating with the hybrid system in the same scenario, the production of hydrogen was less, while the (2×430 kW) electrolyzer has worked only a few months during the year from May to August at 50 m hub height and from March to September at 120 m hub height. The (1×860 kW) electrolyzer has not worked at all.

The second scenario of [500 kW WT (50 m, 120 m) + PV2 + electrolyzer] same as in the first scenario the electrolyzer most productive of hydrogen was (18×48 kW), as shown in Figure 5.2b, but with amount less than in the previous scenario with 87.33 m^3H_2, 97.33 m^3H_2 for 50 m and 120 m, respectively.

The third scenario of [2000 kW WT (50 m, 120 m) hub heights + PV1 + electrolyzer], for this scenario all the electrolyzers have worked and the produced hydrogen is increased in all cases of electrolyzers, as shown in Figure 5.2c. The maximum amount of hydrogen production was at (18×48 kW) and (4×215 kW) electrolyzers with 180 m^3H_2, 200 m^3H_2 respectively.

The fourth scenario of [2000 kW WT (50 m, 120 m) + PV2 + electrolyzer], same as in the third scenario but with a slight decrease in the amount of hydrogen production, as shown in Figure 5.2d. The maximum value of hydrogen production was 200 m^3H_2 at 120 m hub height with (4×215 kW) electrolyzer.

2. For Wasit, the scenario of [500 kW WT (50 m, 120 m) + PV1 + electrolyzer] found that the (18×48 kW) electrolyzer has worked all months of the year, the maximum amount of hydrogen was in June and July with 40.67 m^3H_2, 40.65 m^3H_2 at 50 m hub height and 58 m^3H_2, 56.77 m^3H_2 at 120 m hub height. For the (4×215 kW) electrolyzer produced a little amount of hydrogen through the year with a maximum amount of 25.81 m^3H_2 at 50 m hub height, and minimum amount around 0-1.61 m^3H_2 in the winter's months, while the scenario with 120 m hub height the maximum amount was 46.67 m^3H_2. The (2×430 kW) electrolyzer has worked only in July in the scenario of 50 m hub height with only 3.33 m^3 of H_2 and has worked for four months during the year in the scenario of 120 m hub height. The (1×860 kW) electrolyzer has not worked at all, as shown in Figure 5.3a

The second scenario of [500 kW WT (50 m, 120 m) + PV2 + electrolyzer] same as in the first scenario the electrolyzer most productive of hydrogen was (18×48 kW), as shown in Figure 5.3b, but with amount less than in the previous scenario because the power received from PV2 be lower than those in PV1.

The third scenario of [2000 kW WT (50 m, 120 m) + PV1 + electrolyzer], for this scenario all the electrolyzers have worked and the produced hydrogen increased in all cases of electrolyzers. The maximum amount of hydrogen production was at (18×48 kW) and (4×215 kW) electrolyzers with 166 m^3H_2, 178.33 m^3H_2 respectively, as shown in Figure 5.3c.

The fourth scenario of [2000 kW WT (50 m, 120 m) + PV2 + electrolyzer], same as in the third scenario but with a decrease in the amount of hydrogen production, as shown in Figure 5.3d. The minimum value of hydrogen production was around 0-6.45 m^3H_2 at 50 m hub height with (1×860 kW) electrolyzer.

3. For Anbar, the scenario of [500 kW WT (50 m, 120 m) + PV1 + electrolyzer] found that the (18×48 kW) electrolyzer has worked all months of the year, the maximum amount of hydrogen was in June with 28 m^3H_2 at 50 m hub height and 41.67 m^3H_2 at

120 m hub height. For the (4×215 kW) electrolyzer produced a little amount of hydrogen through the year with a maximum amount of 11.67 m^3H_2 at 50 m hub height, while the scenario with 120 m hub height the maximum amount was 26.67 m^3H_2. The (2×430 kW) electrolyzer has worked only in two months in the scenario of 50 m hub height with only 3.23 m^3 of H_2 and has worked for four months during the year in the scenario of 120 m hub height. The (1×860 kW) electrolyzer has not worked at all, as shown in Figure 5.4a.

The second scenario of [500 kW WT (50 m, 120 m) +PV2+electrolyzer] same as in the first scenario the electrolyzer most productive of hydrogen was (18×48 kW) electrolyzer, as shown in Figure 5.4b. But, the amount produced less than in the previous scenario due to the fact that the power received from PV2 is lower than that in PV1.

The third scenario of [2000 kW WT (50 m, 120 m) +PV1+electrolyzer], for this scenario the most productive electrolyzers were (18×48 kW) and (4×215 kW), as shown in Figure 5.4c. The maximum amount of hydrogen production was 93.67 m^3H_2 for 18×48 kW electrolyzer at 50 m hub height and 133.33 m^3H_2 for 4×215 kW electrolyzer at 120 m hub height.

The fourth scenario of [2000 kW WT (50 m, 120 m) +PV2+electrolyzer] is the same as in the third scenario but with a decrease in the amount of hydrogen production, as shown in Figure 5.4d. The minimum amount of produced hydrogen was in (1×860 kW) electrolyzer where it has not worked most months of the year.

As a result of comparing the monthly average of hydrogen production for the hybrid system that considered highest and lowest rated power wind turbines (500 kW, 2000 kW) working at two hub heights (50 m, 120 m) for each selected city. Found that the maximum amount of produced hydrogen was in Basra followed by Wasit and Anbar. The best scenario was [2000 kW WT at 120 m hub height + PV1+ (4×215 kW) electrolyzer] for Basra, while for both Wasit and Anbar, the best scenario was [2000 kW WT at 120 m hub height + PV1 + (18×48 kW) electrolyzer].

It can be concluded that the hybrid system with the low rated power electrolyzer can generate hydrogen more than the higher rated power electrolyzer because the last one needs to more energy on the contrary of the low rated power electrolyzer that can operate at low energy. Because of that, the (18×48 kW) electrolyzer for the proposed scenarios produced hydrogen more than of the (1×860 kW) electrolyzer.

Tables 5.2, 5.3 and 5.4 show the operating hours for each electrolyzer in the scenario of [500 kW WT at 50 m + PV1 + electrolyzers] and [2000 kW WT at 50 m + PV1 + electrolyzers] for Basra, Wasit and Anbar respectively, it is obviously that the operating hours for all electrolyzers are increased with the increasing of the rated power of wind turbine. These tables can help to determine the optimal size of the electrolyzer units.

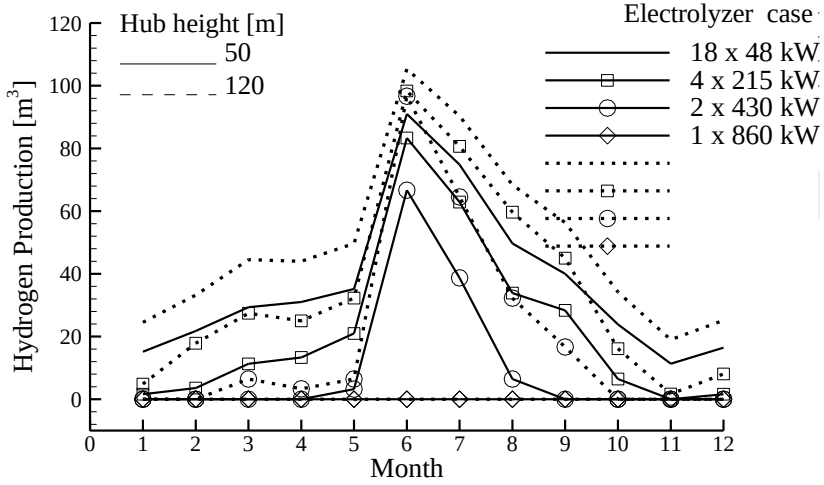

(a) 500 kW (P_{WT}) wind turbine integrated with PV1 case

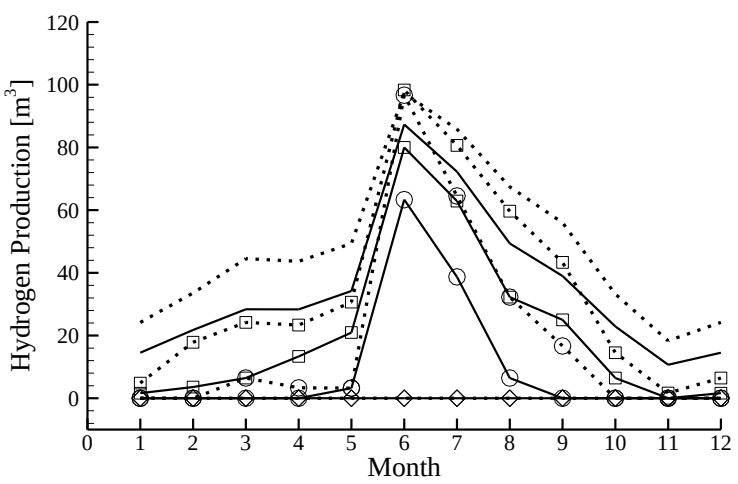

(b) 500 kW (P_{WT}) wind turbine integrated with PV2 case

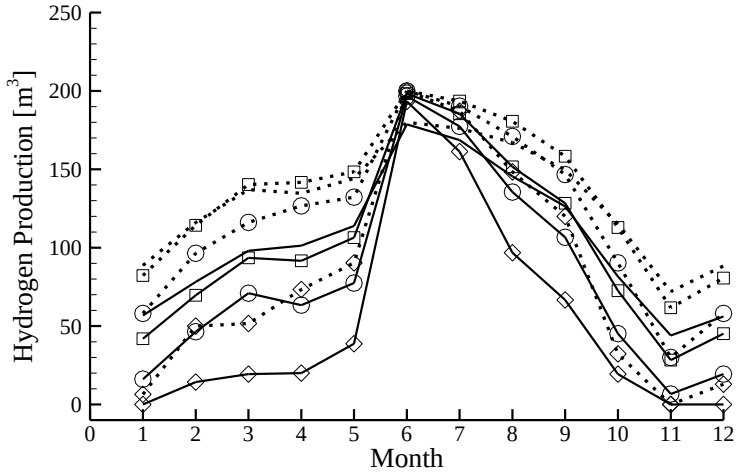

(c) 2000 kW (P_{WT}) wind turbine integrated with PV1 case

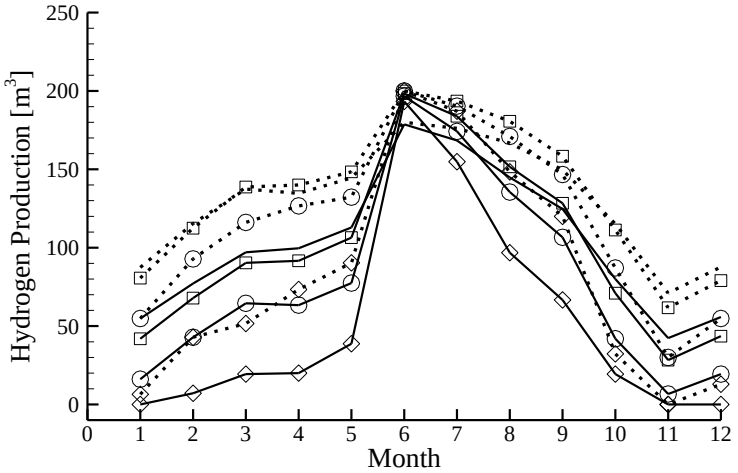

(d) 2000 kW (P_{WT}) wind turbine integrated with PV2 case

Figure 5.2 Variation of monthly hydrogen production in Basra (PV1 case: Panasonic PV modules PV2 case: Kyocera PV modules)

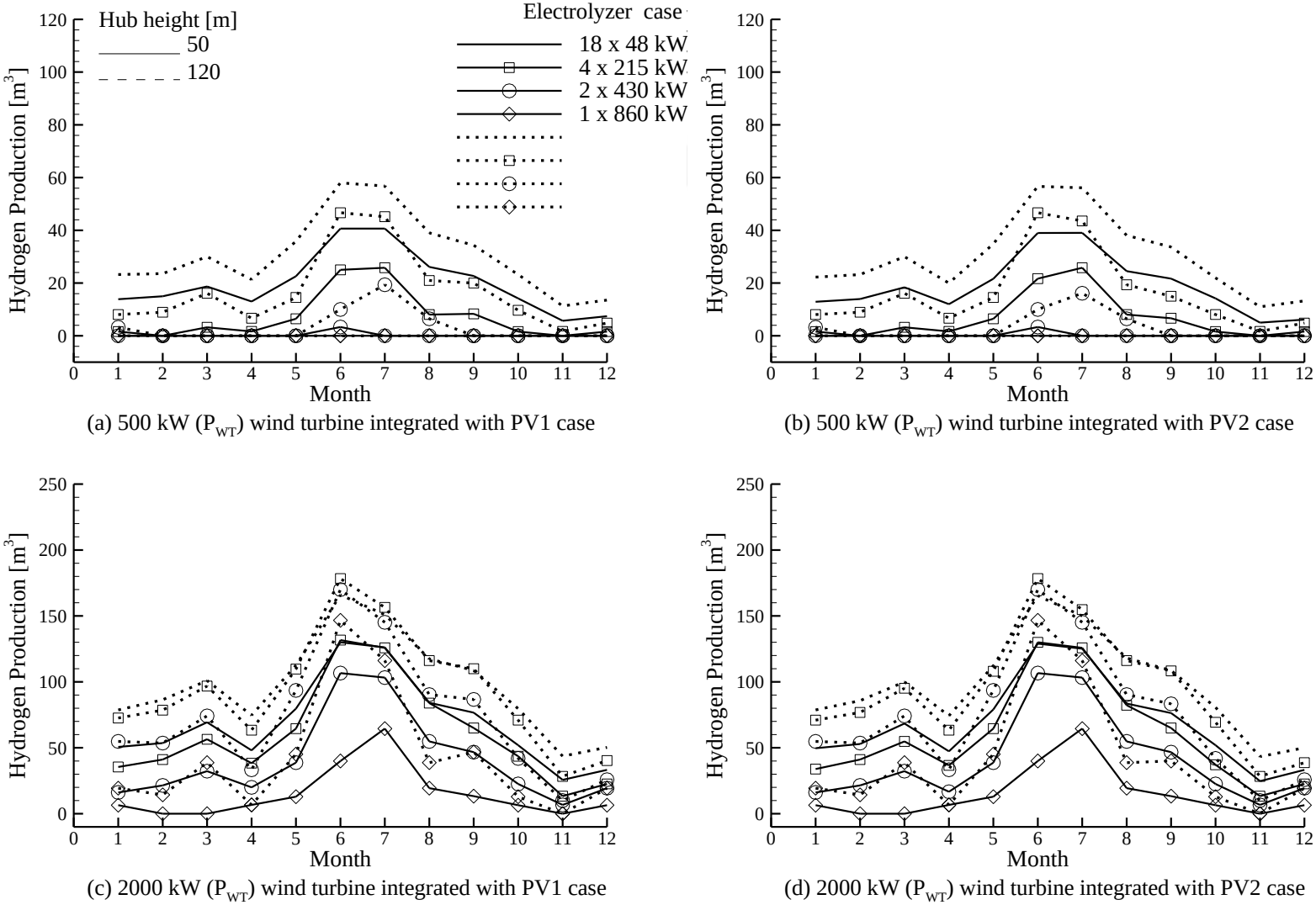

(a) 500 kW (P_{WT}) wind turbine integrated with PV1 case

(b) 500 kW (P_{WT}) wind turbine integrated with PV2 case

(c) 2000 kW (P_{WT}) wind turbine integrated with PV1 case

(d) 2000 kW (P_{WT}) wind turbine integrated with PV2 case

Figure 5.3 Variation of monthly hydrogen production in Wasit (PV1 case: Panasonic PV modules PV2 case: Kyocera PV modules)

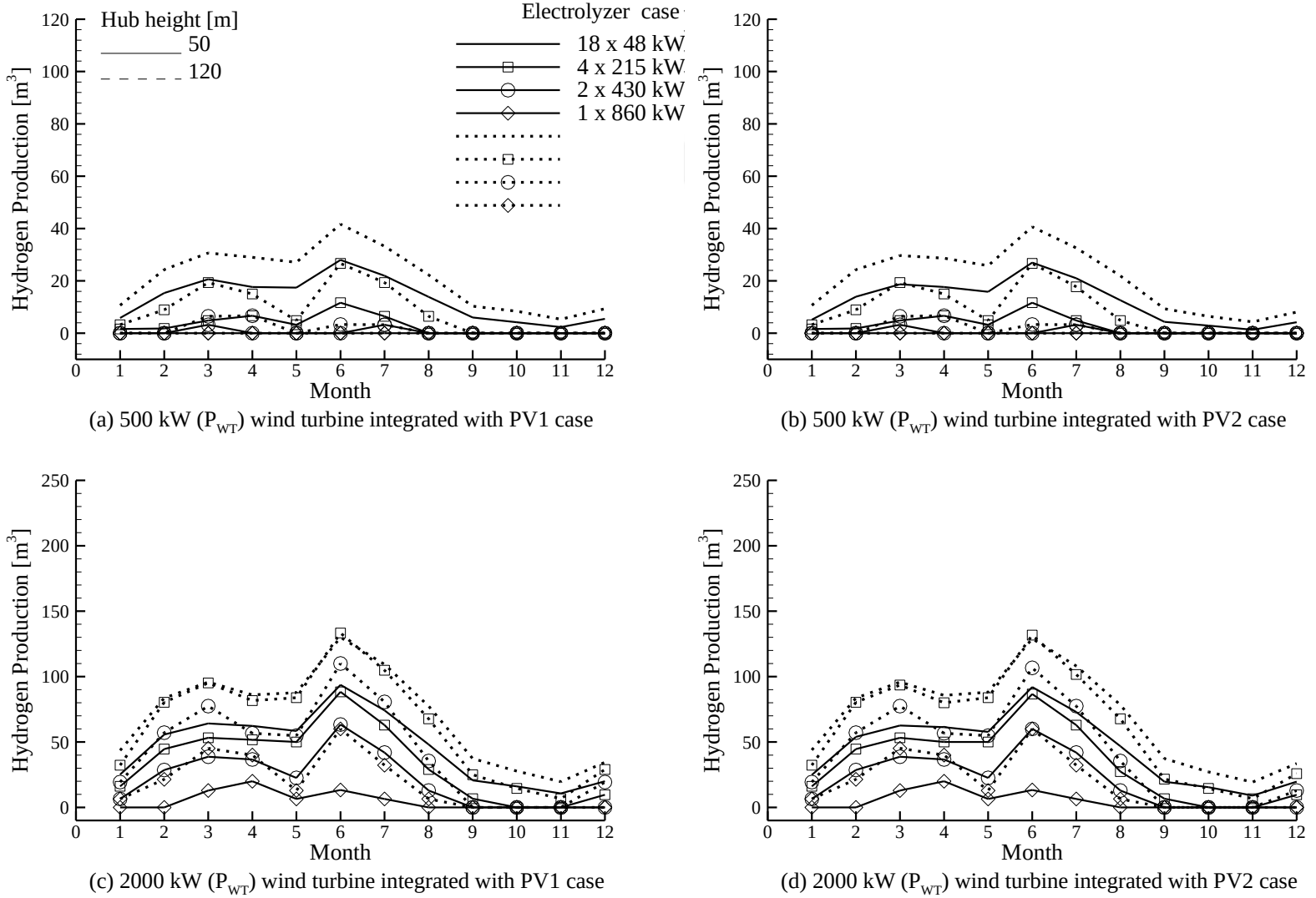

(a) 500 kW (P_{WT}) wind turbine integrated with PV1 case

(b) 500 kW (P_{WT}) wind turbine integrated with PV2 case

(c) 2000 kW (P_{WT}) wind turbine integrated with PV1 case

(d) 2000 kW (P_{WT}) wind turbine integrated with PV2 case

Figure 5.4 Variation of monthly hydrogen production in Anbar (PV1 case: Panasonic PV modules PV2 case: Kyocera PV modules)

Table 5.2 Operating hours for each electrolyzer in the scenario of [500 kW wind turbine at 50 m+PV1+electrolyzers] and [2000 kW wind turbine at 50 m+PV1+electrolyzers] in Basra

Electrolyzer	18*48 kW																	
	y1*	y2	y3	y4	y5	y6	y7	y8	y9	y10	y11	y12	y13	y14	y15	y16	y17	y18
500 kW	8424	6648	4584	3432	2640	1968	1464	1152	840	624	360	0	0	0	0	0	0	0
2000 kW	8688	8592	8184	7680	7224	6600	6048	5304	4680	4248	3792	3504	3336	3168	2856	2688	2448	2256

Electrolyzer	4*215 kW			
	y1	y2	y3	y4
500 kW	3072	840	0	0
2000 kW	7440	4728	3264	2304

Electrolyzer	2*430 kW	
	y1	y2
500 kW	840	0
2000 kW	4728	2304

Electrolyzer	1*860 kW
	y1
500 kW	0
2000 kW	2304

* y = the electrolyzer

Table 5.3 Operating hours for each electrolyzer in the scenario of [500 kW wind turbine at 50 m+PV1+electrolyzers] and [2000 kW wind turbine at 50 m+PV1+electrolyzers] in Wasit

Electrolyzer	18*48 kW																	
	y1	y2	y3	y4	y5	y6	y7	y8	y9	y10	y11	y12	y13	y14	y15	y16	y17	y18
500 kW	7032	4464	2832	1584	840	432	240	120	24	24	0	0	0	0	0	0	0	0
2000 kW	8232	7536	6624	5928	5064	4368	3864	3432	2928	2400	2160	1824	1536	1344	1080	888	768	648

Electrolyzer	4*215 kW			
	y1	y2	y3	y4
500 kW	1200	24	0	0
2000 kW	5520	2928	1464	648

Electrolyzer	2*430 kW	
	y1	y2
500 kW	24	0
2000 kW	2928	648

Electrolyzer	1*860 kW
	y1
500 kW	0
2000 kW	648

Table 5.4 Operating hours for each electrolyzer in the scenario of [500 kW wind turbine at 50 m+PV1+electrolyzers] and [2000 kW wind turbine at 50 m+PV1+electrolyzers] in Anbar

Electrolyzer	18*48 kW																	
	y1	y2	y3	y4	y5	y6	y7	y8	y9	y10	y11	y12	y13	y14	y15	y16	y17	y18
500 kW	5928	2784	1536	648	264	192	120	48	48	0	0	0	0	0	0	0	0	0
2000 kW	7560	6456	5184	4056	3144	2640	2136	1800	1584	1176	1032	792	624	576	432	336	264	216

Electrolyzer	4*215 kW			
	y1	y2	y3	y4
500 kW	480	48	0	0
2000 kW	3576	1608	600	216

Electrolyzer	2*430 kW	
	y1	y2
500 kW	48	0
2000 kW	1608	216

Electrolyzer	1*860 kW
	y1
500 kW	0
2000 kW	216

The annual hydrogen production is illustrated in Figures 5.5, 5.6 and 5.7. The maximum value was in Basra that obtained from [2000 kW WT at 120 m hub height + PV1 + (4×215 kW) electrolyzer], the annual hydrogen production for this scenario achieved 49150 m^3H_2/year. Followed by Wasit with 35620 m^3H_2/year from [2000 kW at 120 m hub height +PV1 + (18×48 kW) electrolyzer]. While the minimum amount of hydrogen production produced in Anbar in the case of using only with the turbine having rated powers of 2000 kW and with 1300kW at 120 m hub height.

As aforementioned, four electrolyzers with different rated power are considered to integrate with the PV/WT hybrid system to investigate the hydrogen production in the selected cities. Results can be summarized as follows:

1. The scenario of PV/WT hybrid system with (18×48 kW) electrolyzer: this scenario was the best scenario, where the hydrogen production values almost the highest values in all cases.

2. The scenario of PV/WT hybrid system with (4×215 kW) electrolyzer, which produced high values of hydrogen production, follows the (18×48 kW) electrolyzer. The amount of hydrogen production increased with increasing the rated power of the wind turbines and the increasing in the hub heights.

3. The scenario of PV/WT hybrid system with (2×430 kW) electrolyzer: hydrogen production is decreased in this electrolyzer because it needs to more power than the previous electrolyzers do. The maximum value of produced hydrogen was 43100 m^3H_2/year, 26800 m^3H_2/year, 15500 m^3H_2/year from [2000 kW WT at 120 m hub height + PV1] for Basra, Wasit, and Anbar respectively.

4. The scenario of PV/WT hybrid system with (1×860 kW) electrolyzer: despite the high rate of hydrogen production in this type of electrolyzer (200 m^3/hour), it has produced only a few quantities because it has not worked in most of the considered scenarios due to necessity of high energy.

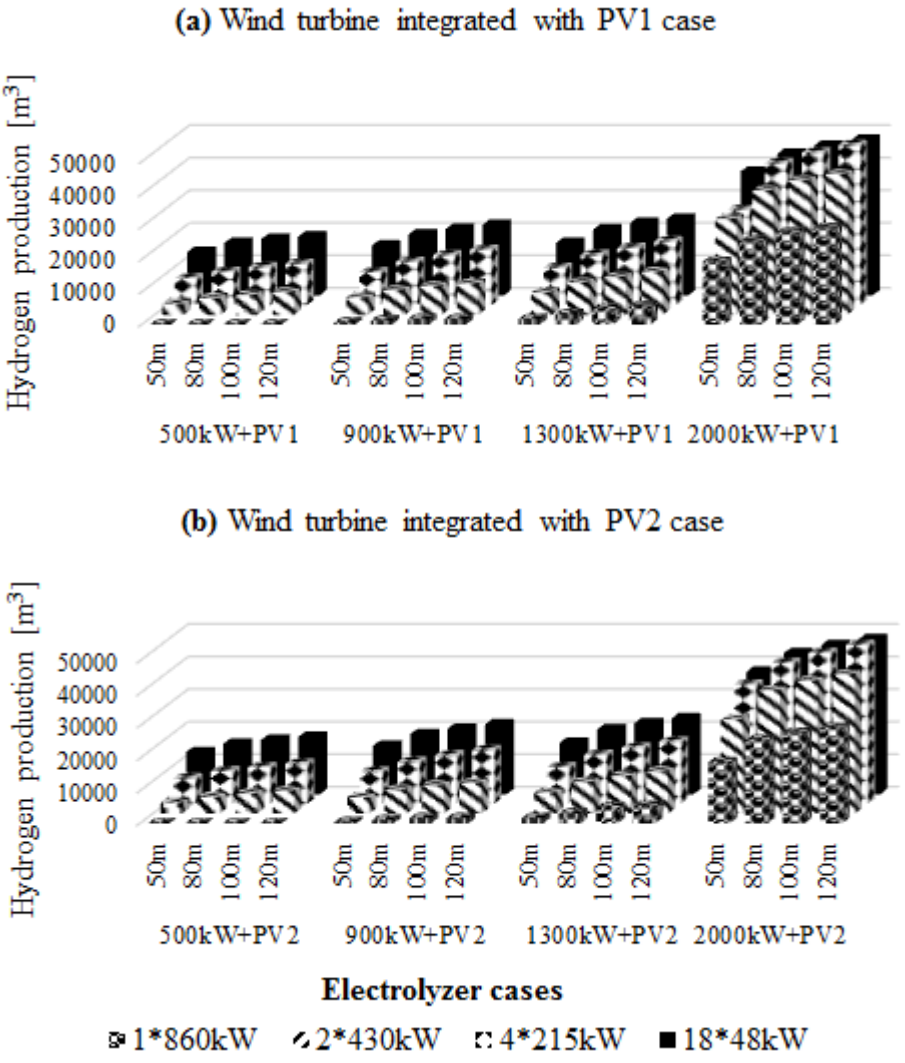

Figure 5.5 Annual hydrogen production for considered cases in Basra (PV1 case: Panasonic PV modules PV2 case: Kyocera PV modules)

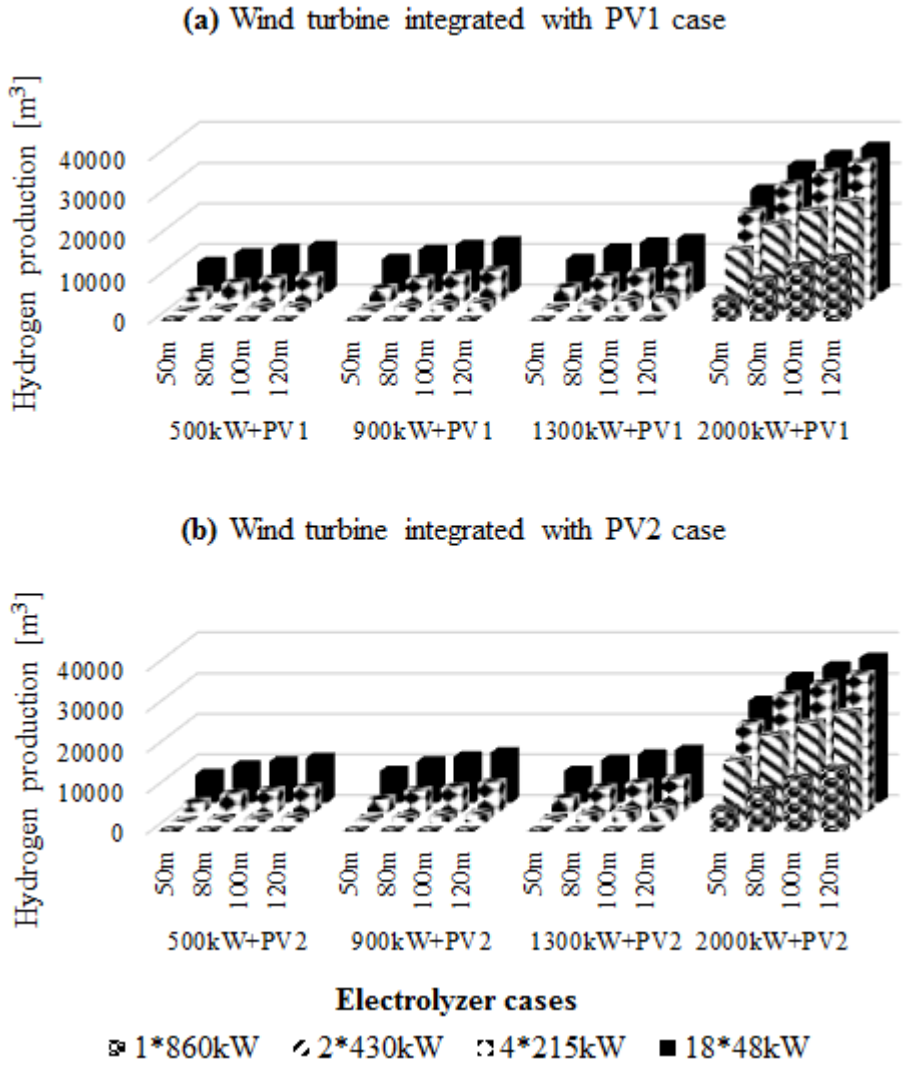

Figure 5.6 Annual hydrogen production for considered cases in Wasit (PV1 case: Panasonic PV modules PV2 case: Kyocera PV modules)

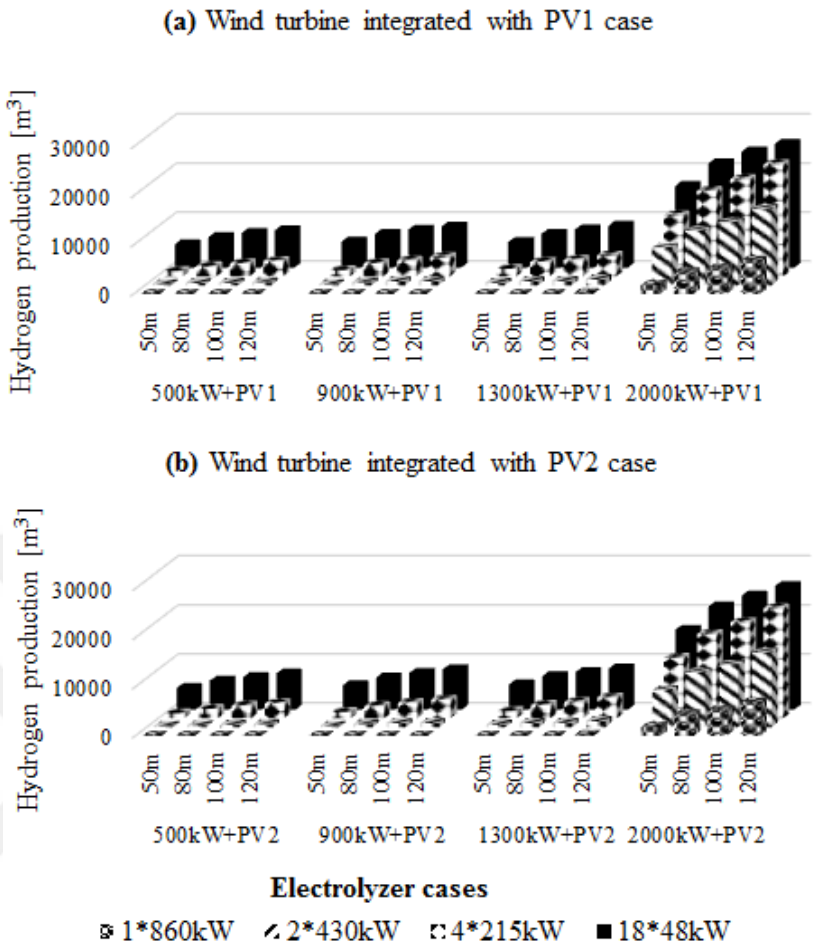

Figure 5.7 Annual hydrogen production for considered cases in Anbar
(PV1 case: Panasonic PV modules PV2 case: Kyocera PV modules)

5.3. The Cost Analysis of Hydrogen Production from Solar/Wind Hybrid System

The costs of hydrogen production for all cases of the hybrid system are calculated by counting the annual cost of electric energy that obtained from the PV/WT hybrid system and consumed by electrolyzer, as well as taking into consideration the annual cost of the electrolyzer, operation and maintenance cost of the electrolyzer, and annual hydrogen production. Levelized cost of hydrogen (LCOH) can be expressed by the following equation:

$$\mathrm{LCOH}_1 = \frac{C^*_{EZ} + C_{electric} + C^*_{o,m}}{m_{H_2}} \qquad (5.3)$$

Where $LCOH_1$ is levelized cost of hydrogen for stand-alone hybrid system, m_{H_2} is the annual hydrogen production, C^*_{EZ} is the annual cost of electrolyzer, $C_{electric}$ is the annual cost of electric energy, $C^*_{0,m}$ is the operation and maintenance cost of the electrolyzer.

The annual cost of electrolyzer can be calculated from the following equation:

$$C^*_{EZ} = C_{EZ} + C_{EZ} \cdot \frac{(1+e)^{10}}{(1+i)^{10}} + C_{EZ} \cdot \frac{(1+e)^{20}}{(1+i)^{20}} + C_{EZ} \cdot \frac{(1+e)^{25}}{(1+i)^{25}} \quad (5.4)$$

Where C^*_{EZ} is the cost of electrolyzer with considering the lifetime of the hybrid system, C_{EZ} is the cost of the electrolyzer.

In order to estimate the cost of hydrogen, the following assumptions are proposed:

- The lifetime of the electrolyzer system (l) =10 years.
- Discount rate (i) = 12%.
- Escalation ratio (e) of the electrolyzer system = 4%.

The cost of electrolyzer must be multiplied by CRF, as expressed by the following equation:

$$C_{EZ} = C_{first\,EZ} \cdot \mathrm{CRF} \quad (5.5)$$

The annual cost of electric energy that consumed by electrolyzer is calculated by counting the power of electrolyzer that consumed per hour, and the annual operation hour of the electrolyzer multiplied by the electric cost from the hybrid system, expressed as:

$$C_{electric} = P_{EZ} \cdot operation\ hour.LCOE \quad (5.6)$$

where P_{EZ} is the power of electrolyzer.

The following equation is used to calculate the operation and maintenance costs of electrolyzer:

$$C^*_{o,m} = \frac{C_{o,m}}{(i-e)}\left(1 - \frac{(1+e)^l}{(1+i)^l}\right) \quad (5.7)$$

$$C_{o,m} = C_{first} \cdot \frac{0.15}{l} \quad (5.8)$$

where C_{first} is the operation and maintenance costs of electrolyzer for the first year.

Another case for analyzing the cost of hydrogen is considered which assumed that excess energy is sold to the grid for 0.10 $ per kW to reduce the cost of hydrogen production, as expressed by the following equation:

$$LCOH_2 = \frac{C_{EZ}^{*} + C_{electric} + C_{o,m}^{*} - C_{Grid}}{m_{H_2}} \quad (5.9)$$

where $LCOH_2$ is the levelized cost of hydrogen considered the exporting of excess energy from the electrolyzer to the grid, C_{Grid} is the excess energy from the electrolyzer.

5.3.1. Results and Discussions

The cost calculations of hydrogen production are applied for each proposed scenario in all selected cities. The results are given in the Tables 5.5, 5.6 and 5.7. The obtained results can be summarized as follows:

i. The PV/WT hybrid system that integrated with 18 electrolyzers that have rated power 48 kW: in this scenario, the costs of hydrogen production are estimated using (18×48 kW) electrolyzer with the hybrid system that consists of different WTs rated power at four different hub height and two types of PV modules. The calculations of costs are applied for each selected citis.

The minimum value of hydrogen production cost was 1.577 $/m^{3}H$_2$ from [2000 kW WT at 120 m hub height+PV2] in Basra because it had a high amount of produced hydrogen of 47660 m^{3}H$_2$/year and low value of electricity cost. The maximum value of hydrogen production cost was 14.165 $/m^{3}H$_2$ [500 kW WT at 50 m hub height+PV2] in Anbar.

ii. The PV/WT hybrid system that integrated with four electrolyzers that have rated power 215 kW: in this scenario, The costs of hydrogen production were estimated using (4×215 kW) electrolyzer with the hybrid system that consists of different WTs rated power at four different hub height and two types of PV modules, this scenario achieved low costs for hydrogen production. The minimum value of hydrogen production cost was 0.851 $/m^{3}H$_2$ [2000 kW WT at 120 m hub height + PV1] in Basra because it has a high amount of produced hydrogen of 49150 m^{3}H$_2$/year, while the maximum value of hydrogen production cost was 27.331 $/m^{3}H$_2$ from [500 kW WT at 50 m hub height+PV2] in Anbar.

iii. In this scenario, the costs of hydrogen production are estimated using PV/WT hybrid system that integrated with two electrolyzers which have rated power 430

kW (2×430 kW electrolyzer). The minimum value of hydrogen production cost was 0.768 $/m^{3}H$_2$ from [2000 kW WT at 120 m hub height + PV1] in Basra where it has an amount of produced hydrogen of 43100 m^{3}H$_2$/year.

iv. In this scenario, the costs of hydrogen production are estimated using PV/WT hybrid system that integrated with one electrolyzers that have rated power 860 kW (1×860 kW electrolyzer). The high power that needs to produce hydrogen is the reason why this electrolyzer did not work in most of the proposed cases. The minimum value of hydrogen production cost in this electrolyzer was 0.754 $/m^{3}H$_2$ from [2000 kW WT at 120 m hub height+PV1] in Basra where it has amount of produced hydrogen of 29600 m^{3}H$_2$/year.

The costs of hydrogen production decreased with the increasing of WTs rated power and the increasing of hub height. The cost of hydrogen production of the hybrid system which consists of PV1 modules is less than of the hybrid system that consists of PV2 modules due to it produces hydrogen more than the system with PV2. Nevertheless, when the system with a 2000 kW WT is considered, the less value of hydrogen production cost varies between the scenario that considered PV1 modules and the scenario that considered PV2 modules because the produced hydrogen increased and the cost of electricity in the system with PV2 is lower than in the system with PV1.

By comparisons of the costs of hydrogen production for the four types of electrolyzers for all considered scenarios were given in Tables 5.2, 5.3, 5.4, notice that (4×215 kW) electrolyzer achieved low costs for produced hydrogen because the quantity of hydrogen production was high and the cost of electrolyzers was lower than the others. Although the (18×48 kW) electrolyzer produced amounts of hydrogen more than the other electrolyzers; because of its low rated power but the (4×215 kW) electrolyzer achieved low costs in most scenarios because of its capital cost less than of the (18×48 kW) electrolyzer.

For the second case of Levelized cost of hydrogen (LCOH$_2$), the cost of hydrogen production decreased because the excess energy from electrolyzer sold to the grid.

Table 5.5 Levelized cost of hydrogen [$/m^3$H_2$] in Basra

WT	Hub Height	LCOH	m_{H_2}(18×48 kW)		m_{H_2}(4×215 kW)		m_{H_2}(2×430 kW)		m_{H_2}(1×860 kW)	
			+PV1	+PV2	+PV1	+PV2	+PV1	+PV2	+PV1	+PV2
500 kW	50 m	$LCOH_1$	4.710	4.855	3.631	3.784	6.240	6.392	-	-
		$LCOH_2$	4.707	4.852	3.612	3.764	6.171	6.323	-	-
	80m	$LCOH_1$	3.920	4.030	2.923	2.941	4.306	4.282	-	-
		$LCOH_2$	3.918	4.027	2.906	2.924	4.254	4.232	-	-
	100m	$LCOH_1$	3.641	3.763	2.565	2.630	3.671	3.648	-	-
		$LCOH_2$	3.639	3.761	2.550	2.615	3.625	3.604	-	-
	120 m	$LCOH_1$	3.485	3.560	2.347	2.389	3.201	3.225	-	-
		$LCOH_2$	3.483	3.558	2.333	2.375	3.161	3.185	-	-
900kW	50 m	$LCOH_1$	4.570	4.681	3.360	3.402	4.558	4.784	24.249	36.093
		$LCOH_2$	4.567	4.679	3.344	3.386	4.511	4.735	23.697	35.275
	80m	$LCOH_1$	3.738	3.784	2.579	2.639	3.286	3.391	12.300	14.658
		$LCOH_2$	3.736	3.782	2.566	2.626	3.249	3.352	11.975	14.271
	100m	$LCOH_1$	3.438	3.467	2.271	2.308	2.860	2.875	9.302	9.288
		$LCOH_2$	3.436	3.465	2.260	2.296	2.826	2.841	9.040	9.031
	120 m	$LCOH_1$	3.236	3.256	2.060	2.092	2.653	2.664	9.277	9.264
		$LCOH_2$	3.234	3.254	2.050	2.082	2.620	2.631	8.998	8.989
1300kW	50 m	$LCOH_1$	4.535	4.620	3.176	3.210	3.878	4.070	9.588	9.577
		$LCOH_2$	4.532	4.618	3.163	3.196	3.842	4.032	9.380	9.374
	80m	$LCOH_1$	3.636	3.682	2.413	2.439	2.739	2.773	5.008	5.294
		$LCOH_2$	3.634	3.679	2.402	2.428	2.711	2.745	4.886	5.165
	100m	$LCOH_1$	3.307	3.350	2.136	2.149	2.367	2.373	3.477	3.466
		$LCOH_2$	3.305	3.348	2.126	2.139	2.342	2.348	3.392	3.383
	120 m	$LCOH_1$	3.119	3.131	1.931	1.954	2.105	2.120	3.018	3.101
		$LCOH_2$	3.116	3.129	1.922	1.945	2.083	2.098	2.942	3.023
2000 kW	50 m	$LCOH_1$	2.020	2.029	1.144	1.144	1.103	1.110	1.116	1.126
		$LCOH_2$	2.014	2.023	1.135	1.135	1.087	1.093	1.083	1.091
	80m	$LCOH_1$	1.747	1.747	0.965	0.964	0.874	0.871	0.868	0.862
		$LCOH_2$	1.740	1.740	0.956	0.954	0.860	0.858	0.839	0.834
	100m	$LCOH_1$	1.646	1.646	0.897	0.897	0.807	0.808	0.794	0.796
		$LCOH_2$	1.638	1.638	0.887	0.887	0.794	0.794	0.766	0.767
	120 m	$LCOH_1$	1.580	1.577	0.851	0.849	0.768	0.767	0.754	0.752
		$LCOH_2$	1.571	1.568	0.841	0.840	0.754	0.753	0.725	0.723

Table 5.6 Levelized cost of hydrogen [$/m^3$H_2$] in Wasit

WT	Hub Height	LCOH	m_{H_2}(18×48kW)		m_{H_2}(4×215kW)		m_{H_2}(2×430 kW)		m_{H_2}(1×860kW)	
			+PV1	+PV2	+PV1	+PV2	+PV1	+PV2	+PV1	+PV2
500 kW	50 m	$LCOH_1$	8.561	8.961	11.372	12.031	213.595	213.557	-	-
		$LCOH_2$	8.556	8.955	11.318	11.975	211.770	211.797	-	-
	80m	$LCOH_1$	6.665	6.841	6.501	6.687	30.665	30.634	-	-
		$LCOH_2$	6.661	6.837	6.468	6.654	30.361	30.339	-	-
	100m	$LCOH_1$	5.973	6.180	5.384	5.553	23.876	26.810	-	-
		$LCOH_2$	5.969	6.176	5.357	5.526	23.621	26.529	-	-
	120 m	$LCOH_1$	5.576	5.682	4.742	4.947	17.938	19.527	-	-
		$LCOH_2$	5.572	5.679	4.717	4.922	17.736	19.311	-	-
900kW	50 m	$LCOH_1$	8.542	8.890	9.654	10.065	43.581	43.570	-	-
		$LCOH_2$	8.538	8.885	9.611	10.021	43.203	43.204	-	-
	80m	$LCOH_1$	6.707	6.855	5.952	6.136	20.133	20.119	-	-
		$LCOH_2$	6.703	6.851	5.925	6.109	19.929	19.921	-	-
	100m	$LCOH_1$	6.013	6.137	5.078	5.434	13.222	15.897	-	-
		$LCOH_2$	6.010	6.134	5.054	5.408	13.082	15.728	-	-
	120 m	$LCOH_1$	5.600	5.652	4.364	4.585	10.322	11.839	-	-
		$LCOH_2$	5.597	5.649	4.344	4.563	10.209	11.708	-	-
1300kW	50 m	$LCOH_1$	8.980	9.262	9.531	9.653	31.773	31.774	-	-
		$LCOH_2$	8.976	9.258	9.493	9.616	31.515	31.526	-	-
	80m	$LCOH_1$	6.839	6.969	5.830	5.865	12.866	12.860	-	-
		$LCOH_2$	6.836	6.966	5.807	5.842	12.748	12.745	-	-
	100m	$LCOH_1$	6.042	6.169	4.886	4.963	8.813	9.437	-	-
		$LCOH_2$	6.039	6.166	4.865	4.942	8.729	9.348	-	-
	120 m	$LCOH_1$	5.606	5.646	4.201	4.294	7.113	7.294	-	-
		$LCOH_2$	5.603	5.643	4.184	4.277	7.043	7.223	-	-
2000 kW	50 m	$LCOH_1$	3.142	3.158	1.947	1.967	2.087	2.090	3.290	3.283
		$LCOH_2$	3.140	3.155	1.939	1.959	2.067	2.070	3.203	3.198
	80m	$LCOH_1$	2.540	2.545	1.513	1.508	1.526	1.524	1.914	1.936
		$LCOH_2$	2.537	2.542	1.506	1.501	1.510	1.508	1.862	1.883
	100m	$LCOH_1$	2.333	2.340	1.371	1.370	1.341	1.349	1.532	1.558
		$LCOH_2$	2.330	2.337	1.364	1.363	1.326	1.334	1.491	1.516
	120 m	$LCOH_1$	2.195	2.193	1.267	1.271	1.231	1.227	1.359	1.365
		$LCOH_2$	2.191	2.189	1.260	1.263	1.217	1.214	1.321	1.327

Table 5.7 Levelized cost of hydrogen [$/m^3$H_2$] in Anbar

WT	Hub Height	LCOH	m_{H_2}(18×48 kW)		m_{H_2}(4×215kW)		m_{H_2}(2×430 kW)		m_{H_2}(1×860kW)	
			+PV1	+PV2	+PV1	+PV2	+PV1	+PV2	+PV1	+PV2
500 kW	50 m	$LCOH_1$	12.983	14.165	26.151	27.331	106.994	106.945	-	-
		$LCOH_2$	12.975	14.156	26.047	27.229	106.342	106.331	-	-
	80m	$LCOH_1$	10.044	10.594	13.789	14.788	53.596	71.334	-	-
		$LCOH_2$	10.038	10.588	13.729	14.726	53.205	70.832	-	-
	100m	$LCOH_1$	8.826	9.443	10.760	11.125	42.906	42.866	-	-
		$LCOH_2$	8.821	9.437	10.712	11.077	42.567	42.542	-	-
	120 m	$LCOH_1$	8.193	8.475	9.240	9.498	35.778	35.740	-	-
		$LCOH_2$	8.188	8.470	9.197	9.456	35.477	35.451	-	-
900kW	50 m	$LCOH_1$	12.762	13.612	22.308	23.124	107.937	107.944	-	-
		$LCOH_2$	12.755	13.605	22.219	23.038	107.236	107.281	-	-
	80m	$LCOH_1$	9.980	10.462	11.549	12.163	36.582	36.577	-	-
		$LCOH_2$	9.974	10.456	11.501	12.115	36.306	36.314	-	-
	100m	$LCOH_1$	8.868	9.184	9.677	9.806	27.602	27.594	-	-
		$LCOH_2$	8.864	9.179	9.636	9.765	27.378	27.380	-	-
	120 m	$LCOH_1$	8.192	8.410	8.062	8.239	27.537	27.527	-	-
		$LCOH_2$	8.187	8.406	8.027	8.204	27.295	27.294	-	-
1300kW	50 m	$LCOH_1$	13.565	13.948	19.584	20.809	44.492	44.532	-	-
		$LCOH_2$	13.559	13.943	19.516	20.740	44.235	44.291	-	-
	80m	$LCOH_1$	10.404	10.588	11.093	11.809	28.128	28.144	-	-
		$LCOH_2$	10.399	10.584	11.053	11.767	27.932	27.957	-	-
	100m	$LCOH_1$	9.259	9.451	9.677	9.938	25.024	25.032	-	-
		$LCOH_2$	9.254	9.447	9.639	9.901	24.832	24.848	-	-
	120 m	$LCOH_1$	8.461	8.617	7.823	7.904	18.993	18.996	72.365	72.368
		$LCOH_2$	8.457	8.613	7.793	7.875	18.839	18.849	71.355	71.396
2000 kW	50 m	$LCOH_1$	4.732	4.818	3.240	3.264	3.773	3.807	8.872	8.868
		$LCOH_2$	4.729	4.815	3.227	3.252	3.741	3.775	8.677	8.678
	80m	$LCOH_1$	3.707	3.734	2.382	2.405	2.680	2.674	3.992	3.986
		$LCOH_2$	3.704	3.732	2.372	2.394	2.654	2.649	3.899	3.895
	100m	$LCOH_1$	3.332	3.373	2.114	2.126	2.349	2.356	3.419	3.412
		$LCOH_2$	3.330	3.370	2.105	2.116	2.324	2.331	3.332	3.327
	120 m	$LCOH_1$	3.110	3.111	1.869	1.888	2.005	2.035	2.721	2.714
		$LCOH_2$	3.106	3.108	1.862	1.880	1.985	2.014	2.652	2.647

CHAPTER 6

CONCLUSIONS AND RECOMMENDATIONS

6.1. Conclusions

This thesis deals with two renewable energy systems (wind turbines and photovoltaic modules). Many scenarios were proposed to investigate the potential of renewable energies (solar, wind, and hydrogen energy) for three different locations in Iraq. The energy obtained from solar and wind energy system has been exploited to produce hydrogen.

From this study, it can be concluded the following:

1. The southern and middle regions of Iraq have more potential in the wind and solar energy than the western and northern regions. According to calculations carried out in this study, Basra (southern Iraq) has annual average solar radiation of 19.11 MJ/m^2 on a horizontal surface, 4380 h of daylight hours per year, and daily average wind speed that estimated at 50 m was 6.32 m/s.
2. The photovoltaic/wind turbine hybrid system can be achieved uninterrupted energy with lower costs, unlike the system that consists of a single renewable energy such as wind turbine system alone or solar panels system.
3. The disparity in the amounts of energy that can be generated from renewable energies (wind, solar) during the seasons of the year, from the results, summer is more appropriate because of the increasing in wind speed and solar radiation.
4. Energy production can increase with increasing the efficiency of solar panels, rated power of wind turbine, and hub height.
5. The costs of power generation and hydrogen production can be reduced by selecting the optimum size of the hybrid system.

6. In order to increase the amount of electrical energy and hydrogen, the numbers of the photovoltaic modules and wind turbines in the hybrid system can be increased.

6.2. Recommendations

Iraqi cities suffer from an insufficient energy and power outage, on the other hand, renewable energy to produce energy and meet the shortfall is available. The research and continuous efforts striving to reduce the costs of energy that produced from renewable energies to compete against conventional fuels.

The researcher recommends that the Iraqi government should be the supporter and encourage the researchers to conduct more searches to identify the increasing potential of renewable energy; Iraq must be among the interested countries with this clean energy and opens the door for investment and exploitation of the sustainable energies that are available in the country.

REFERENCES

[1] Mostafaeipour, A., 2011. Wind energy feasibility study for city of Shahrbabak in Iran. **Renewable and Sustainable Energy Reviews, 15**: pp. 2545–2556.

[2] Wagner, H.J. and Mathur, J., 2013. Introduction to wind energy system. **Green Energy and Technology**, DOI: 10.1007/978-3-642-32976-0-1.

[3] Durak, M. and Özer, S., 2008. Wind energy: theory and application.

[4] Moriarty, P., Honnery, D., 2007. Intermittent renewable energy: the only future source of hydrogen. **Int J Hydrogen Energy, 32**: pp. 1616–1624.

[5] ABS Energy Research. The wind power report. 7th ed.; 2010. London, UK.

[6] Global Wind Energy Council (2015).

[7] **http://science.howstuffworks.com/environmental/green-science/wind**. (Access Date: October 2016).

[8] Ackermann, T., Soder, L., 2002. An overview of wind energy-status. **Renewable and Sustainable Energy Reviews, 6**: pp. 67–128.

[9] Yi Feng, 2015. Overview of wind power generation in China: Status and development. **Renewable and Sustainable Energy Reviews, 50**: pp. 847–858.

[10] Szafron, C., 2011. Wind energy conversion systems grid connection.

[11] Global Wind Energy Council (GWEC) Report 2013.

[12] Zou Y., Elbuluk M., Sozer Y., 2010. A complete modeling and simulation of induction generator wind power systems. IEEE industry applications society annual meeting (IAS), pp. 1–8.

[13] Wind turbine design, **http://windturbinezone.com/wind-technology/windturbine-design 2013**. (Access Date: October 2016)

[14] Prakash Mahela, O., Abdul Gafoor Shaik, 2016. Comprehensive overview of grid interfaced wind energy generation systems. **Renewable and Sustainable Energy Reviews, 57**: pp. 260–281.

[15] Celik, A. N., 2003. A statistical analysis of wind power density based on the Weibull and Rayleigh models at the southern region of Turkey. **Renewable Energy, 29**: pp. 593-604.

[16] Genc, M.S., 2010. Economic Analysis of Large-Scale Wind Energy Conversion Systems in Central Anatolian Turkey, **Clean Energy Systems and Experiences**, Kei Eguchi (Ed.), ISBN: 978-953-307-147-3.

[17] Cousineau, D., 2009. Fitting the three-parameter Weibull distribution: review and evaluation of existing and new methods. **IEEE Transactions on Dielectrics and Electrical Insulation.** 10.1109/TDEI.2009.4784578. pp. 281 – 288.

[18] Kuruoglu, E., Zerubia, J., Modeling SAR images with a generalization of the Rayleigh distribution. **IEEE Transactions on Image Processing. Volume: 13, Issue 4**, April 2004 pp. 527 – 533.

[19] Chansoo Kim, Keunhee Han, 2009. Estimation of the scale parameter of the Rayleigh distribution under general progressive censoring. **Journal of the Korean Statistical Society, 38**: pp. 239–246.

[20] Kazem, Hussein A., Chaichan, Miqdam T., 2012. Status and future prospects of renewable energy in Iraq. **Renewable and Sustainable Energy Reviews, Volume 16, Issue 8**: pp. 6007–6012.

[21] Archer, Cristina L. Jacobson, Mark Z., 2013. Geographical and seasonal variability of the global "practical" wind resources. **Applied Geography, 45**: pp. 119-130.

[22] The Lowest Priced and Best Solar Companies in California, 2015. **www.California solar center.org**.

[23] Nathan S. Lewis, 2005. Basic research needs for solar energy utilization, Report on the Basic Energy Sciences Workshop on Solar Energy Utilization. **California Institute of Technology.**

[24] "The History of Solar" U.S. Department of Energy, 2004.

[25] Koberle A.C., Gernaat, D., E.H.J., Vuuren, D., P. van, 2015. Assessing current and future techno-economic potential of concentrated solar power and photovoltaic electricity generation. **Energy, 89**: pp. 739-756.

[26] **From a solar cell to a PV system.svg** (Access Date: June 2016).

[27] **SBS Institute Publications Solar Photovoltaic.aspx** (Access Date: June 2016).

[28] **www.solarcell.net.in** (Access Date: June 2016).

[29] Patrick Doyle and Khalidah Jaafar, 2010. Iraq Has an Opportunity to Become a Solar Leader. **DAI's Developments Newsletter.**

[30] AL-Riahi, M., AL-Jumaily, K. J., Ali, H. Z., 1997. Modeling clear weather day solar irradiance in Baghdad, Iraq. **Energy Convers. Mgmt Vol. 39, No. 12**: pp. 1289-1294.

[31] AL-Riahi, M., AL-Kayssi, A., 1998. Some comments on time variation in solar radiation over Baghdad, Iraq. **Renewable Energy, Vol. 14, Nos. I-4**: pp. 479-484.

[32] Al-Karaghouli, A., Kazmerski, L.L., 2010. Optimization and life-cycle cost of health clinic PV system for a rural area in southern Iraq using HOMER software. **Solar Energy, 84**: pp. 710–714.

[33] Dihrab, S., Sopian, K., 2010. Electricity generation of hybrid PV/wind systems in Iraq. **Renewable Energy, 35**: pp. 1303–1307.

[34] Kazem, H., Chaichan, M., 2012. Status and future prospects of renewable energy in Iraq. **Renewable and Sustainable Energy Reviews, 16**: pp. 6007–6012.

[35] Amori, K., Al-Najjar, H., 2012. Analysis of thermal and electrical performance of a hybrid (PV/T) air based solar collector for Iraq. **Applied Energy, 98**: pp. 384–395.

[36] Hussein, B., Essa, I., Hussein, D., 2013. Introducing a PV Design Program Compatible with Iraq Conditions. **Energy Procedia, 36**: pp. 852 – 861.

[37] Ali, M., Salih, S., 2013. A Visual Basic-Based Tool for Design of Stand-alone Solar Power Systems. **Energy Procedia, 36**: pp. 1255 – 1264.

[38] Mahdi, E., Obaid, A., Khadim, I., Fadeel, A., Jaffer, A., Muhseen, E., Al-Shahup Jasim, A., Al-Gani, A., Mustuf, F.I., 2013. Design and evalution of a solar PV system. **Iraqi Journal of Physics, Vol.11, No.21**: pp. 67-74.

[39] Al-Hilphy, A., 2013. A theoretical and practical study for the incident solar radiation intensity in the Basrah province (south of Iraq). **IOSR Journal of Engineering (IOSRJEN), Vol. 3, Issue 9:** (September. 2013), ||V2|| pp. 25-35.

[40] Hasan, H., 2013. A New Study on Optimization and Control of Solar-Wind Power Sources in both Autonomous and Grid-Linked Applications. Basra University, College of Engineering, Master Thesis, Basra.

[41] Kadhim, M., 2013. Estimating the Optimal Design of a Hybrid Renewable Energy System in Basra City. Basra University, College of Engineering, Master Thesis, Basra.

[42] Abed, F., Al-Douri, Y., Al-Shahery, G., 2014. Review on the energy and renewable energy status in Iraq: The outlooks. **Renewable and Sustainable Energy Reviews, 39**: pp. 816–827.

[43] Kazem, A., Chaichan, M., T., Kazem, H., 2014. Dust effect on photovoltaic utilization in Iraq: Review article. **Renewable and Sustainable Energy Reviews, 37**: pp. 734–749.

[44] Jawad Khadim, I., Mahdi, E., Ubaid, A., 2014. Determining tilt angle for fixed solar panel tosites of Iraq's provinces by using the programs on NASA and google earth websites. **Eng. &Tech. Journal, Vol. 32, Part (B), No.3**, 2014.

[45] Hunaish, A., 2014. PLC Based Implementation of Solar Photovoltaic Energy Maximum Power Point Tracking Techniques. Basra University, College of Engineering, Master Thesis., Basra.

[46] Seth Dunn, 2001. Hydrogen Futures: Toward a Sustainable Energy System. Worldwatch Institute, Worldwatch paper 157, **www.worldwatch.org**.

[47] Das, D., Esmaili, R., Xu, L., Nichols, D., 2005. An Optimal Design of a Grid Connected Hybrid Wind/Photovoltaic/Fuel Cell System for Distributed Energy Production. 31st Annual Conference of IEEE Industrial Electronics Society, 2005. IECON 2005.

[48] Ahmed, N., Miyatake, M., Al-Othman, A.K., 2008. Power fluctuations suppression of stand-alone hybrid generation combining solar photovoltaic/wind turbine and fuel cell systems. **Energy Conversion and Management, 49**: pp. 2711–2719.

[49] Zhou, W., Lou C., Li Z., Lin Lu, Yang, H., 2010. Current status of research on optimum sizing of stand-alone hybrid solar–wind power generation systems. **Applied Energy, 87**: pp. 380–389.

[50] Caballero, F., Sauma, E., Yanine, F., 2013. Business optimal design of a grid - connected hybrid PV (photovoltaic) - wind energy system without energy storage for an Easter Island's block. **Energy, 61**: pp. 248-261.

[51] Maouedj, R., Mammeri, A., Draou, M.D., Benyoucef, B., 2014. Performance evaluation of hybrid Photovoltaic-Wind power systems. **Energy Procedia, 50**: pp. 797 – 807.

[52] Rahimi, M., Banybayat, M., Tagheie, Y., Valeh-e-Sheyda, P., 2015. An insight on advantage of hybrid sun–wind-tracking over sun-tracking PV system. **Energy Conversion and Management, 105**: pp. 294–302.

[53] Nguyen, D., Fujita, G., 2016. Analysis of sensorless MPPT method for hybrid PV–Wind system using DFIG Wind Turbines. **Sustainable Energy, Grids and Networks, 5**: pp. 50–57.

[54] Al Busaidi, A., Kazem, H., Al-Badi, A., Khan, M., 2016. A review of optimum sizing of hybrid PV–Wind renewable energy systems in Oman. **Renewable and Sustainable Energy Reviews, 53**: pp. 185–193.

[55] Emsley John, 2003. Nature's Building Blocks: An A-Z Guide to the Elements, OUP Oxford press, pp.229.

[56] Filippo Agresti, 2010. Hydrogen Storage in Metal and Complex Hydrides: from Possible Niche Applications towards Promising High Performance Systems. **paduaresearch.cab.unipd.it**.

[57] Boundless. "Properties of Hydrogen." Boundless Chemistry Boundless, 26 May. 2016. Retrieved 22 Dec. 2016 from **https://www.boundless.com/chemistry/textbooks/boundless-chemistry_textbook/nonmetallic-elements-21/hydrogen-148/properties-of-hydrogen-571-3498.**

[58] Mustafa Balat and Mehmet Balat, 2009. Political, economic and environmental impacts of biomass-based hydrogen. **International journal of hydrogen energy, 34**: pp. 3589-3603.

[59] **www.eere.energy.gov/hydrogenandfuelcells**. (Access Date: October 2016)

[60] Hydrogen Production and Storage R&D Priorities and Gaps. **International Energy Agency**, OECD/IEA, 2006. Hydrogen Implementing Agreement.

[61] Molburg, John, C., Doctor, Richard, D., 2003. Hydrogen from Steam-Methane Reforming with CO_2 Capture. **Argonne National Laboratory**, 9700 S. Cass Avenue, Argonne, Illinois 60439.

[62] Hotza, D., Diniz da Costa, J.C., 2008. Fuel cells development and hydrogen production from renewable resources in Brazil. **International Journal of Hydrogen Energy, 33**: pp. 4915-4935.

[63] Ulleberg Øystein, 2003. Modeling of advanced alkaline electrolyzers: A system simulation approach. **International Journal of Hydrogen Energy, 28(1)**: pp. 21-33. DOI: 10.1016/S0360-3199(02)00033-2.

[64] Schalenbach, M., Carmo, M., Fritz, David L., Mergel, J., Stolten, D., 2013. Pressurized PEM water electrolysis: Efficiency and gas crossover. **International Journal of Hydrogen Energy, 38**: pp. 14921-14933.

[65] Stempien, J. Pawel, Sun, Q., Hwa Chan, S., 2013. Solid Oxide Electrolyzer Cell Modeling: A Review. **Journal of Power Technologies, 93 (4)**: pp. 216–246.

[66] More on Nomenclature and the Water Splitting Reaction Requirements. Solar Hydrogen Generation. **http://www.briangwilliams.us**. Last Updated 24 Dec 2016.

[67] Meng Ni, Dennis Y.C. Leung, Michael K.H. Leung, K. Sumathy, 2006. An overview of hydrogen production from biomass. **Fuel Processing Technology, 87**: pp. 461 – 472.

[68] Lin, S.Y., Harada, M., Suzuki, Y., Hatano, H., 2005. Process analysis for hydrogen production by reaction integrated novel gasification (HyPr-RING). **Energy Conversion and Management, 46**: pp. 869.

[69] Lin, S.Y., Harada, M., Suzuki, Y., Hatano, H., 2002. Development an innovative method, HyPr-RING, to produce hydrogen from hydrocarbons. **Energy Conversion and Management, 43**: pp. 1283.

[70] Züttel, A., April 2004. Hydrogen storage methods. **Naturwissenschaften, Volume 91, Issue 4**: pp. 157-172.

[71] Momirlan, M., Veziroglu, T.N., 2002. Current status of hydrogen energy. **Renewable and Sustainable Energy Reviews, 6**: pp. 141–179.

[72] Campen, A., Mondala, K., Wiltowski, T., 2008. Separation of hydrogen from syngas using a regenerative system. **International Journal of Hydrogen Energy, 33**: pp. 332–339.

[73] Dupont V., 2007. Steam reforming of sunflower oil for hydrogen gas production. **Helia, 30 (46)**: pp.103–32.

[74] Dutton, A.G., Bleijs, J.A.M., Dienhart, H., Falchetta, M., Hug, W., Prischich, D., Ruddell, A.J., 2000. Experience in the design, sizing, economics, and implementation of autonomous wind-powered hydrogen production systems. **International Journal of Hydrogen Energy, 25**: pp. 705-722.

[75] Honnery, D., Moriarty, P., 2009. Estimating global hydrogen production from wind. **International Journal of Hydrogen Energy, 34**: pp.727-736.

[76] Khan, M.J., Iqbal, M.T., 2009. Analysis of a small wind-hydrogen stand-alone hybrid energy system. **Applied Energy, 86**: pp. 2429–2442.

[77] Zolezzi, J.M., Garay, A., Reveco, M., 2010. Large scale hydrogen production from wind energy in the Magallanes area for consumption in the central zone of Chile. **Journal of Power Sources, 195**: pp. 8236–8243.

[78] Javier Pino, Fco., Valverde, L., Rosa, F., 2011. Influence of wind turbine power curve and electrolyzer operating temperature on hydrogen production in wind hydrogen systems. Influence of wind turbine power curve and electrolyzer operating temperature. **Journal of Power Sources, 196**: pp. 4418–4426.

[79] Genc, M. S., Celik, M., Karasu, I., 2012. A review on wind energy and wind–hydrogen production in Turkey: A case study of hydrogen production via electrolysis system supplied by wind energy conversion system in Central Anatolian Turkey. **Renewable and Sustainable Energy Reviews, 16**: pp. 6631–6646.

[80] Genc, G., Celik, M., Genc, M.S., 2012. Cost analysis of wind-electrolyzer-fuel cell system for energy demand in Pınarbaşı-Kayseri. **International Journal of Hydrogen Energy, 37 (17)**: pp. 12158–12166.

[81] Zhang, G., Wan, X., 2014. A wind-hydrogen energy storage system model for massive wind energy curtailment. **International Journal of Hydrogen Energy, 39**: pp. 1243-1252.

[82] Sarrias-Mena, R., Fernandez-Ramı´rez, L. M., Garcı´a-Vazquez, C. A., Jurado, F., 2015. Electrolyzer models for hydrogen production from wind energy systems. **International Journal of Hydrogen Energy, 40**: pp. 2927-2938.

[83] Hussain Siyal, S., Mentis, D., Mortberg, U., Samo, S., Howells, M., 2015. A preliminary assessment of wind generated hydrogen production potential to reduce the gasoline fuel used in road transport sector of Sweden. **International Journal of Hydrogen Energy, 40**: pp. 6501-6511.

[84] Douak, M., Settou, N., 2015. Estimation of hydrogen production using wind energy in Algeria. **Energy Procedia, 74**: pp. 981 – 990.

[85] Valverde-Isorna, L., Ali, D., Hogg, D., Abdel-Wahab M., 2016. Modelling the performance of wind–hydrogen energy systems: Case study the Hydrogen Office in Scotland/UK. **Renewable and Sustainable Energy Reviews, 53**: pp. 1313–1332.

[86] Hollmuller, P., Jean-Marc Joubert, Lachal, B., Yvon, K., 2000. Evaluation of a 5 kWp photovoltaic hydrogen production and storage installation for a residential home in Switzerland. **International Journal of Hydrogen Energy, 25**: pp. 97-109.

[87] Kazim, A., Veziroglu, T.N., 2001. Utilization of solar–hydrogen energy in the UAE to maintain its share in the world energy market for the 21st century. **Renewable Energy, 24**: pp. 259–274.

[88] Thomas L. Gibson, Nelson A. Kelly, 2008. Optimization of solar powered hydrogen production using photovoltaic electrolysis devices. **International Journal of Hydrogen Energy, 33**: pp. 5931-5940.

[89] Chun-Hua Li, Xin-Jian Zhu, Guang-Yi Cao, Sheng Sui, Ming-Ruo Hu, 2009. Dynamic modeling and sizing optimization of stand-alone photovoltaic power systems using hybrid energy storage technology. **Renewable Energy, 34**: pp. 815–826.

[90] Amao, K., Hamano, A., Shimizu, K., 2012. Development of artificial leaf for solar hydrogen production. **Energy Procedia, 29**: pp. 21 – 25.

[91] Boudries, R., 2013. Analysis of solar hydrogen production in Algeria: Case of an electrolyzer-concentrating photovoltaic system. **International Journal of Hydrogen Energy, 38**: pp. 11507-11518.

[92] Boudries, R., Khellaf, A., Aliane, A., Ihaddaden, L., Khida, F., 2014. PV system design for powering an industrial unit for hydrogen production. **International Journal of Hydrogen Energy, 39**: pp. 15188 – 15195.

[93] Zafar, S., Dincer, I., 2014. Thermodynamic analysis of a combined PV/T-fuel cell system for power, heat, fresh water and hydrogen production. **International Journal of Hydrogen Energy, 39**: pp. 9962 - 9972.

[94] Giuseppe Mura, P., Baccoli, R., Innamorati, R., Mariotti, S., 2015. An energy autonomous house equipped with a solar PV hydrogen conversion system. **Energy Procedia, 78**: pp. 1998 – 2003.

[95] Motalleb, M., Đuki, A., Firak, M., 2015. Solar hydrogen power system for isolated passive house. **International Journal of Hydrogen Energy,** x x x: pp. 1-9.

[96] Jesper Jacobsson, T., Fjällström, V., Edoff , M., Edvinsson, T., 2015. CIGS based devices for solar hydrogen production spanning from PEC-cells to PV-electrolyzers: A comparison of efficiency, stability and device topology. **Solar Energy Materials & Solar Cells, 134**: pp. 185–193.

[97] Yilmaz, F., Tolga Balta, M., Selbaş, R., 2016. A review of solar based hydrogen production methods. **Renewable and Sustainable Energy Reviews, 56**: pp. 171–178.

[98] Sellami, M.Hassen and Loudiyi, K., 2016. Electrolytes behavior during hydrogen production by solar energy. **Renewable and Sustainable Energy Reviews;** xxxx–xxxx.

[99] Dalapati, G. K., Chin Sheng Chua,Ajay Kushwaha, Siao Li Liew,Vignesh Suresh, Dongzhi Chi, 2016. All earth abundant materials for low cost solar-driven hydrogen production. **Materials Letters, 183**: pp. 183–186.

[100] Bhattacharyya, R., Apurva Misra, Sandeep, K.C., 2017. Photovoltaic solar energy conversion for hydrogen production by alkaline water electrolysis: Conceptual design and analysis. **Energy Conversion and Management, 133**: pp. 1–13.

[101] Agbossou, K., Chahine, R., Hamelin, J., Laurencelle, F., Anouar, A., St-Arnaud, J.-M., Bose, T.K., 2001. Renewable energy systems based on hydrogen for remote applications. **Journal of Power Sources, 96**: pp. 168-172.

[102] Gosselink, J.W., 2002. Pathways to a more sustainable production of energy: sustainable hydrogen—a research objective for Shell. **International Journal of Hydrogen Energy, 27**: pp. 1125–1129.

[103] Stojic, D., Marceta, M. P., Sovilj, S. P., Miljanic, S. S., 2003. Hydrogen generation from water electrolysis—possibilities of energy saving. **Journal of Power Sources, 118**: pp. 315–319.

[104] Agbossou, K., Kolhe, M., Hamelin, J., Bose, T. K., 2004. Performance of a Stand-Alone Renewable Energy System Based on Energy Storage as Hydrogen. **IEEE Transactions on Energy Conversion, VOL. 19, NO. 3**: September 2004.

[105] Mills, A., Al-Hallaj, S., 2004. Simulation of hydrogen-based hybrid systems using Hybrid2. **International Journal of Hydrogen Energy, 29**: pp. 991–999.

[106] Ando, Y., Tanaka, T., 2004. Proposal for a new system for simultaneous production of hydrogen and hydrogen peroxide by water electrolysis. **International Journal of Hydrogen Energy, 29**: pp. 1349–1354.

[107] Levene, J.I., Mann, M.K., Margolis, R., Milbrandt, A., 2005. An Analysis of Hydrogen Production from Renewable Electricity Sources. **National Renewable Energy Laboratory,** Conference Paper NREL/CP-560-37612 September 2005.

[108] Shakya, B.D., Lu Aye, Musgrave, P., Technical feasibility and financial analysis of hybrid wind–photovoltaic system with hydrogen storage for Cooma. **International Journal of Hydrogen Energy, 30**: pp. 9–20.

[109] Meng Ni, K.H. Leung, M., Sumathy, K., Leung, D.Y.C., 2006. Potential of renewable hydrogen production for energy supply in Hong Kong. **International Journal of Hydrogen Energy, 31**: pp. 1401–1412.

[110] Wang, C., Hashem Nehrir, M., 2008. Power Management of a Stand-Alone Wind/Photovoltaic/Fuel Cell Energy System. **IEEE Transactions on Energy Conversion, VOL. 23, NO. 3**.

[111] Sopian, K., Fudholi, A., Ruslan, M., Sulaiman, M. Y., ALghoul, M., Yaha, M., Amin, N., Chin Haw, L., Zaharim, A., 2009. Hydrogen Production from Combined Wind/PV Energy Hybrid System in Malaysia. **Proceedings of the 4th IASME / WSEAS International Conference on Energy & Environment (EE'09).**

[112] Ratlamwala, T.A.H., Gadalla, M.A., Dincer, I., 2011. Performance assessment of an integrated PV/T and triple effect cooling system for hydrogen and cooling production. **International Journal of Hydrogen Energy, 36**: pp. 11282-11291.

[113] Caldero´n, M., Caldero´n, A.J., Ramiro, A., Gonza´lez, J.F., Gonza´lez, I., 2011. Evaluation of a hybrid photovoltaic-wind system with hydrogen storage performance using exergy analysis. **International Journal of Hydrogen Energy, 36**: pp. 5751-5762.

[114] Khalilnejad, A., Riahy, G.H., 2014. A hybrid wind-PV system performance investigation for the purpose of maximum hydrogen production and storage using advanced alkaline electrolyzer. **Energy Conversion and Management, 80**: pp. 398–406.

[115] Posso, F., Zambrano, J., 2014. Estimation of electrolytic hydrogen production potential in Venezuela from renewable energies. **International Journal of Hydrogen Energy, 39**: pp. 11846-11853.

[116] Maleki, A., Askarzadeh, A., 2014. Comparative study of artificial intelligence techniques for sizing of a hydrogen-based stand-alone photovoltaic/wind hybrid system. **International Journal of Hydrogen Energy, 39**: pp. 9973-9984.

[117] Lee, Duu-H., 2012. Toward the clean production of hydrogen: Competition among renewable energy sources and nuclear power. **International Journal of Hydrogen Energy, 37**: pp. 15726-15735.

[118] Chang, Pao.-L., Hsu, Chiung-W., Hsiung, Chih-M., Lin, Chiu-Y., 2013. Constructing an innovative bio-hydrogen integrated renewable energy system. **International Journal of Hydrogen Energy, 38**: pp. 15660-15669.

[119] Rahmouni, S., Settou, N., Chennouf, N., Negrou, B., Houari, M., 2014. A technical, economic environmental analysis of combining geothermal energy with carbon sequestration for hydrogen production. **Energy Procedia, 50**: pp. 263 – 269.

[120] Yilmaz, C., Kanoglu, M., Abusoglu, A., 2015. Thermoeconomic cost evaluation of hydrogen production driven by binary geothermal power plant. **Geothermics, 57**: pp. 18–25.

[121] Klimova, V., Pakhaluev, V., Shcheklein, S., 2016. On the problem of efficient production of hydrogen reducing gases for metallurgy utilizing nuclear energy. **International Journal of Hydrogen Energy,** x x x: pp. 1-6.

[122] Al-Azzawi, S.I., Zeki, N.A., 1987. Comparison between the characteristics of wind power calculations and solar radiation energy of some meteorological stations in Iraq. **Solar & Wind Technology, Volume 4, Issue 4**: pp. 513-516.

[123] Darwish, A.S.K., Sayigh, A.M., January 1988. Wind energy potential in Iraq. **Journal of Wind Engineering and Industrial Aerodynamics, Volume 27, Issues 1–3**: pp. 179-189.

[124] Al-Alawy, I.T., Mohammed, Abdul-Ilah Y., 1984. A mathematical model of wind energy for selected locations in Iraq. **Solar & Wind Technology, Volume 1, Issue 3**: pp. 187-191.

[125] Mynett, John A., Hussain, I., M., 1978. Availability of Solar Energy at Baghdad, Iraq: Performance and Design Data for Flat Plate Collectors. **Sun: Mankind's Future Source of Energy, Volume Two**: pp. 1160-1164.

[126] King W., C., Eugene J., West Point P., N., Y., Anderson P., G., Cowher D., D., Dalton J., B., et, al., 2003. In: Malinowski Jon C, editor. Iraq: a geography. **Department of Geography and Environmental Engineering United States Military Academy**.

[127] Genc, M., S., 2010. Economic Analysis of Large-Scale Wind Energy Conversion Systems in Central Anatolian Turkey, Clean Energy Systems and Experiences, Kei Eguchi (Ed.), ISBN: 978-953-307-147-3, **InTech**. **http://www.intechopen.com/books/clean-energy-systems-and experiences/ economic-analysis-of-large-scale-wind-energy-conversion-systems-in- central-anatolian-turkey.**

[128] Zolezzi, J.M., Garay, A., Reveco, M., 2010. Large scale hydrogen production from wind energy in the Magallanes area for consumption in the central zone of Chile. **Journal of Power Sources, 195**: pp. 8236–8243.

[129] Abed Al-Dulaimy, F., M., and Al-Shahery, G., Y., M., May 2010. Estimation of Global Solar Radiation on Horizontal Surfaces over Haditha, Samara, and Beji, Iraq. **The Pacific Journal of Science and Technology, Volume 11, Number 1**. **http://www.akamaiuniversity.us/PJST.htm**.

[130] Akpabio, Louis E., Etuk, Sunday E., 2003. "Relationship between Global Solar Radiation and Sunshine Duration for Onne, Nigerra". **Turk J. Phys., 27**: pp. 161-167.

[131] Abdul-Wahid, S., N., Mahdi, W., H., and Hamdan, H., J., Abdul-Wahid, F., N., June 2010. Estimation and Comparison of Diffuse Solar Radiation over Iraq. **Kufa Journal of Engineering; ISSN 2071-5528, Volume 1, Number 2**: pp. 153-174.

[132] Al-Hilphy, A., R., September 2013. A theoretical and practical study for the incident solar radiation intensity in the Basrah province (south of Iraq). **IOSR Journal of Engineering (IOSRJEN); e-ISSN: 2250-3021, p-ISSN: 2278-8719 Vol. 3, Issue 9, V2**: pp. 25-35, **www.iosrjen.org**

[133] Supriya C.S., 2001. Optimization and Sizing of a Grid-Connected Hybrid PV-Wind Energy System. **International Journal of Engineering Science and Technology (IJEST), Vol. 3 No. 5**: pp. 4296- 4323

[134] **https://www.alibaba.com/product-detail/500Kw-WIND-TURBINE-Direct-Drive**. (Access Date: February 2016).

[135] Karim, M., AlZu'bi, H., Diabat, A., 2010. Design of a hybrid solar-wind power plant using optimization. **Proceedings of IEEE Second International Conference on Engineering System Management and Applications**, pp. 1-6.

[136] **https://www.solar-nu-webshop.nl/webshop/zonnepanelen-pv/detail/360/panasonic-zonnepaneel-330w-hit-vbhn330sj471590x1053x35mm.html**. (Access Date: February 2016).

[137] **http://www.eco-distributing.com** (Access Date: February 2016).

[138] **https://www.alibaba.com/product-detail/High-quality-CE-water-electrolyzer-hydrogen_60452272801.html?spm=a2700.7724838.0.0.joEufy** (Access Date: April 2016)

[139] **http://www.hgenerators.com** (Access Date: April 2016).

PROFILE

PERSONAL INFORMATION

Name, Surname: Masad Mezher HASAN

Nationality: Iraqi

Date and Place of Birth: October 27, 1984, Basra

Tel: +90 553 544 33 70

Email: maishasan15@gmail.com

Address: Iraq/ Basra

EDUCATION

Degree	Institution	Graduation Date
Master of Science	Erciyes University/ Engineering College	-
B.Sc.	Technical College of Basra/ Fuel and Energy Dep.	2006
High School	Al-Euruba High School, Basra	2002

WORK EXPERIENCES

Year	Institution	Task
2007- still	Technical College of Basra	Research Assistant

FOREIGN LANGUAGE

English - Turkish